Rational Synthesis and Application of Aryl Iodides in Electrochemical Reactions and Theoretical Studies on the CBS Catalyst

Kumulative Dissertation

zur Erlangung des Doktorgrades der Naturwissenschaften
(Dr. rer. nat.)

dem Fachbereich Chemie der Philipps-Universität Marburg
vorgelegt von

M.Sc.

Robert Möckel

aus Lörrach

Marburg, 2018

Erstgutachter: Prof. Dr. G. Hilt

Zweitgutachterin: Prof. Dr. S. Dehnen

Erklärung

Ich erkläre, dass eine Promotion noch an keiner anderen Hochschule als der Philipps-Universität Marburg, Fachbereich Chemie, versucht wurde. Weiterhin versichere ich, dass ich meine vorgelegte Dissertation "Rational Synthesis and Application of Aryl Iodides in Electrochemical Reactions and Theoretical Studies on the CBS Catalyst" selbst und ohne fremde Hilfe verfasst, nicht andere als die in ihr angegebenen Quellen oder Hilfsmittel benutzt, alle vollständig oder sinngemäß übernommenen Zitate als solche gekennzeichnet sowie die Dissertation in der vorliegenden oder einer ähnlichen Form noch bei keiner anderen in- oder ausländischen Hochschule anlässlich eines Promotionsgesuchs oder zu anderen Prüfungszwecken eingereicht habe.

Marburg, den 24. August 2018

Robert Möckel

Eingereicht am 24. August 2018.

Vom Fachbereich Chemie der Philipps-Universität Marburg (Hochschulkennziffer: 1180) als Dissertation angenommen am _____

Tag der mündlichen Prüfung: 6. November 2018

Erstgutachter:	Herr Prof. Dr. Gerhard Hilt
Zweitgutachterin:	Frau Prof. Dr. Stefanie Dehnen

Die vorliegende Arbeit wurde am Fachbereich Chemie der Philipps-Universität Marburg unter der Anleitung von Prof. Dr. Gerhard Hilt in der Zeit von Januar 2015 bis September 2018 angefertigt.

Publications published as part of this dissertation so far:

Peer-reviewed Publications:

1. A. R. Nödling, R. Möckel, R. Tonner, G. Hilt, *"*Lewis *Acids as Activators in CBS-Catalysed* Diels-Alder *Reactions: Distortion Induced* Lewis *Acidity Enhancement of* $SnCl_4$*",Chem. Eur. J.* **2016**, 13171.

2. R. Möckel, J. Hille, E. Winterling, S. Weidemüller, T. M. Faber, G. Hilt, *"Electrochemical Synthesis of Aryl Iodides by Anodic Iododesilylation"*, *Angew. Chem.* **2018**, *130*, 450; *Angew. Chem. Int. Ed.* **2018**, *58*, 442.

3. R. Möckel, E. Babaoglu, G. Hilt, *"Iodine(III)-mediated Electrochemical Trifluoroethoxylactonisation - Rational Reaction Optimisation and Prediction of Mediator Activity"*, **2018**, *Chem. Eur. J.*, **2018**, *24*, 15781.

Poster Presentations:

1. R. Möckel, G. Hilt, *"Electrochemical Synthesis of Aryl Iodides by Anodic Iododesilylation"*, Summer School on Electrosynthesis, **17.-20.09.2017**, Mainz.

2. R. Möckel, G. Hilt, *"Distortion Induced Lewis Acidity Enhancement of* $SnCl_4$ *in CBS-Catalysed Diels-Alder Reactions"*, Orchem 2016, **05.-07.09.2016**, Weimar.

Conference Talks:

1. R. Möckel, G. Hilt, *"'Synthesis of Iodobenzene Derivatives by Electrochemical TMS-Iodine Exchange"'* German-Japanese Symposium on Electrosynthesis 2017, **14.09.2017**, Mainz.

Alex und Emmi

Danksagungen

Mein besonderer Dank gilt Herrn Prof. Dr. Gerhard Hilt für die ausgezeichnete Betreuung im Rahmen dieser Arbeit. Darüber hinaus möchte ich mich auch für die große Freiheit bedanken die du mir gegeben hast, mich auch auf Organik-fernen Gebieten versuchen zu dürfen, bei denen ein Gelingen nicht immer von vornherein zu erwarten war.

Frau Prof. Dr. Stefanie Dehnen danke ich für die Bereitschaft und die damit verbundene Arbeit, sich als Zweitgutachterin dieser Arbeit zur Verfügung zu stellen. Bedanken möchte ich mich ebenfalls bei Herrn Prof. Dr. Gottfried und Dr. Ralf Tonner für ihre Bereitwilligkeit, sich als Prüfer zur Verfügung zu stellen.

Für die angenehme und für mich sehr lehrreiche Zusammenarbeit möchte ich mich speziell bei Herrn Dr. Ralf Tonner bedanken.

Allen aktuellen und ehemaligen Mitgliedern der Arbeitsgruppe Hilt danke ich ganz herzlich für die angenehme Arbeitsatmosphäre und die tolle Zusammenarbeit der ganzen letzten Jahre. Mein Dank gilt hierbei Alexander Nödling, Julian Kuttner, Philipp Röse, Laura Kersten, Anastasia Schmidt, Patrick Baumann, Lea Brechmann und Erik Winterling. Ganz besonders jedoch Felicia Weber, Emre Babaoglu, Corinna Kohlmeyer, Lars Sattler, Sebastian Weber und Luomo Li – dank euch war auch das Umziehen immer wieder eine große Freude. Von Anne Ruffing und Max Franz aber ganz besonders auch von Ludmila Hermann und Natalia Krom wurden wir in Oldenburg sehr herzlich empfangen.

Auch maßgeblich am Gelingen dieser Arbeit beteiligt waren meine Bachelor Studenten Tianqi Shen, Tabea Faber, Stefan Weidemüller und Simon Werner, als auch die von mir betreuten Vertiefungsstudenten Erik Winterling, Patrick Baumann, Christoph Priem, Fabian Daus, Jessica Hille, Laura Werel, Lukas Alig, Malte Hofferth, Marvin Lübcke, Simon Werner, Stefan Weidemüller, Tabea Faber und Niklas Braun.

Für ihre hervorragende Arbeit, die den reibungslosen Ablauf meiner Forschung ermöglichten, möchte ich den Mitarbeitern der Serviceabteilungen des Fachbereichs Chemie in Marburg sowie des Instituts für Chemie in Oldenburg danken.

Mein besonderer Dank gilt Emre, für die dank dir deutlich schönere Zeit in Oldenburg, als auch die sehr entspannte (und immer häufiger organisierte) Kooperation. Wir werden dich sehr als Frieda und Emmi Sitter sowie als leidlichen Squash und Codenames Spieler vermissen.

Bei Alex N. möchte ich mich für zahlreiches Korrekturlesen, die großartige Kooperation, als auch für die schöne Zeit in und außerhalb des Labors bedanken. Du hast mich mit dem Arbeit-

skreis bekannt gemacht, durch dein "kritisches Hinterfragen"' hast du mir immer wieder neue Gedankenanstöße gegeben und mich dadurch vom Stillstand abgehalten.
Ein riesiger Dank gilt allen meinen Freunden, ohne deren Hilfe und Unterstützung die Zeit in Marburg nicht wie im Flug vergangen wäre. Zu nennen wären hier zum einen die Chemie Homies Lisa, Marius, Friedrich, Nico und Steffen. Als auch die "Überbleibsel" meiner glorreichen Medizin-Karriere Laura und Philipp, Franzi und Daniel, Sarina und Pavel, Julia und David und nicht zuletzt Berit. Dank euch war die Zeit in Marburg grossartig!
Für etliche schöne Abende, Tage und Unternehmungen gilt mein Dank Flule - ihr seid einfach die Besten! Auf viele weitere gemeinsame Jahre, bis ganz bald in Süddeutschland!
Für die zahlreiche Unterstützung und die Aufmunterungen der ganzen letzten Jahre möchte ich meinen Eltern, meiner Schwester Resi, sowie Muma und Papu danken. Eine Auflistung wäre unendlich und unmöglich. Ohne euch hätte ich das nie geschafft!
Zu guter Letzt gilt mein größter Dank Alex. Dafür, dass du immer für mich da bist, mir den Rücken freihält, die beste vorstellbare Freundin und die Mutter unserer wunderbaren Tochter bist. Danke!

Contents

Chapter 1

Introduction

1.1 Lewis acidity

Lewis acids are an indispensable tool for modern organic chemistry with a wide scope of applications.[1,2] Despite their broad application, the prediction of an optimal Lewis acid for a given application is still challenging. The reason for this can be deduced from their definition. According to the IUPAC definition (which is close to the original definition by Lewis[3]) Lewis acids are:

"A molecular entity (and the corresponding chemical species) that is an electron-pair acceptor and therefore able to react with a Lewis *base to form a* Lewis *adduct, by sharing the electron pair furnished by the* Lewis *base."*[4]

Even if this definition seems to be clear at first glance, the actual determination of a compounds Lewis acidity (which is one of the essential factors for the choice of a suitable Lewis acid) is challenging. At close inspection of this definition, it becomes clear, that the absolute acidity is not an intrinsic property of the acid, but is rather determined by the interplay with an electron pair donor (the Lewis base). The Lewis base itself as well as steric parameters affect the strength of the respective Lewis interaction noticeably.[5]
Due to the importance and structural diversity of Lewis acids, a large number of concepts has been developed to rationalise and predict a compounds Lewis acidity. Roughly, those concepts can be divided into two different approaches which are discussed in the following.

Experimental Determination of Lewis Acidity

One is the experimental quantification using spectroscopic Lewis base probes. This approach is based on the change of the electron structure of a Lewis base upon coordination to a Lewis acid with an accompanying change of a spectroscopic measurable parameter. The advantage doing this is that by using a specific base, steric as well as electronic interactions are captured. However, this in turn means, that the results are specific only for this Lewis base and can't be transferred to structurally or electronically different bases and are therefore only meaningful for the retrospective quantification. Several spectroscopic probes have been reported. Most known are the ones by Childs who used ^{1}H NMR shifts of crotonaldehyde, Hilt who used ^{2}H NMR shifts of *d*-quinolizidine and Gutmann and Beckett who used the ^{31}P NMR shift of triethylphosphine oxide as probe.[6–9]

Theoretical Determination of Lewis Acidity

The second group of approaches is based on theoretical methods. The first works on this topic mainly relied on the determination and comparison of the bond energy or formation energy of structural similar Lewis adducts as measure for the acidity of the respective acid.[5] This was achieved either by direct calculation or by application of empirical methods. To be mentioned in this context are the studies of Gutmann (donor number) and Mulliken (ΔH_{bond} of charge transfer complexes).[10–12] The drawback of those methods is their inability to generate a universal Lewis acidity scale as all energies are calculated with respect to a specific Lewis base. A step into direction of a universal acidity scale was done by Drago who introduced specific parameters for the acid and the base by which the formation energy could be estimated. Thereby, a first comparison of different Lewis acids without consideration of a specific base was possible.[13,14] Another example towards this direction was proposed by Pearson who developed the HSAB concept (hard and soft acids and bases). Thereby a qualitatively prediction of Lewis acidity is possible.[15] This concept was further expanded by Klopman, Salem and Parr which led to the definition of the electronic chemical potential μ and the hardness η.[16–19] Later on, Parr calculated the global electrophilicity index ω from μ and η which has successfully been used as global acidity scale.[20,21] An approach in the same direction has been developed by Evanseck who used the valence deficiency as measure for the intrinsic base independent Lewis acidity.[22] Another recently very popular scale is the fluoride ion affinity scale (FIA) which is based on the formation energy of a Lewis acid with a fluoride ion. As this energy gives only a measure for the

interaction with a hard base, this approach was expanded to chloride, iodide and methylate ion affinity scales in order to cover soft LEWIS acids as well.[23,24] Although this approach provides a global acidity scale it is referring to a specific LEWIS base and therefore it is often misleading. A last approach is the combination of the described experimental probes with quantum mechanical methods. Doing this, LEWIS acid coordinated probes and their respective predictive parameters (e.g. NMR shift, IR frequency or theoretical parameters like charge or HOMO/LUMO energies) are calculated by theoretical means. This facilitates a very good prediction of LEWIS acidity with respect to the resulting activity in a reaction of interest. This is due to the ability to design the theoretical probe in a manner that it resembles the system of interest ideally. This approach has been demonstrated among others by LASZLO who used theoretically obtained LUMO energies of LEWIS acid coordinated crotonaldehyde for the prediction of the LEWIS acid catalysed ene reaction of β-pinene with methyl acrylate.[25,26]

Energy Decomposition Analysis

A theoretical method for the analysis of chemical bonds which is of particular use with respect to the analysis of LEWIS acid-base adducts is *Energy Decomposition Analysis* (EDA). It considers the bond-forming process of the fragments A^0 and B^0 in its respective electronic and geometric ground state Ψ_A^0 and Ψ_B^0 with the energies E_A^0 and E_B^0 yielding the product AB with E_{AB} and Ψ_{AB}. In a first step A^0 and B^0 are distorted to the geometries in AB to A and B with Ψ_A and Ψ_A and E_A and E_B. The therefore necessary energy is the preparation energy ΔE_{prep}.

$$\Delta E_{prep} = E_A - E_A^0 + E_B - E_B^0 \tag{1.1}$$

The interaction energy ΔE_{int} is defined as

$$\Delta E_{int} = E_{AB} - E_A - E_B \tag{1.2}$$

Using EDA the interaction energy can be analysed in more detail. In a first step, A and B are moved with frozen electron distribution from infinite distance to the position in the molecule forming $\Psi_A\Psi_B$ with E_{AB}^0. The associated energy change corresponds to ΔE_{elstat}. In a second step, $\Psi_A\Psi_B$ is antisymmetrised and renormalised yielding Ψ^0. This procedure allows the spins of the two fragments to interact. The occurring energy difference corresponds to ΔE_{Pauli}. In a last step, Ψ^0 is relaxed, by that means ΔE_{orb} can be obtained.[27–29]

$$\Delta E_{int} = \Delta E_{elstat} + \Delta E_{Pauli} + \Delta E_{orb} \tag{1.3}$$

By this splitting of ΔE_{int} into its components, a thorough analysis of the individual energy contributions to a respective bond can be done which is especially useful for LEWIS acid-base adducts.[30] An extension of this method is its combination with natural orbitals for the chemical valence (NOCV) theory. In this way, ΔE_{orb} can be further broken down into pairwise contributions of interacting orbitals of the two fragments. The thereby obtained NOCVs Ψ_k can be used for a graphical analysis of the corresponding deformation densities $\Delta\rho_k(r)$ which depicts the change of the electron structure in the bond forming process. This is of special use as thereby, a visual assignment of different bonding types (σ, π, etc.) to the energetic contributions of the respective $\Delta\rho_k(r)$ is possible.[28,29,31–34]

1.2 Organic Electrochemistry

Organic chemistry has undergone a dramatic change during the last decade. Due to an increasing sensibility for environmental issues newly developed methods today have to satisfy multiple requirements, usually according to the 12 principles of green chemistry by Anastas.[35] As little catalysts and reagents as possible shall be used in order to reduce waste production. The applied components have to be non-toxic, preferably easy to control, and energy-saving conditions should be applied. Because of this broad range of demands, the recent rise of methods like highly efficient catalyst systems or photochemistry can be explained. Another method which rides on the wave of sustainability is organic electrochemistry.[36,37]

By replacement of classical reductants or oxidants with electricity, most of the described demands can be fulfilled. The waste is minimised or even eliminated and the reaction can be controlled much better due to multiple adjustable parameters (potential, current density). However, this entails new challenges. The experimental effort is increased (need of galvanostats and special cells) and due to a large number of additional parameters (e.g. applied charge, current density, electrode material, electrolyte, cell type), optimisation is more difficult. Further information regarding the experimental as well as the theoretical background, are summarised in the reviews by Dan Little and Jean-Michel Saveant.[38,39]

Despite all such challenges, a broad range of new reactions has been developed in recent years covering a large selection of challenges of organic chemistry. This includes complex oxidation and reduction reactions or C–C and C–heteroatom coupling reactions.[36,37,40–46] Several advances covering reactions relevant to the presented work are detailed in the following sections.

Electrochemical iodination reactions

Due to the widespread use of aryl iodides in chemistry, their synthesis is of central importance.[47–51] Classically, they are synthesised by electrophilic aromatic substitution. The necessary electrophilic iodine species can either be generated *in situ* by oxidation of iodine to iodonium ions using stoichiometrical amounts of oxidant or by using preformed electrophilic iodination regents like NIS or ICl. Both approaches lack atom efficiency for which reason an electrochemical generation of iodonium ions for the synthesis of aryl iodides is tantalising.[52,53]

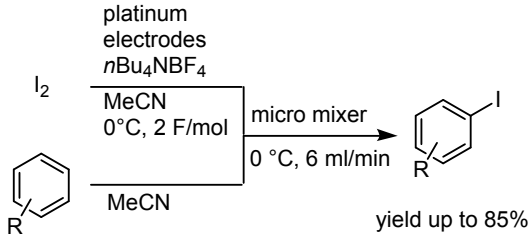

Scheme 1.1 – Electrochemical iodination protocol by YOSHIDA based on reaction of a preformed iodonium-pool with arenes in a micro-mixer.[54]

The first example of such a transformation was reported by CAMPBELL nearly 50 years ago. They were able to synthesise structurally simple aryl iodides by direct electrolysis of iodine with the respective aromatic hydrocarbons in acetonitrile using a divided cell. The yields were mostly low due to not further specified side reactions. However, by preforming a iodonium pool which was subsequently reacted with the substrate yields between 80 and 100 % could be obtained.[55] Further extensive work on electrochemical iodination reactions of aromatic hydrocarbons has been done by YOSHIDA (Scheme 1.1). Using micro-mixing techniques, he could obtain predominantly good yields and regioisomer ratios.[54] The drawback of all reported methods is on one hand the lack of regioselectivity control and on the other hand the inability of performing the reactions in a one-pot fashion but rather to be forced to separate the generation of the iodonium ions from their reaction with the substrate.

Iodine(III)-mediated Electrochemical Reactions

One rather recent application of aryl iodides is the field of hyper-coordinate iodine(III) reagents. Iodine(III) compounds possess a unique reactivity which resembles partially the one of transition metals. They can undergo oxidative additions as well as reductive eliminations and thereby are able to mediate bond-forming processes.[51,56–59]

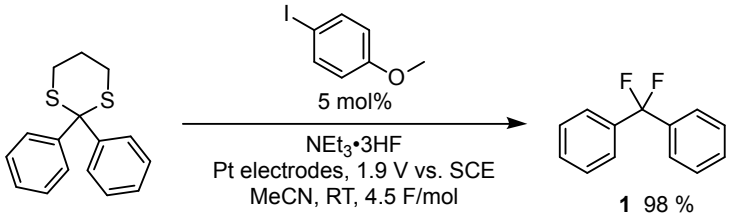

Scheme 1.2 – *p*-Iodoanisole mediated electrochemical *gem*-difluorination of dithio-ketals.[60]

The origin of their reactivity stems from the fascinating bonding situation of the iodine. Albeit they are often described as hypervalent due to a postulated 4e3c bond, recent investigations suggest an eight-electron configuration and thus a normal valency. In extreme cases of iodine(III) compounds with only one carbon ligand, e.g. PIFA or PIDA, the iodine atom actually exists in a hypovalent six electron configuration.[61,62]

The picture of ionic bound ligands with an electron deficient iodine implies several special features. Due to the electron deficiency of the iodine it is a LEWIS acid and furthermore prone to reductive elimination what makes it a strong oxidant.[63,64] As the ligands are bound in a ionic way, they are highly nucleophilic and therefore strongly activated. A last implication of the refusal of the iodine to increase its valency implies that substrates coordinate probably by electrostatic interactions which are not strongly directional and thus very flexible.[58,61–65] By use of those features, a multitude of applications of the various iodine(III) reagents have been developed. However, an inherent problem to all cases is the lack of atom efficiency as in all cases stoichiometric amounts of oxidants have to be used to generate the iodine(III) species from the respective aryl iodides.[49,51,51,66]

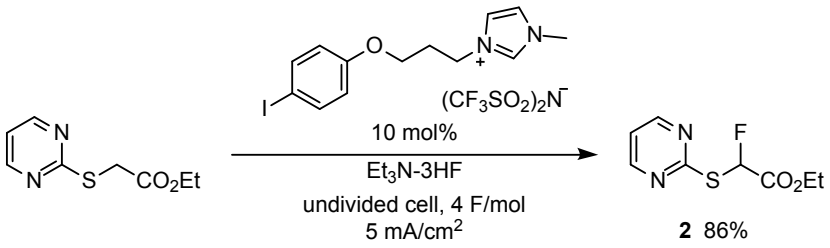

Scheme 1.3 – Ionic liquid aryl iodide mediated electrochemical fluorination of pyrimidinylthio acetates.[67]

An elegant approach to avoid this problem is the utilisation of electrochemistry. Pioneering work on this approach has been done by FUCHIGAMI. Using various aryl iodide derivatives as mediators in substoichiometrical amounts, they could fluorinate a range of substrates in good to excellent yields. A common theme of all applied substrates is the presence of sulphur containing functional groups in neighbourhood to the reaction centre in order to stabilise occurring cationic intermediates. In early investigations they used, as shown in Scheme 1.2, simple aryl iodide mediators.[i] A divided cell and controlled potential electrolysis had to be used to obtain good

[i] They state that *para* substituted aryl iodides have to be used to prevent homo coupling but did not further investigate the influence of the mediator substitution on reaction yield.

yields.[60,68] To improve atom efficiency, they used the concept of mediator recycling in later studies. The recycling was possible in two distinct approaches. The first approach was the application of an aryl iodide containing ionic liquid (Scheme 1.3). This approach brought two advantages. The product could be separated from the mediator after the reaction by simple extraction with organic solvents. Furthermore, due to the bulkiness of the mediator, reduction of the iodine(III) was not a severe problem and thus an undivided cell could be used.[67] The second approach made use of polystyrene bound aryl iodides in combination with chloride as co-mediator for the fluorination of benzylcarbonothioates yielding benzyl fluorides. In this case the mediator could be recycled simply by filtration. Within 10 recycling cycles, they didn't observe any deterioration of the mediator activity.[69] The last literature known example for an in-cell use of iodine(III) compounds as mediators has been reported by Hara in which they fluorinated 1,3-dicarbonyls following the procedure of Fuchigami.[70,71] Astonishingly, all other reported applications of iodine(III) as electrochemical mediator have been done in an ex-cell manner which strongly diminishes the benefits of electrochemistry.[71] One such example for the ex-cell use is shown in Scheme 1.4, in which an ionic iodine(III) reagent was synthesised electrochemically (using hexafluoro-*iso*-propanolate or trifluoroethoxylate as ligands) and subsequently reacted with imines yielding benzoxazoles.[72]

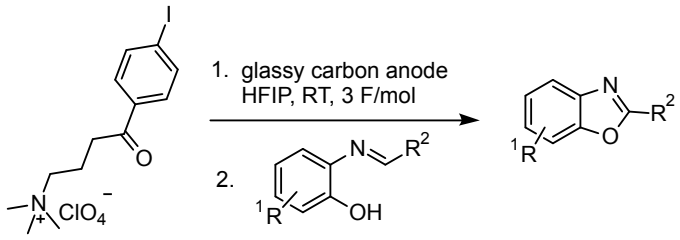

Scheme 1.4 – Iodine(III)-mediated electrochemical ex-cell synthesis of benzoxazoles.[72]

1.3 Statistical Tools for Reaction Optimisation

An intrinsic problem for modern method development in chemistry is the vast number of parameters that can be controlled. In "classical" organic reactions "chemical parameters" like applied catalysts, and additives or solvent, as well as "physical parameters" like temperature or pressure can and should be optimised to get an as efficient reaction as possible. In organic electrochemical reactions, this problem is even worse. Electrochemical parameters such as electrolyte, cell type or electrode material have to be considered additionally. Several approaches can be chosen to cope with the enormous amount of conditions that need to be screened to find optimal performance. The approach most often used today is parallelisation. By decreasing reaction size, the number of possible experiments that can be done in parallel is drastically increased, allowing the screening of many factors in a limited time. This approach can also be applied in electrochemical method development, although the instrumental requirements are high due to the necessity of power supply and special electrochemical cells.[46] These difficulties have been diminished by miniaturisation leading to micro-electrode arrays at which hundreds of reactions can be done at the same time. Nevertheless, this method is experimentally challenging and not broadly applicable.[73] Another approach is the implementation of electrochemistry to flow conditions which allows a fast screening of different reaction conditions as well, but is instrumentally challenging, too.[74–76]

These problems arising in a "classical" reaction optimisation can be drastically diminished by the two other optimisation approaches. Those two approaches, Design of Experiment (DoE) and Multivariate Linear Regression Analysis (MLR)), try to solve the optimisation problem not by increasing the number of experiments but tackle the problem with a better interpretation of the obtained data and by shifting the data generation to theoretical methods.

Multivariate Linear Regression Analysis

The most basic method to increase optimisation efficiency and thereby to decrease the number of necessary reactions that have to be done is to extract as much information as possible from the data at hand. In chemical environment, most often data is evaluated by transforming continuous variables into dummy variables (yes/no, better/worse, etc.). This approach allows an intuitively data handling that does not require any statistical background, however due to the dimensional reduction by the transformation process, most of the information at hand is not used.[77,78]

A common method which allows the use of all data is linear regression analysis. Using this

method, it is possible to connect the measured output Y_i with an input variable X_i in a mathematical model and thereby using all n data points (1.4) which improves significance (the error ϵ_i is taken into account) and further allows predictions.

$$y_i = \alpha + \beta x_i + \epsilon_i \qquad i = 1, ..., n,\ \alpha,\ \beta\ \epsilon \in\ \mathbb{R} \tag{1.4}$$

$$\sum_{i=1}^{n} (Y_i - \alpha - \beta x_i)^2 \rightarrow \min_{\alpha,\beta} \tag{1.5}$$

Different methods for the determination of α and β are available, most commonly used is the least squares method (1.5) in which the squared difference between predicted and observed values is minimised. The generation of a mathematical model for Y_i has multiple advantages. By comparison of the measured with the predicted output the variance σ^2 can be determined (1.6) .

$$\hat{\sigma}^2 = \frac{1}{n-2} \sum_{i=1}^{n} \hat{\epsilon}_i^2 = \frac{1}{n-2} \sum_{i=1}^{n} (Y_i - \hat{Y}_i) \tag{1.6}$$

This allows a quantitative assessment of the quality of the experimental data. Although this doesn't directly improve optimisation efficiency, it prevents unfounded decisions. This is of particular relevance with respect to outliers which thereby can be identified using various methods (e.g. T-test) and are a severe problem for optimisations done in a binary approach.
Furthermore, the use of calculated values α and β allows an improved optimisation efficiency. Using the predictive capabilities, new Y_i can be predicted for given X_i. This allows to save experiments by interpolation over the existing data. As the linear functions described so far do not allow the modelling of an optimum, quadratic functions have to be incorporated for a quantitative optimisation (1.7).[77]

$$y_i = \alpha + \beta_1 x_i + \beta_2 x_i^2 + \epsilon_i \tag{1.7}$$

Although this approach possesses multiple advantages, it is inherently restricted to unidimensional questions, which is a big drawback for an application in a chemical context. To overcome this disadvantage, multivariate linear regression was developed. In general, it is the transformation of univariate linear regression and all connected methods to an p-dimensional space (1.8).[77]

$$y_i = \alpha + \beta_1 x_{i1} + ... + \beta_p x_{ip} + \epsilon_i \tag{1.8}$$

Using this generalisation, the method is much better applicable in a chemical context since multiple descriptors can be used at once to predict an outcome Y_i. For multivariate linear regression, the determination of the significance σ is of particular relevance. Using modified

tests, the significance of each β_p can be assessed and thereby the importance of the respective influence factor can be quantitatively determined. Especially when descriptors are incorporated whose relevance is not known, the calculation of the respective p-values (probability that the Null-hypothesis is fulfilled) allows an instant boolean effect/no effect classification. If functions of higher order are included, it is possible to map the chemical space in p dimensions in a quantitative way.[77]

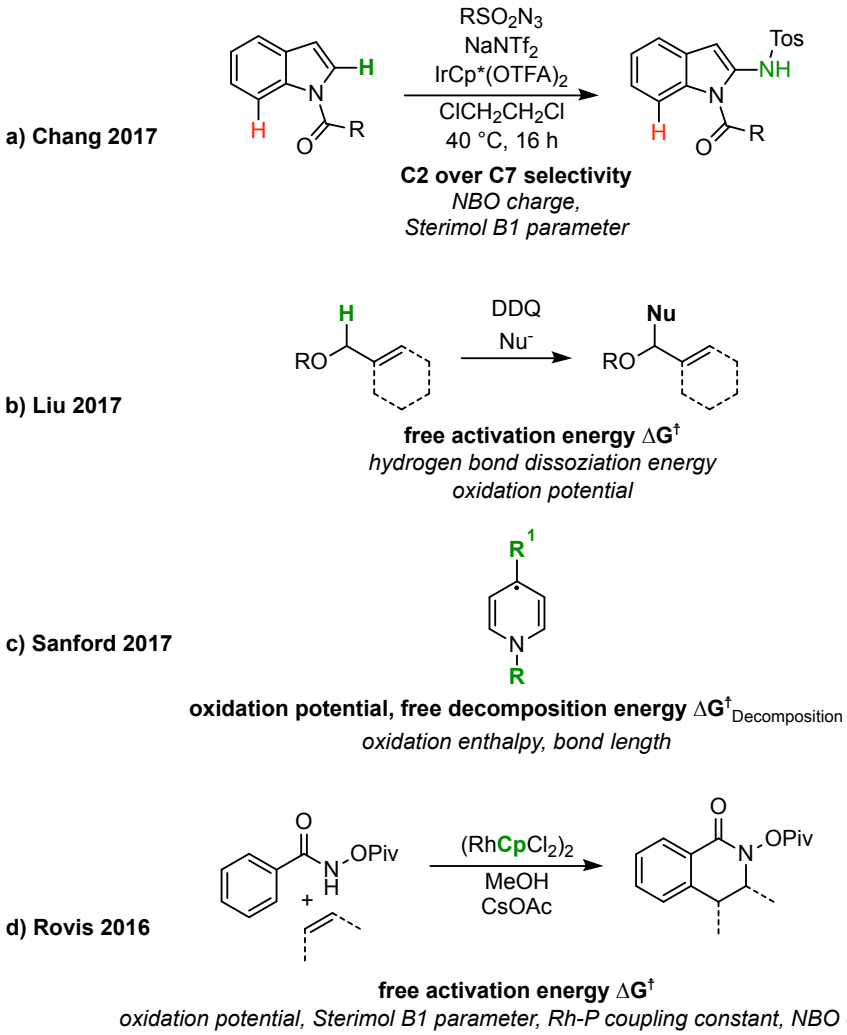

Figure 1.1 – Overview of some resent applications of MLR; a) Ir(III) catalysed amidation,[79] b) DDQ mediated CH activation,[80] c) Pyridinium anolytes for Redox-Flow batteries,[81] d) Rhodium-catalysed CH activation using different Cp-ligands.[82] Target variable bolt, descriptor variables in italic, centre of optimisation marked in green.

In a chemical context MLR is often used for two different applications. On the one hand, it is needed in design of experiments theory in order to generate the resulting model (for more information see 1.3). One the other hand it is often combined with computational methods like density functional theory (DFT). In this combination, the parameter set X_i is calculated by DFT methods and subsequently used as input in a MLR model for the prediction of the parameter of interest Y_i. Common descriptors that are being used are for example ionisation-, oxidation/reduction-, or dissociation energies, point charges, IR frequencies, NMR shifts and many steric parameters like bond lengths or torsion angles and more complicated ones like Charton, Taft or Sterimol parameters. However, in order to be able to generate the model, the respective Y_i have to be determined experimentally though. Nevertheless, as soon as the model has been established, it can be used in a so-called virtual screening to predict new Y_i without any experimental but only with computational input. Due to no scaling problems of modern clusters, this is very efficient and allows broad screenings that would be not possible experimentally.[83–88] The approach of using MLR analysis, especially for virtual screenings, has experienced a boom in recent years in all areas of chemistry. A small survey over some important contributions from the last years with the respective output variable and the applied descriptor variables can be seen in Figure 1.1.

Design of Experiments

Design of Experiments (DoE) is a statistical method that deals with the optimisation of optimisation processes. Classical, reactions are optimised step by step in a one-dimensional way altering only one variable at a time until an optimum is reached while all other variables are fixed (one factor at a time (OFAT)). This approach has one big advantage which is probably the reason why it is used nearly exclusively in chemistry. As only one parameter is altered, variations in the output variable (e.g. yield or enantiomeric excess) can directly be linked to this change.[78]

Although this approach is intuitively and directly evaluable, it has the substantial disadvantage that interactions of the parameters are not captured. This severe drawback is illustrated in Figure 1.2 a and b. In this fictional example, time and temperature shall be improved. In an OFAT optimisation starting from a fixed temperature of 20 °C, two reasonable quadratic fits can be obtained with an acceptable yield of 60 %. Due to strong interactions of the two parameters, this is however far off the global optimum as it can be seen in the contour plot of the reaction space in Figure 1.2 c (black points).[78]

A second drawback is the high number of necessary experiments. As only one parameter is varied at a time, the respective data points can only be linked with this specific variable. This is why for each factor the same number of experiments has to be done which in turn leads to a high amount of experiments when considering a larger number of factors.

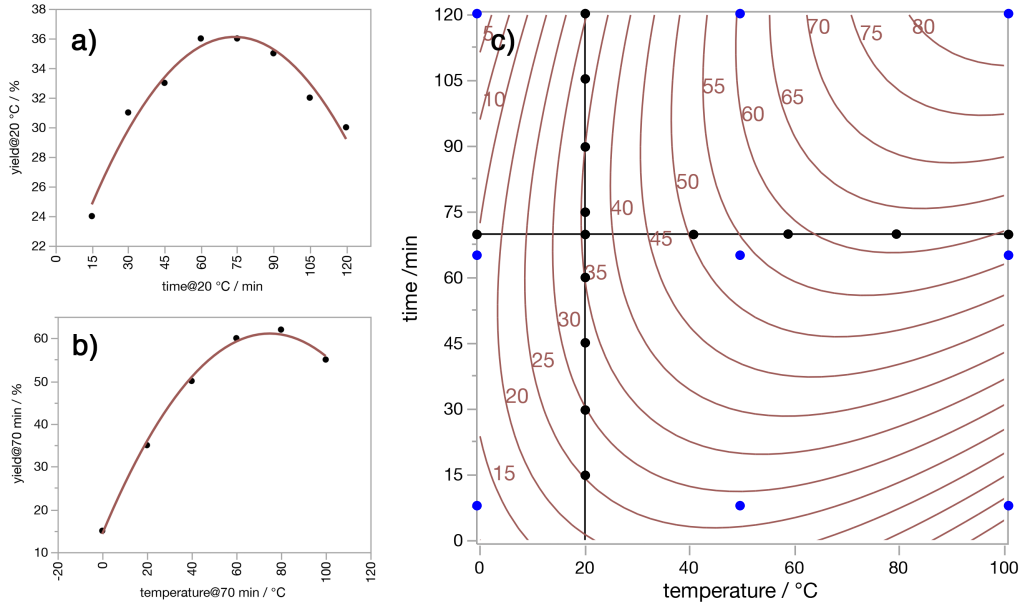

Figure 1.2 – a) OFAT optimisation of the time at 20 °C (optimum: 70 min); b) OFAT optimisation of the temperature at 70 min (optimum: 75 °C); c) contour plot obtained from DoE optimisation (black point: OFAT data points, blue points: DoE data points).

Design of experiments theory deals with those two problems. By distributing the data points not on single axes within the reaction space but rather spreading them as symmetrically and evenly as possible over the complete reaction space those two problems can be avoided. This becomes apparent if the example in Figure 1.2 is considered from an DoE point of view. The blue dots in the contour plots show the collected data points of a central composite design. Their distribution over the complete reaction space allows the fitting of a MLR model. This is not only capable of depicting the, in this case important, cross interaction but exhibits furthermore a higher statistical significance. This is due to the fact that for each term in the model all respective data points can be used which implies a higher significance with at the same time lower number of necessary experiments.[78]

In this rather basic example only numeric continuous factors were optimised.[ii] In order to be able to optimise other factors like discrete numeric, categorical, mixture or covariate variables and in order to address different optimisation purposes (screening, quantitative optimisation), a large number of specialised DoE designs have been developed. A short overview of the most important designs is shown in Table 1.1.[78,89] Historically, full factorial and central composite designs are the most important ones as they have been developed firstly and have the advantage that they can be evaluated manually. Due to the drawback of a limitation to numerical factors, today mainly optimal (with D-optimal being the most important) designs are used as they are highly flexible with respect to the type of input data and as they can be used for screening as well as for quantitative purposes. A disadvantage of optimal designs is their iterative generation which requires the use of computers mandatory.

In case of the application of DoE to a larger optimisation problem, most often multiple designs are used. In a first step, using a screening design (factorial, definitive or D-optimal), only the main effects are investigated in order to select from a large number of possible factors the important ones. Only now the remaining factors are investigated quantitatively using a more sophisticated design (central composite, D-optimal). This combined approach satisfies the demand for a low number of experiments with at the same time a maximal output of information. Being superior to OFAT optimisation in every aspect (apart from simplicity), DoE is been used vastly in the industrial environment. All important reaction types have been improved using DoE with often spectacular results.[90] Nevertheless, it is seldom used in academic organic method development. A possible reason for this may be the deterring mathematical background which entails the mandatory use of specialised software. Nonetheless, DoE is experiencing an upswing in recent years.[91–97] Surprisingly, in the field of optimisation demanding organo-electrochemistry, except one exemplary report only, DoE has not been applied yet.[98]

[ii] continuous factor: all values between the limits are experimentally accessible, discrete numerical factors: only specific values between the boarders are experimentally accessible, categorical factor: properties that can not be expressed in numbers, mixture factors: proportion between two or more variables, covariate factor: variables that can't be influenced

Table 1.1 – Selection of the most important DoE designs.

DoE design	**application**	**experiments (for N factors)**	**advantages**	**disadvantages**
factorial	screening	$\geq$ N+1	very efficient	only main effects & 2-factor interactions, only continuous factors
full factorial	screening	N^2	all interactions estimable	high number of experiments, only continuous factors
central composite	quantitative	$(N+1)^2$	all interactions estimable	high number of experiments, only continuous factors
factorial central composite	quantitative	$\geq$ 3N+4	efficient	only main effects & 2-factor interactions, only continuous factors
definitive	semi quant.	2N+1	quadratic terms sometimes estimable	minimum of six factors, categorical factors disfavoured
D-optimal	screening	$\geq$ N+1	all kinds of factors, individually configurable	only evaluable by computer
D-optimal	quantitative	$\geq$ 2N+1	all kinds of factors, individually configurable	only evaluable by computer

Chapter 2

Project Scope and Motivation

Due to the ever-increasing clear global resources finiteness, the awareness of the necessity of sustainable processes increases. In a chemical method development context, this shows up in the nearly exclusive goal in development of atom efficient and catalytic reactions. Nonetheless, as soon as changes of the oxidation state of the substrates are involved, stoichiometric amounts of oxidants/reductants have to be used, which diminishes any efficiency. Another hidden problem are the costs for optimisation. Within these processes, not just material goods but also manpower is often used in an excessive way.

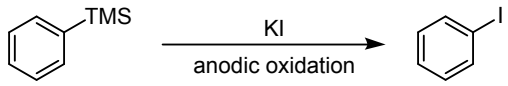

Scheme 2.1 – Targeted electrochemical Iododesilylation reaction for the synthesis of aryl iodides.

Within the scope of this dissertation those two efficiency problems should be tackled. Therefore, new electrochemical methods using the unique features of iodine chemistry should be developed. This idea was based on results of the authors master thesis, in which a new protocol for a chemical iododesilylation reaction for the synthesis of aryl iodides was developed. As this reaction required stoichiometrical amounts of an oxidant for the generation of the active iodonium ions, it was not atom efficient. Hence, an electrochemical mutation of the protocol was to be developed in order to eliminate this efficiency problem. In a second step, the obtained aryl iodides should be used as mediators in iodine(III)-mediated reactions. Those are currently under heavy investigation, as reactivities similar to the ones of transition metals can be obtained with at the

same time the benefits of main group catalysis. The drawback is once more the necessity of the stoichiometrical use of oxidants for the generation of the active iodine(III) species, which is why this type of reaction is a perfect candidate for the development of electrochemical protocols. The specific reaction that should be optimised was a lactonisation reaction yielding isochromanones, which has been reported in prior studies with the use of classical oxidants. The choice for this specific reaction was influenced by its complexity as two new bonds are formed, and drug-like compounds of pharmaceutical interest are obtained.

To tackle the problem of unnecessary use of manpower as well as chemicals due to inefficient optimisation, two statistical approaches should be tested on those reactions – design of experiments and multivariate linear regression analysis. Although both methods are well established statistical tools for classical reactions, their previously untested applicability to electrochemical reaction optimisation should be established.

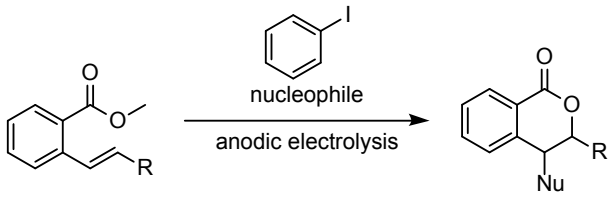

Scheme 2.2 – Targeted electrochemical iodine(III)-mediated reaction for the synthesis of isochromanones.

In a third cooperation project, the activation of the CBS catalyst by different Lewis acids should be investigated. Starting point of this investigation were studies of Dr. Alexander Nödling who used a deuterated CBS catalyst derivative as ^{2}H NMR probe for the prediction of the activity of different Lewis acids in a CBS catalysed Diels Alder reaction. In order to prove the predictive capabilities of this approach, he determined rate constants of a model Diels Alder reaction and correlated these with the measured NMR shifts. Doing this, unexplained outliers occurred which should be investigated using density functional theory. For one, reasons for the existence of the different outliers should be found using bonding analysis. Furthermore, a quantum mechanical probe for the prediction of the activation of the CBS catalyst by those different Lewis acids should be developed which should be able to predict the outliers correctly. Here again, the focus was on the efficient prediction of reactivities and the avoidance of experimental work in favour of computer based methods.

Chapter 3

Cumulative part

This dissertation consists of two publications, to which I contributed the majority and one publication (no. 1) to which I contributed half. In this chapter, these publications will be discussed in the following order:

1. A. R. Nödling, R. Möckel, R. Tonner, G. Hilt, *"*Lewis *Acids as Activators in CBS-Catalysed* Diels-Alder *Reactions: Distortion Induced* Lewis *Acidity Enhancement of* $SnCl_4$ *",Chem. Eur. J.* **2016**, 13171.

2. R. Möckel, J. Hille, E. Winterling, S. Weidemüller, T. M. Faber, G. Hilt, *"Electrochemical Synthesis of Aryl Iodides by Anodic Iododesilylation"*, *Angew. Chem.* **2018**, *130*, 450; *Angew. Chem. Int. Ed.* **2018**, *58*, 442.

3. R. Möckel, E. Babaoglu, G. Hilt, *"Iodine(III)-mediated Electrochemical Trifluoroethoxylactonisation - Rational Reaction Optimisation and Prediction of Mediator Activity"*, *Chem. Eur. J.* **2018**, *24*, 15781.

3.1 Lewis Acids as Activators in CBS-Catalysed Diels-Alder Reactions: Distortion Induced Lewis Acidity Enhancement of $SnCl_4$

A. R. Nödling, R. Möckel, R. Tonner, G. Hilt, *Chem. Eur. J.* **2016**, 13171.

Abstract: The effect of several Lewis acids on the CBS catalyst (named after Corey, Bakshi and Shibata) was investigated in this study. While ^{2}H NMR spectroscopic measurements served as gauge for the activation capability of the Lewis acids, *in situ* FT-IR spectroscopy was employed to assess the catalytic activity of the Lewis acid oxazaborolidine complexes. A correlation was found between the $\Delta\delta(^2\mathrm{H})$ values and rate constants k_{DA}, which indicates a direct translation of Lewis acidity into reactivity of the Lewis acid-CBS complexes. Unexpectedly, a significant deviation was found for $SnCl_4$ as Lewis acid. The $SnCl_4$-CBS adduct was much more reactive than the $\Delta\delta(^2\mathrm{H})$ values predicted and gave similar reaction rates as those observed for the prominent $AlBr_3$ CBS adduct. To rationalise these results, quantum mechanical calculations were performed. The frontier molecular orbital approach was chosen and a good correlation between the LUMO energies of the Lewis acid-CBS-naphthoquinone adducts and k_DA could be found. For the $SnCl_4$-CBS-naphthoquinone adduct an unusual distortion was observed leading to an enhanced Lewis acidity. Energy decomposition analysis with natural orbitals for chemical valence (EDA-NOCV) calculations revealed the relevant interactions and activation mode of $SnCl_4$ as Lewis acid in Diels-Alder reactions.

Contents: Chiral oxazaborolidines (with the *S*-proline derived catalyst named CBS-catalyst being the most well known) are an important class of Lewis acid catalysts for various applications. One example is their application in asymmetric 4+2 cycloaddition reactions where, however, they have to be activated by additional Brønsted super acids or strong Lewis acids.

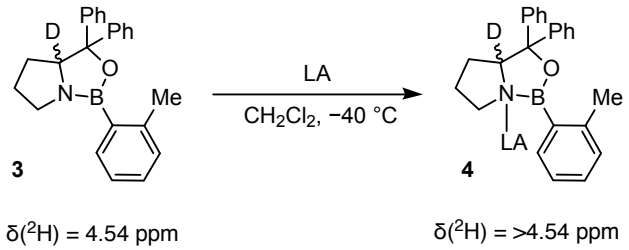

Scheme 3.1 – ^{2}H NMR spectroscopic quantified activation $\Delta\delta(^2\mathrm{H})$ of d-**4** upon Lewis acid coordination at −40 °C.

Due to investigations by Corey, the most common activation is accomplished by protonation using a Brønsted acid. In cases of Lewis acid activation nearly exclusively aluminium tribromide is used. We were interested whether other Lewis acids are able to activate the CBS catalyst as well and furthermore if their catalytic activity can be predicted using a NMR-probe. Rate constants k_{DA} of different Lewis acids were determined using *in situ* FT-IR spectroscopy in a model Diels-Alder reaction of isoprene with naphthoquinone. Subsequently, these kinetic data should be correlated with ^{2}H NMR shifts $\Delta\delta(^2\mathrm{H})$ obtained from the complexation of the respective Lewis acids with the deuterated CBS catalyst probe d-**3** (Scheme 3.1).

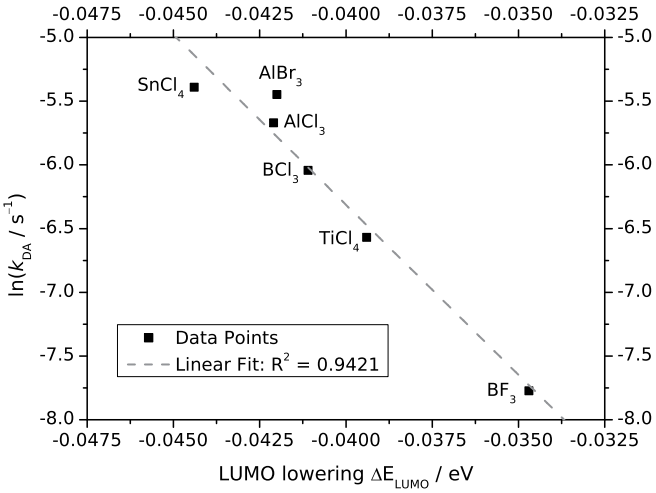

Figure 3.1 – Correlation of k_{DA} with ΔE_{LUMO}.

A mediocre correlation between the rate constants k_{DA} of the model reaction with the $\Delta\delta(^2H)$ shifts was obtained. However, there were two outliers – $SnCl_4$ and the group of indium LEWIS acids ($InCl_3$, $InBr_3$ and InI_3). In case of the indium acids low k_{DA} were observed, opposed to high activation according to their $\Delta\delta(^2H)$ values. In case of $SnCl_4$, although being only weakly acidic according to its $\Delta\delta(^2H)$ shift, it showed a catalytic activity as high as $AlBr_3$. To explain these phenomena, the system was analysed more thoroughly using density functional theory. First we applied frontier molecular orbital (FMO) theory using the LUMO lowering $\Delta E_{LUMO} = E_{LUMO_{(CBS-LA-napthoquinone)}} - E_{LUMO_{(napthoquinone)}}$ as theoretical probe. This approach was successful, and we could thereby predict the activity of all LEWIS acids including the one of $SnCl_4$ and the indium acids. This finding implied that the coordination of naphthoquinone to the LEWIS acid-CBS adduct is important which is why those structures were analysed in more detail.

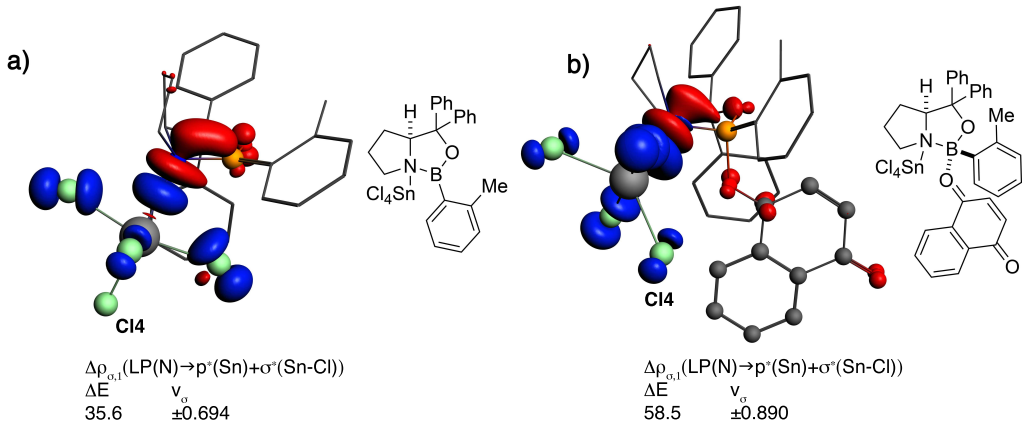

Figure 3.2 – Plots of the NOCVs with the highest eigenvalue ($\Delta\rho_{\sigma,1}$) representing the donor-acceptor interaction (LP(N_{CBS})→LP*(Sn) + σ^*(Sn-Cl)) at BP86/TZ2P+. a) The missing participation of the fourth chlorine atom of $SnCl_4$ in the CBS-$SnCl_4$ bond can be seen. b) The deformation-induced participation of this atom in the (naphthoquinone-CBS)-$SnCl_4$ bond is visible. Colour coding: red = decrease-, blue = increase of electron density.

The low catalytic activity of the indium LEWIS acids could thereby be attributed to a coordination of the respective LEWIS acid to the oxygen of naphthoquinone in the LA-CBS-naphthoquinone complex rather than to the CBS nitrogen atom. This prevents an efficient activation of the CBS catalyst. As the $\Delta\delta(^2H)$ were measured without naphthoquinone, this neatly explains the observed discrepancy.

In order to understand the unusual high activity of $SnCl_4$, EDA-NOCV calculations were con-

ducted. Doing this, the unexpected behaviour of $SnCl_4$ could be attributed to a conformational change of the fourth chlorine atom at the tin centre. In the $SnCl_4$-CBS complex it is arranged axially to the Sn-N bond (which is the expected conformation for $SnCl_4$). Upon coordination of naphthoquinone, this chlorine atom is moved to an equatorial position (leading to a square pyramidal conformation of $SnCl_4$). Due to this coordination change the fourth chlorine atom can now participate in LEWIS interaction leading to a much higher interaction energy ΔE_{int} overcompensating the simultaneously increased preparation energy ΔE_{prep}. This phenomenon could be attributed to an disproportional increase of the orbital interaction ΔE_{Orb} due to an increased LEWIS basicity of the CBS fragment upon coordination of the naphthoquinone fragment. The unambiguous participation of the fourth chlorine was proven by the analysis of the most important NOCVs. In Figure 3.2 their respective highest eigenvalue $\Delta\rho_{\sigma,1}$ are plotted for the complex with and without naphthoquinone. While in Figure 3.2-a no electron density shift to the fourth chlorine can be observed, in Figure 3.2-b, due to the conformational change, the fourth chlorine atom is participating in electron density withdrawal from the CBS nitrogen. Using NOCV theory (natural orbitals of the chemical valence) a further interaction of the fourth chlorine with the H-atom in position 5 could be found which further stabilises the equatorial conformation by raising ΔE_{Orb}.

Own contribution: The initial project was developed by Alexander Nödling and Gerhard Hilt. The idea for theoretical investigations and the selection of the appropriate methods was done by myself. All experimental works were done by Alexander Nödling. All computational investigations (structural optimisations, FMO and EDA-NOCV investigations) were done by myself. The manuscript was co-written by Alexander Nödling (experimental part) and myself (theoretical part) with support by Ralf Tonner and Gerhard Hilt.

3.2 Electrochemical Synthesis of Aryl Iodides by Anodic Iododesilylation

R. Möckel, J. Hille, E. Winterling, S. Weidemüller, T. M. Faber, G. Hilt, *Angew. Chem.* **2018**, *130*, 450; *Angew. Chem. Int. Ed.* **2018**, *58*, 442.

Abstract: An electrochemical access to iodinated aromatic compounds starting from trimethylsilyl-substituted arenes is presented. By design of experiments, highly efficient and mild conditions were identified for a wide range of substrates. A functional group stability test and the synthesis of an important 3-iodobenzylguanidine radiotracer illustrate the scope of this process.

Contents: Aryl iodides have multiple applications in chemistry and therefore a variety of approaches for their synthesis have been developed. Most often, their synthesis is accomplished by electrophilic aromatic substitution. Therefore, either pre-generated electrophilic iodination reagents or stoichiometric amounts of oxidants have to be used. To circumvent this atom inefficient approach electrochemistry is an appealing solution. Seminal work has been done by Yoshida who reported direct aromatic iodination reactions using electrochemically generated iodonium species. The drawback of this method is the lack of regioselectivity.

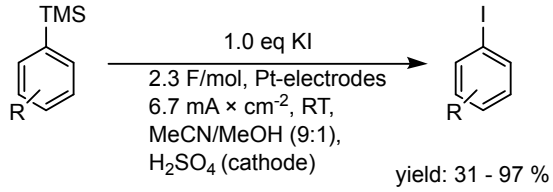

Scheme 3.2 – Design of Experiments optimised reaction conditions for the electrochemical iododesilylation reaction.

In this work we combined this electrochemical with a leaving group approach in order to gain control over regioselectivity. We chose the trimethylsilyl-group as its potential as directing group could previously be demonstrated by the author in a reaction using stoichiometric amounts of oxidants. [48]

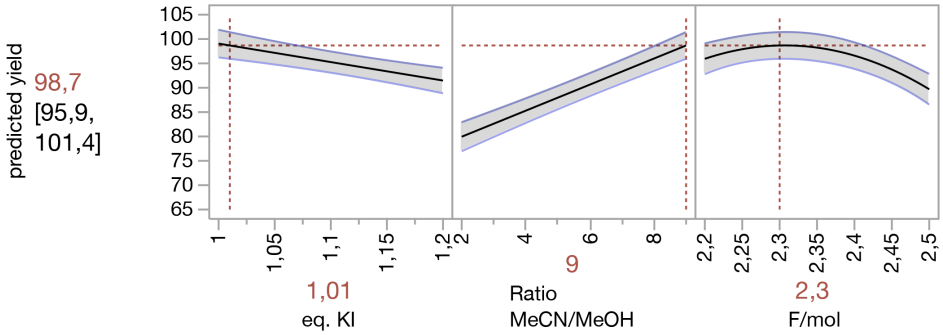

Figure 3.3 – Analysis plot of the model, obtained by DoE optimisation. Optimal values are given in red.

We first optimised the reaction in a classic OFAT way using trimethylsilyl benzene as screening substrate. During this optimisation, methanol as co-solvent was identified to be crucial for good yields. Unfortunately, low yields were observed for substrates bearing a methyl group due to a benzylic methoxylation side reaction. In order to cover the reaction space in a better way, a DoE approach was applied. We used a central composite design covering the methanol concentration, the potassium iodide loading and the applied charge. Using the conditions predicted by the DoE model (Figure 3.3), we were able to subject a range of substrates to the reaction with mainly excellent yields (Scheme 3.2). To check for further functional group tolerance, a compatibility test was conducted. This method is based on the addition of additives containing a certain functional group. To test the reaction compatibility, the yield of the desired product and the amount of additive recovered after the reaction are determined, which gives an indication for the stability of the respective additional functional group under the applied reaction conditions. The test showed oxidative labile groups (e.g. indole and other heterocycles) and functional groups with an intrinsic reactivity towards iodonium ions (e.g. alkenes, alkynes) not to be tolerant, whereas many other functional groups are stable towards the reaction conditions (e.g. esters, nitriles, halides, phosphonium salts). To further demonstrate the applicability of the new reaction, we synthesised the Boc-protected radiotracer *m*-iodobenzylguanidine **5** in a very good yield of 88 % (Scheme 3.3).

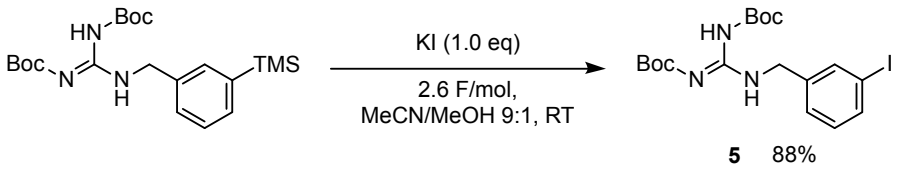

Scheme 3.3 – Synthesis of Boc-protected radiotracer *m*-iodobenzylguanidine **5**.

Own contribution: The initial project idea was developed by Gerhard Hilt. The transmission to electrochemical conditions including the DoE approach was developed by myself. The classical optimisation reactions were done by Tabea Faber, Stephan Weidemüller and Erik Winterling under my supervision. Elaboration, execution and evaluation of the DoE optimisation was done by myself. Most of the reported substrates were synthesised and subjected to the reaction by Jessica Hille under my supervision, a minor number was done by myself. The compatibility test as well as the radiotracer synthesis were completely done by myself. Analytical investigations (^{1}H and ^{13}C NMR, FT-IR, GC/MS, GC/FID) were done by myself or in some cases under my supervision. High resolution mass spectrometric measurements were performed by the Mass Spectrometry core facility. The manuscript was written by myself with support from Gerhard Hilt.

3.3 Iodine(III)-mediated Electrochemical Trifluoroethoxylactonisation - Rational Reaction Optimisation and Prediction of Mediator Activity

R. Möckel, E. Babaoglu, G. Hilt, *Chem. Eur. J.*, **2018**, *24*, 15781.

Abstract: A new electrochemical iodine(III)-mediated cyclisation reaction for the synthesis of 4-(2,2,2-trifluoroethoxy)isochroman-1-ones is presented. Based on this reaction we used design of experiments and multivariate linear regression analysis to demonstrate their first application in an electrochemical reaction. The broad applicability of these reaction conditions could be shown by a range of substrates and an extensive compatibility test.

Contents: In this report, we presented the literature unknown combination of design of experiments with multivariate linear regression analysis in an electrochemical reaction. Thereby, the reaction conditions as well as the applied mediator should be optimised in an efficient way proving the concept for an electrochemical reaction.

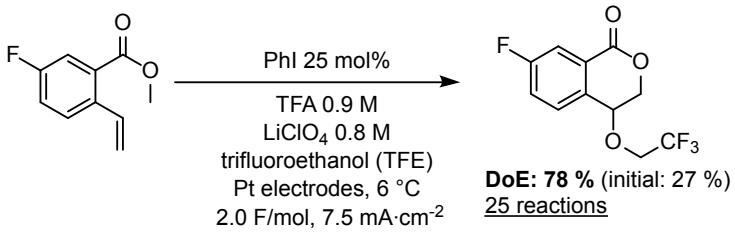

Scheme 3.4 – DoE optimised reaction conditions for the electrochemical synthesis of 4-(2,2,2-trifluoroethoxy)isochroman-1-ones.

The approach was demonstrated for a new iodine(III)-mediated trifluoroethoxylactonisation reaction yielding 4-(2,2,2-trifluoroethoxy)isochroman-1-ones (see Scheme 3.4). An iodine(III)-mediated reaction was chosen because of the unique properties of hypovalent iodine compounds (reactivity comparable to transition metals) and because of the fact that only a very limited number of examples for their mediative in-cell use in electrochemical reactions are known. In a first step, the reaction was optimised using DoE. We firstly applied a D-optimal screening design to be able to investigate a multitude of factors (electrolyte (type + concentration), acid (type + concentration), mediator loading, applied charge, temperature, electrode, current density). In a

second step we optimised the most influential factors quantitatively. Application of the obtained model lead to an increase in yield from 28 to 78 %.

In a second step, multivariate linear regression analysis was applied in order to obtain a model predicting the yield for different mediators from theoretical values. Therefore, multiple descriptors (Enthalpies, HOMO/LUMO energies, IR frequencies, steric parameters and natural charges) were calculated for a large range of commercially available aryl iodides using density functional theory (DFT).[i] From this set we chose 18 mediators for the training and 6 for the validation set using a D-optimal design. A multivariate model could be obtained (Figure 3.5) showing good RMSE (root mean square error (average deviation of the predicted from the measured values)) of 5.6 % in the validation set. In order to further demonstrate the predictive power of the model, the yields for a third test set including chiral mediators were predicted with a very good RMSE of just 4.0 %.

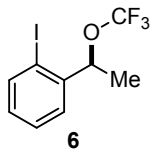

6

Figure 3.4 – Mediator **6**, obtained from the virtual screening.

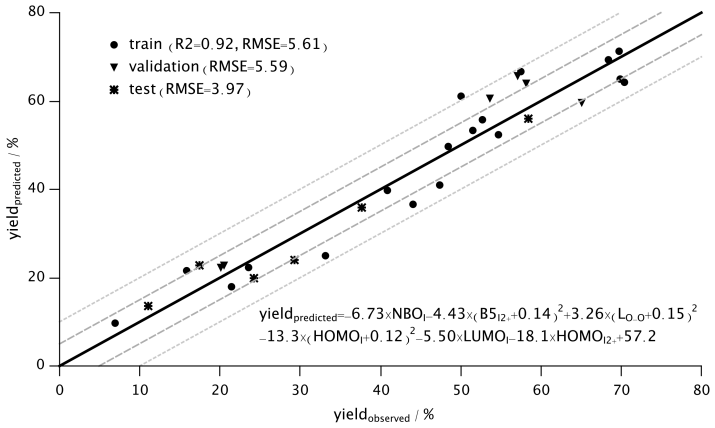

Figure 3.5 – Multivariate linear regression model for the prediction of the yield for different iodine(III) mediators in the electrochemical trifluoroethoxylactonisation.

Literature unknown mediators were included in the test set which were derived using the model and which showed in case for mediator **6** (see Figure 3.4) good yields of up to 56% (compared to the throughout low yields of all tested literature known mediators). This impressively illustrates the benefits but as well the capabilities of this virtual screening approach for the search of new structural motifs of chiral mediators. Furthermore, using cyclic voltammetry (CV), the parameters of the model ($HOMO_I$, $HOMO_{I2+}$, $LUMO_I$, NBO_I, L_{O-O} and $B5_{I2+}$) were attrib-

[i]For each mediator three distinctive structures were calculated. The aryl iodide, its di-cation and the bis trifluoroacetate coordinated iodine(III) species.

uted to two different factors that determine the activity of the mediator; for one the stability of the mediator with respect to degradation processes, and second the reactivity towards the substrate.

In a last step, a range of substrates was subjected to the optimised reaction conditions using iodobenzene as mediator to show the broad applicability. Yields between 32 and 60 % could be obtained (see Figure 3.6). Electron rich substrates gave lower yields (in case of a methoxy substituted substrate no product was obtained) whereas various substitution patterns at the aromatic core did not influence the reaction yield. For substrates bearing a substituent at the vinylic position, diastereomer ratios between 64: 36 and 90:10 (*syn:anti*) could be obtained with at the same time slightly lower yields.

To further demonstrate functional group tolerance, an extensive compatibility test was carried out. Oxidative labile or groups which show reactivity towards iodine(III) compounds (e.g. alkenes, alkynes) are not compatible, whereas many other functional groups including e.g. electron deficient heterocycles, amides, nitriles or aldehydes are stable. Using MLR, the additive yields could furthermore be correlated to two calculated descriptors – there HOMO energy and a point charge showing that mainly oxidative stability determines the additive yields. Nonetheless, the correlation revealed two groups of outliers – the discussed additives which show intrinsic reactivity towards iodine(III) and a group of basic additives which probably are protonated and thus more stable under the reaction conditions than predicted by the model.

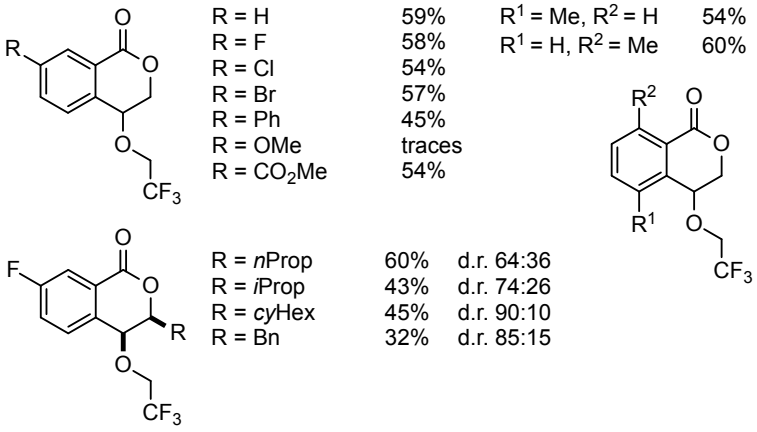

Figure 3.6 – Products obtained from the electrochemical iodobenzene mediated lactonisation reaction.

Own contribution: The project was mainly developed by myself with help of Gerhard Hilt and Emre Babaoglu. Design, execution and evaluation of the DoE optimisation was done by myself. All necessary reactions were performed by myself. The multivariate linear regression analysis was planned, carried out and the results were statistically evaluated in all parts by myself. All necessary DFT calculations for the generation of the descriptor variables set were done by myself. Substrates were synthesised and subjected to the reaction by me.
The compatibility test was executed mainly by myself with minor contributions of Emre Babaoglu. The statistical evaluation of the compatibility test results was done by Emre Babaoglu under my supervision. Necessary analytical experiments (^{1}H and ^{13}C NMR, FT-IR, CV, GC/MS, GC/FID) were performed by myself. Execution of the single-crystal X-ray diffraction experiments were done by the X-ray core facility. Solving and refinement of the obtained data was done by myself.
The synthesis of the chiral mediators and as well as their application in the reaction was done by Emre Babaoglu. The manuscript was written by myself (co-corresponding author) with support of Gerhard Hilt and Emre Babaoglu.

Chapter 4

Summary

Within this dissertation three different projects are discussed. The underlying theme of all projects is the application of computational and/or statistical methods in order to decrease the experimental effort and to increase the information output at the same time.

DFT investigations in Lewis acid activation of the CBS catalyst

The first project was a cooperation with Dr. Alexander Nödling on the quantification of Lewis acid activation of the CBS catalyst in a CBS-catalysed Diels-Alder reaction of naphthoquinone with isoprene. This was achieved by determination of $\Delta\delta(^2\mathrm{H})$ shifts of different Lewis acids using a deuterated CBS catalyst as ^{2}H NMR probe and subsequent correlation with rate constants k_{DA} measured using *in situ* FT-IR spectroscopy. Thereby $SnCl_4$ and the group of indium Lewis acids ($InCl_3$, $InBr_3$ and InI_3) were identified as outlier. Whereas the indium acids showed k_{DA} lower than predicted by their $\Delta\delta(^2\mathrm{H})$, $SnCl_4$ activated the CBS catalyst much better than predicted by its $\Delta\delta(^2\mathrm{H})$. In order to explain those outliers, quantum mechanical calculations were done. On the one hand, a quantum mechanical probe should be established by which the outliers can be predicted correctly other than by NMR. On the other hand, an explanation for the presence of the outliers should be found. Using a frontier molecular orbital approach $\Delta E_{LUMO} = E_{LUMO_{(CBS-LA-naphthoquinone)}} - E_{LUMO_{(naphthoquinone)}}$ could be established as a probe which predicts the reactivities of all Lewis acids, including the one of $SnCl_4$ and the indium acids, reliably. The low activation of the indium acids could be attributed to a coordination of the indium Lewis acid to naphthoquinone rather than to the CBS nitrogen in the LA-CBS-naphthoquinone complex which leads to a low activation of the CBS catalyst.

The unexpected high catalytic activity of the CBS catalysts with $SnCl_4$ could be rationalised using energy decomposition analysis (EDA) in combination with natural orbitals of the chemical valence (NOCV). It was attributed to an unexpected coordination change of the forth chlorine atom from an axial position in the LA-CBS complex to an equatorial position in the LA-CBS-naphthoquinone complex. This change allows the fourth chlorine to participate in LEWIS interaction rendering $SnCl_4$ a strong LEWIS acid which is an alternative to the commonly used AlB_3.

Electrochemical synthesis of aryl iodides

A new electrochemical synthesis of aryl iodides was established in the second project. This was achieved by electrochemical generation of iodonium ions from potassium iodide. By introduction of a trimethylsilyl group as leaving group in the aryl moieties, the reaction could be accomplished in a regioselective way. A classical OFAT optimisation of the system yielded reaction conditions, which did not tolerate benzylic positions. However, a second DoE optimisation approach revealed reaction conditions which tolerate benzylic positions and gave mostly excellent yields with often no need for chromatographic purification. To check on electronic as well as steric effects, electron deficient/rich and sterically demanding substrates were subjected to the reaction conditions but no significant influence could be detected.
To prove functional group tolerance a compatibility test was conducted which showed good compatibility to a broad range of functional groups like nitriles, halogens, or phosphonium salts. To prove the applicability of this new reaction further, the Boc-protected radiotracer *m*-iodobenzylguanidine was synthesised with a very good yield of 88 % in a very short reaction time, to prove the reactions applicability for synthesis of iodine isotopes labelled pharmaceuticals.

Iodine(III)-mediated electrochemical synthesis of Isochromanones

In the third project, a new iodine(III)-mediated electrochemical synthesis of 4-(2,2,2-trifluoroethoxy) isochromanones was developed. This reaction is the first example of an iodine(III)-mediated electrochemical reaction in which two new bonds are formed. A range of statistical methods was applied in order to carry out the whole optimisation process as efficiently as possible. Optimisation of the reaction conditions was done using DoE. Thereby the yield could be improved from 27 to 78 %. Subsequently, the applied mediator was optimised using multivariate linear regression analysis. The necessary descriptor set was obtained using density functional theory and the respective data points were selected by a D-optimal design. A

model with a very good RMSE and R^2 with respect to the training as well as to the validation set could be obtained consisting of five factors ($HOMO_I$, $HOMO_{I2+}$, $LUMO_I$, NBO_I, L_{O-O} and $B5_{I2+}$). Using cyclic voltammetry, four of the factors could be linked to two parameters that determine the furnishing yield of the mediator – stability to oxidative decomposition of the mediator and reactivity towards the substrate. To further prove the models capabilities, a virtual screening on chiral mediators was executed. Therefore, a range of chiral non literature known mediators were calculated and subjected to the model. By this means, a new chiral mediator could be found which delivered a good experimental yield of 56 % which is nearly twice the yield obtained from the top-scorer of literature known chiral mediators.

Furthermore, a range of substrates was subjected to the reaction conditions in order to check for electronic and steric effects. Acceptable yields up to 60 % could be obtained for 13 different substrates with, in case of substrates with a vinylic substituent, diastereomeric ratios of up to 90:10 (*syn:anti*). Using a compatibility test, functional group tolerance could be proved for a large range of groups like electron deficient heterocycles, amides, nitriles or aldehydes. Using MLR once more, it could be shown that predominantly oxidative stability of the functional group determines its compatibility to the reaction.

Chapter 5

Zusammenfassung

Im Rahmen dieser Dissertation werden drei Projekte diskutiert. Gemeinsames Merkmal aller drei Projekte ist die Anwendung von theoretischen und/oder statistischen Methoden um den experimentellen Aufwand zu minimieren und gleichzeitig den Output an Informationen zu erhöhen.

DFT Untersuchungen zur Lewis–Säuren vermittelten Aktivierung des CBS Katalysators

Beim ersten Projekt handelt es sich um eine Kooperation mit Dr. Alexander Nödling zur Quantifizierung der Aktivierung des CBS Katalysators mittels LEWIS-Säuren in einer CBS-katalysierten DIELS–ALDER Reaktion von Naphthochinon mit Isopren. Dazu wurden die $\Delta\delta(^2\mathrm{H})$ Verschiebungen verschiedener LEWIS-Säuren unter Verwendung eines deuterierten CBS Derivats als ^{2}H-Sonde bestimmt und anschließend mit Geschwindigkeitskonstanten k_{DA}, die mittels *in situ* FT-IR Spektroskopie bestimmt wurden, korreliert. Hierbei konnten zwei Ausreißer identifiziert werden – $SnCl_4$ und die Gruppe der Indium LEWIS-Säuren ($InCl_3$, $InBr_3$ and InI_3). Während die Bor basierten Säuren kleinere Geschwindigkeitskonstanten k_{DA} aufwiesen als mittels der entsprechenden $\Delta\delta(^2\mathrm{H})$ Werte vorhergesagt wurde, zeigte $SnCl_4$ eine deutlich höhere Aktivität als vorhergesagt. Um diese Ausreißer zu erklären, wurden quantenmechanische Rechnungen durchgeführt. Zum Einen sollte dadurch eine quantenmechanische Sonde gefunden werden mittels derer eine, im Gegensatz zur ^{2}H-NMR Sonde, zuverlässige Vorhersage der Ausreißer möglich sein sollte. Weiterhin sollte dadurch ein Grund für das Auftreten der Ausreißer gefunden werden.
Unter Verwendung der Grenzorbitaltheorie konnte $\Delta E_{LUMO} = E_{LUMO_{(CBS-LA-Naphthochinon)}} - E_{LUMO_{(Naphthochinon)}}$ als zuverlässiger Prädiktor gefunden werden mittels dem die Aktivität

aller LEWIS-Säuren, einschließlich derer von $SnCl_4$ und der der Indium Säuren, zuverlässig vorhergesagt werden konnte. Die niedrige Aktivierung der Indium LEWIS-Säuren konnte auf eine Koordination der jeweiligen LEWIS-Säure an das Sauerstoffatom des Naphthochinons anstelle des Stickstoffatoms des CBS Katalysators erklärt werden, was zu einer nur schwachen Aktivierung des CBS Katalysators führt.
Die unerwartet hohe Aktivierung des CBS Katalysators durch $SnCl_4$ konnte unter zu Hilfenahme von Energie Dekompositions Analyse (EDA) in Kombination mit Natürlichen Orbitalen für die chemische Valenz Theorie (NOCV) erklärt werden. Sie wurde auf eine Konformationsänderung des vierten Chlors am $SnCl_4$ von einer axialen zu einer äquatorialen Anordnung nach Koordination von Naphthochinon zurückgeführt. Dieser Wechsel erlaubt dem vierten Chloratom an der LEWIS-Aktivierung teilzuhaben, was in diesem Fall $SnCl_4$ zu einer ähnlich starken Säure wie $AlBr_3$ macht.

Elektrochemische Synthese von Aryliodiden

Im Rahmen des zweiten Projekts wurde eine neue elektrochemische Synthese von Aryliodiden entwickelt. Dies wurde durch die elektrochemische Erzeugung von Iodoniumionen aus Kaliumiodid erreicht. Durch Verwendung einer Trimethylsilyl Gruppe am Aromaten konnte die Reaktion regioselektiv durchgeführt werden. Eine klassische ein-Faktor Optimierung der Reaktion ergab Bedingungen, die benzylische Funktionalitäten nicht tolerieren. Durch Statistische Versuchsplanung konnten jedoch Bedingungen gefunden werden, die diese Funktionalität zulassen und zudem größtenteils hervorragende Ausbeuten ergeben wobei auf eine chromtographische Reinigung häufig verzichtet werden konnte. Um auf sterische als auch elektronische Effekte zu prüfen, wurden verschiedenst substituierte Substrate (elektonenarm als auch Elektronen reich, sterisch anspruchsvoll) unter den Reaktionsbedingungen getestet, aber keinerlei Einfluss konnte beobachtet werden. Um die Toleranz gegenüber funktionellen Gruppen zu überprüfen, wurde ein Kompatibilitätstest durchgeführt. Dieser zeigte eine große Bandbreite an kompatiblen funktionellen Gruppen wie Nitrilen, Halogenen oder Phosphoniumsalzen. Um eine Anwendung der Reaktion zu zeigen, wurde weiterhin der Boc-geschützte Radio-Indikator *m*-Iodobenzylguanidinin in einer guten Ausbeute von 88 % und einer kurzen Reaktionszeit dargestellt. Dies zeigt eine mögliche Anwendung der Reaktion zur Synthese Isotopen markierter Pharmazeutika.

Iod(III) vermittelte elektrochemische Synthese von Isochromanonen

Im dritten Projekt wurde eine neuartige Iod(III) vermittelte elektrochemische Synthese von 4-(2,2,2-Trifluroethoxy)isochromanonen entwickelt. Bei dieser Reaktion handelt es sich um das erste Beispiel einer Iod(III) vermittelten elektrochemischen Reaktion bei der zwei neue Bindungen geknüpft werden.

Eine Reihe statistischer Methoden wurde verwendet um den gesamten Optimierungsprozess so effizient wie möglich zu gestalten. Die Optimierung der Reaktionsbedingungen wurde mittels Statistischer Versuchsplanung durchgeführt. Dadurch konnte eine Steigerung der Ausbeute von 27 auf 78 % erreicht werden. Anschließend wurde der Mediator mittels multivariater linearer Regressionsanalyse optimiert. Das hierfür notwendige Prädiktor Set wurde mittels Dichte Funktional Theorie berechnet wobei die einzelnen Einträge mittels D-optimalem Versuchsplan ausgewählt wurden. Es konnte ein Model mit einem sehr guten RMSE und R^2 in Bezug auf das Trainings- als auch das Validierungsset erhalten werden. Das Model besteht aus fünft Prädiktoren ($HOMO_I$, $HOMO_{I2+}$, $LUMO_I$, NBO_I, L_{O-O} und $B5_{I2+}$). Mittels Cyclovoltammetrie konnten die verschiedenen Prädiktoren zwei verschiedenen Einflüssen auf die Ausbeute zugeordnet werden – Stabilität gegenüber oxidativem Abbau und Aktivität gegenüber dem Substrat. Um die Möglichkeiten des Models darüber hinaus zu zeigen, wurde ein virtuelles Screening für neue chirale Mediatoren durchgeführt. Dazu wurden eine Reihe neuartiger, Literatur unbekannter, chiraler Mediatoren berechnet und deren Ausbeute mittels des Models bestimmt. Es konnte ein neuartiger chiraler Mediator gefunden werden, der eine experimentelle Ausbeute von 56 % lieferte, was nahezu doppelt so viel ist wie bei dem besten Literatur-bekannten chiralen Mediator unter den optimierten Reaktionsbedingungen.

Weiterhin wurde eine Reihe von Substraten unter den Reaktionsbedingungen getestet um sterische und elektronische Einflüsse auf die Reaktion zu erfassen. Hierbei konnten akzeptable Ausbeuten von bis zu 60 % für 13 Substrate erhalten werden. Für Substrate mit einem vinylischen Substituenten konnten Diastereoselektivitäten von bis zu 90:10 (*syn:anti*) erhalten werden. Mit Hilfe eines Kompatibilitätstests konnte weiterhin die Kompatibilität zu einer Vielzahl funktioneller Gruppen gezeigt werden, unter anderem Elektronen-arme Heterocyclen, Amide, Nitrile oder Aldehyde. Mittels MLR Analyse konnte weiterhin gezeigt werden, dass die Kompatibilität der Additive vor allem durch ihre oxidative Stabilität bestimmt wird.

Chapter 6

Bibliography

[1] A. Corma, H. García, *Chem. Rev.* **2003**, *103*, 4307–4366.

[2] J. M. Bayne, D. W. Stephan, *Chem. Soc. Rev.* **2016**, *45*, 765–774.

[3] G. N. Lewis, *Valence and the Structure of Atoms and Molecules*, The Chemical Catalog Co., Inc., New York, **1923**.

[4] A. D. McNaught, A. Wilkinson, *IUPAC. Compendium of Chemical Terminology*, Blackwell Scientific Publications, Oxford, 2nd ed., **1997**.

[5] E. I. Davydova, A. Y. Timoshkin, T. N. Sevastianova, A. V. Suvorov, G. Frenking, *J. Mol. Struc.-Theochem.* **2006**, *767*, 103–111.

[6] G. Hilt, F. Pünner, J. Möbus, V. Naseri, M. A. Bohn, *Eur. J. Org. Chem.* **2011**, *2011*, 5962–5966.

[7] M. A. Beckett, G. C. Strickland, J. R. Holland, K. Sukumar Varma, *Polym. Commun.* **1996**, *37*, 4629–4631.

[8] R. F. Childs, D. L. Mulholland, A. Nixon, *Can. J. Chem.* **1982**, *60*, 809–812.

[9] M. A. Beckett, D. S. Brassington, S. J. Coles, M. B. Hursthouse, *Inorg. Chem. Commun.* **2000**, *3*, 530–533.

[10] R. S. Mulliken, *J. Am. Chem. Soc.* **1952**, *74*, 811–824.

[11] V. Gutmann, *Coordin. Chem. Rev.* **1974**, *12*, 263–293.

[12] D. P. N. Satchell, R. S. Satchell, *Chem. Rev.* **1969**, *69*, 251–278.

[13] D. R. McMillin, R. S. Drago, *Inorg. Chem.* **1972**, *11*, 872–879.

[14] R. S. Drago, B. B. Wayland, *J. Am. Chem. Soc.* **1965**, *87*, 3571–3577.

[15] R. G. Pearson, *J. Am. Chem. Soc.* **1963**, *85*, 3533–3539.

[16] G. Klopman, *J. Am. Chem. Soc.* **1968**, *90*, 223–234.

[17] R. G. Pearson, *Acc. Chem. Res.* **1993**, *26*, 250–255.

[18] R. G. Parr, R. G. Pearson, *J. Am. Chem. Soc.* **1983**, *105*, 7512–7516.

[19] L. Salem, *J. Am. Chem. Soc.* **1968**, *90*, 543–552.

[20] A. R. Jupp, T. C. Johnstone, D. W. Stephan, *Dalton Trans.* **2018**, *47*, 7029–7035.

[21] P. K. Chattaraj, D. R. Roy, *Chem. Rev.* **2007**, *107*, PR46–PR74.

[22] J. A. Plumley, J. D. Evanseck, *J. Phys. Chem. A* **2009**, *113*, 5985–5992.

[23] H. Böhrer, N. Trapp, D. Himmel, M. Schleep, I. Krossing, *Dalton Trans.* **2015**, *44*, 7489–7499.

[24] T. E. Mallouk, G. L. Rosenthal, G. Mueller, R. Brusasco, N. Bartlett, *Inorg. Chem.* **1984**, *23*, 3167–3173.

[25] P. Laszlo, M. Teston, *J. Am. Chem. Soc.* **1990**, *112*, 8750–8754.

[26] P. Laszlo, M. Teston-Henry, *Tet. Lett.* **1991**, *32*, 3837–3838.

[27] T. Ziegler, A. Rauk, *Theoret. Chim. Acta* **1977**, *46*, 1–10.

[28] K. Kitaura, K. Morokuma, *Int. J. Quantum Chem.* **1976**, *X*, 325–340.

[29] L. Zhao, M. von Hopffgarten, D. M. Andrada, G. Frenking, *WIREs Comput. Mol. Sci.* **2017**, *8*, e1345.

[30] I. Purushothaman, S. De, P. Parameswaran, *RSC Adv.* **2014**, *4*, 60421–60428.

[31] M. P. Mitoraj, A. Michalak, T. Ziegler, *J. Chem. Theory Comput.* **2009**, *5*, 962–975.

[32] M. Mitoraj, A. Michalak, *J. Mol. Model.* **2008**, *14*, 681–687.

[33] A. Michalak, M. Mitoraj, T. Ziegler, *J. Phys. Chem. A* **2008**, *112*, 1933–1939.

[34] M. P. Mitoraj, A. Michalak, T. Ziegler, *Organometallics* **2009**, *28*, 3727–3733.

[35] P. Anastas, N. Eghbali, *Chem. Soc. Rev.* **2010**, *39*, 301–312.

[36] E. J. Horn, B. R. Rosen, P. S. Baran, *ACS Cent. Sci.* **2016**, *2*, 302–308.

[37] A. Wiebe, T. Gieshoff, S. Möhle, E. Rodrigo, M. Zirbes, S. R. Waldvogel, *Angew. Chem. Int. Ed.* **2018**, *57*, 5594–5619.

[38] R. Francke, R. D. Little, *Chem. Soc. Rev.* **2014**, *43*, 2492–31.

[39] J.-M. Savéant, *Chem. Rev.* **2008**, *108*, 2348–2378.

[40] S. R. Waldvogel, S. Möhle, M. Zirbes, E. Rodrigo, T. Gieshoff, A. Wiebe, *Angew. Chem. Int. Ed.* **2018**, *57*, 6018–6041.

[41] M. Yan, Y. Kawamata, P. S. Baran, *Angew. Chem. Int. Ed.* **2018**, *57*, 4149–4155.

[42] S. R. Waldvogel, S. Lips, M. Selt, B. Riehl, C. J. Kampf, *Chem. Rev.* **2018**, 10.1021–acs.chemrev.8b00233.

[43] J.-i. Yoshida, A. Shimizu, R. Hayashi, *Chem. Rev.* **2017**, *118*, 4702–4730.

[44] M. Yan, Y. Kawamata, P. S. Baran, *Chem. Rev.* **2017**, *117*, 13230–13319.

[45] M. D. Kärkäs, *Chem. Soc. Rev.* **2018**, *58*, 142–80.

[46] C. Gütz, B. Klöckner, S. R. Waldvogel, *Org. Process Res. Dev.* **2016**, *20*, 26–32.

[47] L. Skulski, *Molecules* **2000**, *5*, 1331–1371.

[48] R. Möckel, G. Hilt, *Org. Lett.* **2015**, *17*, 1644–1647.

[49] E. A. Merritt, B. Olofsson, *Angew. Chem. Int. Ed.* **2009**, *48*, 9052–9070.

[50] T. Dohi, Y. Kita, *Iodine Chemistry and Applications* , Wiley, Hoboken, **2014**.

[51] A. Yoshimura, V. V. Zhdankin, *Chem. Rev.* **2016**, *116*, 3328–3435.

[52] B. Hu, W. H. Miller, K. D. Neumann, E. J. Linstad, S. G. DiMagno, *Chem. Eur. J.* **2015**, 6394–6398.

[53] S. R. Waldvogel, K. M. Wehming, *Sci. Synth.* **2007**, 235.

[54] K. Kataoka, Y. Hagiwara, K. Midorikawa, S. Suga, J.-i. Yoshida, *Org. Process Res. Dev.* **2008**, *12*, 1130–1136.

[55] L. L. Miller, E. P. Kujawa, C. B. Campbell, *J. Am. Chem. Soc.* **1970**, *92*, 2821–2825.

[56] M. Saito, Y. Kobayashi, S. Tsuzuki, Y. Takemoto, *Angew. Chem.* **2017**, *129*, 7761–7765.

[57] A. Parra, S. Reboredo, *Chem. Eur. J.* **2013**, *19*, 17244–17260.

[58] D. R. Stuart, *Chem. Eur. J.* **2017**, 1–15.

[59] A. Sreenithya, C. Patel, C. M. Hadad, R. B. Sunoj, *ACS Catal.* **2017**, *7*, 4189–4196.

[60] T. Fuchigami, T. Fujita, *J. Org. Chem.* **1994**, *59*, 7190–7192.

[61] A. Sreenithya, K. Surya, R. B. Sunoj, *WIREs Comput. Mol. Sci.* **2017**, *7*, e1299.

[62] A. Stirling, *Chem. Eur. J.* **2018**, *24*, 1709–1713.

[63] A. Labattut, P.-L. Tremblay, O. Moutounet, C. Y. Legault, *J. Org. Chem.* **2017**, *82*, 11891–11896.

[64] F. Heinen, E. Engelage, A. Dreger, R. Weiss, S. M. Huber, *Angew. Chem. Int. Ed.* **2018**, *57*, 3830–3833.

[65] H. Pinto de Magalhães, A. Togni, H. P. Lüthi, *J. Org. Chem.* **2017**, *82*, 11799–11805.

[66] Y. Li, D. P. Hari, M. V. Vita, J. Waser, *Angew. Chem. Int. Ed.* **2016**, *55*, 4436–4454.

[67] T. Sawamura, S. Kuribayashi, S. Inagi, T. Fuchigami, *Org. Lett.* **2010**, *12*, 644–646.

[68] T. Fujita, T. Fuchigami, *Tet. Lett.* **1996**, *37*, 4725–4728.

[69] T. Sawamura, S. Kuribayashi, S. Inagi, T. Fuchigami, *Adv. Synth. Catal.* **2010**, *352*, 2757–2760.

[70] S. Hara, T. Hatakeyama, S. Q. Chen, K. Ishi-i, M. Yoshida, M. Sawaguchi, T. Fukuhara, N. Yoneda, *J. Fluorine Chem.* **1998**, *87*, 189–192.

[71] M. Elsherbini, T. Wirth, *Chem. Eur. J.* **2018**, 10.1002–chem.201801232.

[72] O. Koleda, T. Broese, J. Noetzel, M. Roemelt, E. Suna, R. Francke, *J. Org. Chem.* **2017**, *82*, 11669–11681.

[73] K. Mitsudo, Y. Kurimoto, K. Yoshioka, S. Suga, *Chem. Rev.* **2018**, *118*, 5985–5999.

[74] M. Atobe, H. Tateno, Y. Matsumura, *Chem. Rev.* **2017**, *118*, 4541–4572.

[75] D. Pletcher, R. A. Green, R. C. D. Brown, *Chem. Rev.* **2018**, *118*, 4573–4591.

[76] C. Gütz, A. Stenglein, S. R. Waldvogel, *Org. Process Res. Dev.* **2017**, *21*, 771–778.

[77] L. Fahrmeir, C. Heumann, R. Künstler, I. Pigeot, G. Tutz, *Statistik*, Springer, Berlin, 8th ed., **2016**.

[78] W. Kleppmann, *Versuchsplanung*, Carl Hanser Fachbuchverlag, München, 9th ed., **2016**.

[79] Y. Kim, Y. Park, S. Chang, *ACS Cent. Sci.* **2018**, *4*, 768–775.

[80] C. A. Morales-Rivera, P. E. Floreancig, P. Liu, *J. Am. Chem. Soc.* **2017**, *139*, 17935–17944.

[81] C. S. Sevov, D. P. Hickey, M. E. Cook, S. G. Robinson, S. Barnett, S. D. Minteer, M. S. Sigman, M. S. Sanford, *J. Am. Chem. Soc.* **2017**, *139*, 2924–2927.

[82] T. Piou, F. Romanov-Michailidis, M. Romanova-Michaelides, K. E. Jackson, N. Semakul, T. D. Taggart, B. S. Newell, C. D. Rithner, R. S. Paton, T. Rovis, *J. Am. Chem. Soc.* **2017**, *139*, 1296–1310.

[83] C. B. Santiago, J.-Y. Guo, M. S. Sigman, *Chem. Sci.* **2018**, *9*, 2398–2412.

[84] J.-Y. Guo, Y. Minko, C. B. Santiago, M. S. Sigman, *ACS Catal.* **2017**, *7*, 4144–4151.

[85] C. B. Santiago, A. Milo, M. S. Sigman, *J. Am. Chem. Soc.* **2016**, *138*, 13424–13430.

[86] M. S. Sigman, K. C. Harper, E. N. Bess, A. Milo, *Acc. Chem. Res.* **2016**, *49*, 1292–1301.

[87] E. N. Bess, A. J. Bischoff, M. S. Sigman, *P. Natl. Acad. Sci.* **2014**, *111*, 14698–14703.

[88] K. C. Harper, E. N. Bess, M. S. Sigman, *Nat. Chem.* **2012**, *4*, 366–374.

[89] B. Jones, C. J. Nachtsheim, *J. Qual. Technol.* **2013**, *45*, 121–129.

[90] S. A. Weissman, N. G. Anderson, *Org. Process Res. Dev.* **2015**, *19*, 1605–1633.

[91] I. Arenas, A. Ferrali, C. Rodríguez-Escrich, F. Bravo, M. A. Pericàs, *Adv. Synth. Catal.* **2017**, *359*, 2414–2424.

[92] A. Echtermeyer, Y. Amar, J. Zakrzewski, A. Lapkin, *Beilstein J. Org. Chem.* **2017**, *13*, 150–163.

[93] P. Renzi, C. Kronig, A. Carlone, S. Eröksüz, A. Berkessel, M. Bella, *Chem. Eur. J.* **2014**, *20*, 11768–11775.

[94] A. L. García-Cabeza, R. Marín-Barrios, R. Azarken, F. J. Moreno-Dorado, M. J. Ortega, H. Vidal, J. M. Gatica, G. M. Massanet, F. M. Guerra, *Eur. J. Org. Chem.* **2013**, *2013*, 8307–8314.

[95] P. M. Murray, F. Bellany, L. Benhamou, D.-K. Bucar, A. B. Tabor, T. D. Sheppard, *Org. Biomol. Chem.* **2016**, *14*, 2373–2384.

[96] V. K. Aggarwal, A. C. Staubitz, M. Owen, *Org. Process Res. Dev.* **2006**, *10*, 64–69.

[97] P. Renzi, M. Bella, *Synlett* **2017**, *28*, 306–315.

[98] T. Gul, R. Bischoff, H. P. Permentier, *Electrochim. Acta* **2015**, *171*, 23–28.

Nomenclature

CV	cyclic voltammetry
DoE	design of experiments
DFT	density functional theory
eq	equivalents
FT-IR	Fourier transformed infra-red spectroscopy
GC	gas chromatograph
HOMO	highest occupied molecular orbital
HR-MS	high resolution mass spectrometry
LUMO	lowest unoccupied molecular orbital
Me	methyl
MLR	multivariate linear regression
MS	mass spectrometry
NBO	natural bond orbital
NMR	nuclear magnetic resonance spectroscopy
NOCV	natural orbitals for chemical valence
TMS	Trimethylsilyl

Chapter 7

Appendix

List of Publications

1. R. Möckel, E. Babaoglu, G. Hilt, *"Iodine(III)-mediated Electrochemical Trifluoroethoxylactonisation - Rational Reaction Optimisation and Prediction of Mediator Activity"*, *Chem. Eur. J.*, **2018**, *24*, 15781.

2. R. Möckel, J. Hille, E. Winterling, S. Weidemüller, T. M. Faber, G. Hilt, *"Electrochemical Synthesis of Aryl Iodides by Anodic Iododesilylation"*, *Angew. Chem.* **2018**, *130*, 450; *Angew. Chem. Int. Ed.* **2018**, *58*, 442.

3. A. R. Nödling, R. Möckel, R. Tonner, G. Hilt, *"*Lewis *Acids as Activators in CBS-Catalysed* Diels-Alder *Reactions: Distortion Induced* Lewis *Acidity Enhancement of* $SnCl_4$*",Chem. Eur. J.* **2016**, 13171.

4. R. Möckel, G. Hilt, *"Synthesis of Polysubstituted Iodobenzene Derivatives from Alkynylsilanes and 1,3-Dienes via* Diels-Alder*/Oxidation/Iodination Reaction Sequence"*, *Org. Lett.* **2015**, *17*, 1644.

5. Z. You, R. Möckel, J. Bergunde, S. Dehnen, *"Organotin-Oxido Cluster-Based Multiferrocenyl Complexes Obtained by Hydrolysis of Ferrocenyl-Functionalized Organotin Chlorides"*, *Chem. Eur. J.* **2014**, *20*, 13491.

Reprints of the Publications

The publications which are part of this dissertation are presented in their original form in the following in the same order as they were discussed in 3. Permissions for re-print articles have been obtained from the publisher. Supporting informations are provided in the supporting informations of the original publications and on CD supplied with this dissertation.

Homogeneous Catalysis

Lewis Acids as Activators in CBS-Catalysed Diels–Alder Reactions: Distortion Induced Lewis Acidity Enhancement of $SnCl_4$

Alexander R. Nödling, Robert Möckel, Ralf Tonner,* and Gerhard Hilt*[a]

Dedicated to Prof. Dr. Gernot Frenking on the occasion of his 70th birthday

Abstract: The effect of several Lewis acids on the CBS catalyst (named after Corey, Bakshi and Shibata) was investigated in this study. While ^2H NMR spectroscopic measurements served as gauge for the activation capability of the Lewis acids, in situ FT-IR spectroscopy was employed to assess the catalytic activity of the Lewis acid oxazaborolidine complexes. A correlation was found between the $\Delta\delta(^2H)$ values and rate constants k_{DA}, which indicates a direct translation of Lewis acidity into reactivity of the Lewis acid–CBS complexes. Unexpectedly, a significant deviation was found for $SnCl_4$ as Lewis acid. The $SnCl_4$–CBS adduct was much more reactive than the $\Delta\delta(^2H)$ values predicted and gave similar reaction rates to those observed for the prominent $AlBr_3$–CBS adduct. To rationalize these results, quantum mechanical calculations were performed. The frontier molecular orbital approach was applied and a good correlation between the LUMO energies of the Lewis acid–CBS–naphthoquinone adducts and k_{DA} could be found. For the $SnCl_4$–CBS–naphthoquinone adduct an unusual distortion was observed leading to an enhanced Lewis acidity. Energy decomposition analysis with natural orbitals for chemical valence (EDA-NOCV) calculations revealed the relevant interactions and activation mode of $SnCl_4$ as Lewis acid in Diels–Alder reactions.

Introduction

Chiral oxazaborolidines were introduced by Itsuno as reagents,[1] and refined by Corey for catalytic use in asymmetric reductions of prochiral ketones with boranes nearly 30 years ago.[2] Due to their widespread use as powerful and versatile catalysts,[3] (*S*)-proline-derived oxazaborolidines **1** are usually referred to as CBS catalysts, stemming from the initials of the authors Corey, Bakshi, and Shibata in their seminal report (Figure 1).[2]

In the last decade, the Corey group could expand the reaction scope of oxazaborolidine catalysts **1** by combining them with superacids such as TfOH or Tf_2NH.[4] This results in protonation of the nitrogen atom of **1**, thus enhancing the Lewis acidity of the adjacent boron atom. These protonated species of type **3** (Scheme 1) are potent catalysts in asymmetric Diels–Alder reactions of α,β-unsaturated carbonyl compounds.[5] Shortly after, (*S*)-valine-derived oxazaborolidine (**2**) was developed by Yamamoto.[6] The combination of Lewis acids (LA), for example, $SnCl_4$, $TiCl_4$ or $FeCl_3$, with **2** led to a similar Lewis acidity enhancement of the boron atom by coordination of the Lewis acid to the nitrogen. In this case, the Lewis acids showed superior reactivities and enantioselectivities in Diels–Alder reactions than the superacids TfOH or Tf_2NH. Corey subsequently found $AlBr_3$ as a highly potent activator of **1b** for Diels–Alder reactions,[7] but mentioned worse results when other Lewis acids, such as BCl_3 or $SnCl_4$, were used.[8] Both catalysts, **1a/b** and **2**, have found regular use, for example, in natural product synthesis, but mainly as their protonated congeners **3a/b**.[5,9] Reports on the use of Lewis acid-activated oxazaborolidines, such as **4**, are scarce,[9g,10] and if Lewis acids are used, $AlBr_3$ is employed almost exclusively.

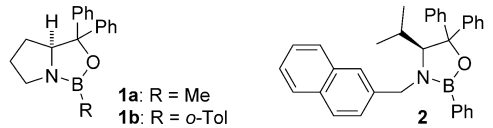

Figure 1. Chiral oxazaborolidines **1a**, **1b** and **2** as introduced by Corey and Yamamoto.

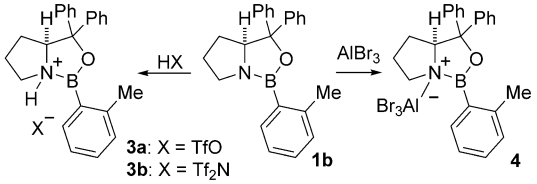

Scheme 1. Activation of oxazaborolidine **1b** by Brønsted or Lewis acid.

[a] Dr. A. R. Nödling, R. Möckel, Dr. R. Tonner, Prof. Dr. G. Hilt
Fachbereich Chemie, Philipps-Universität Marburg
Hans-Meerwein-Straße 4, 35032 Marburg (Germany)
E-mail: Tonner@chemie.uni-marburg.de
Hilt@chemie.uni-marburg.de

Supporting information for this article is available on the WWW under http://dx.doi.org/10.1002/chem.201602394.

© 2016 Wiley-VCH Verlag GmbH & Co. KGaA, Weinheim

Due to our interest in the relation between experimentally quantifiable strength and catalytic activity of Lewis acids,[11] we were curious about the underlying reasons for the apparent superiority of $AlBr_3$ as activator of **1 b** compared to other Lewis acids. We envisaged the polarising effect on the oxazaborolidine framework upon Lewis acid coordination to be experimentally quantifiable by an ^2H NMR spectroscopic probe. Based on our previous experience of quantifying the Lewis acidity of metal(loid) halides with quinolizidine probe [D_1]**5**,[11a] we expected to be able to quantify the activation of **1 b** upon coordination of a Lewis acid via ^2H NMR spectroscopic studies of the deuterated derivative [D_1]**1 b** (Figure 2).

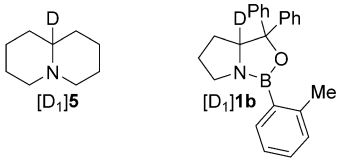

Figure 2. ^2H NMR spectroscopical probes quinolizidine [D_1]**5** and the deuterated CBS catalyst [D_1]**1 b**.

The shift difference $\Delta\delta(^2H)$ between the ^2H NMR shift of the respective Lewis acid–oxazaborolidine complex and the free oxazaborolidine [D_1]**1 b** would serve as quantified activation of [D_1]**1 b**. As encountered in our previous studies,[11a] we anticipated the activation $\Delta\delta(^2H)$ of [D_1]**1 b** in Lewis acid complexes to correlate with catalytic activity of such complexes in organic transformations, such as the Diels–Alder reaction (DA). To probe this relation we intended to conduct kinetic studies of a representative Diels–Alder reaction using in situ FT-IR spectroscopy. Thereby, rate constants, k_{DA}, should be obtained for different Lewis acid–CBS complexes and in addition enantiomeric ratios should be determined for probing the performance of different Lewis acids.

Results and Discussion

Synthesis of deuterated oxazaborolidine probe [D_1]1 b

The deuterated oxazaborolidine [D_1]**1 b** was synthesised by combining a modified procedure of Gilmour for the synthesis of deuterated amino alcohol [D_1]**8** and the condensation protocol reported by Yamamoto (Scheme 2).[12,13] The deuterium content was determined by ^1H NMR spectroscopy after Grignard addition of PhMgBr to deuterated ester [D_1]**7**, and was on average about 80%. The deuterated oxazaborolidine [D_1]**1 b** could be obtained after condensation of [D_1]**8** with tri-*ortho*-tolylboroxine in acceptable yield and with sufficient deuterium content.

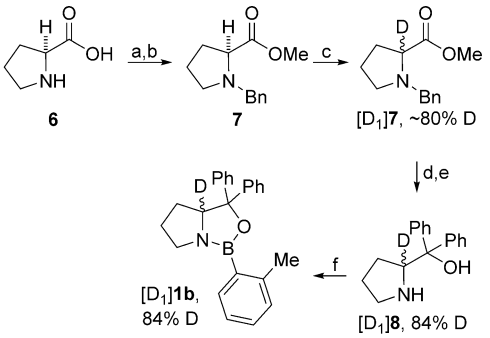

Scheme 2. Synthesis of deuterated oxazaborolidine [D_1]**1 b**. a) $SOCl_2$, MeOH, 0 °C to RT, 16 h; b) toluene/NEt_3 1:1, BnBr, reflux, 16 h, quantitative yield over 2 steps; c) LDA, THF, −20 °C, 1 h, then D_2O, −5 °C to RT, 16 h, 78%; d) PhMgBr, THF, 5 °C to RT, 16 h, 64%, 84% D; e) Pd/C (10% Pd), HCl, H_2 (1 atm), EtOH, quantitative yield; f) tri-*ortho*-tolylboroxine, toluene, reflux, Dean–Stark apparatus, quantitative yield. Bn = benzyl, Ph = phenyl, LDA = lithium diisopropylamide. For details see the Supporting Information.

^2H NMR spectroscopic studies of Lewis acid–CBS complexes of type 6

We chose a number of common Lewis acids for the study, ranging from $BF_3{\cdot}Et_2O$ to very strong $AlBr_3$ and included the frequently used Brønsted acid $HNTf_2$ (Table 1). In order to assess the activation the chemical shift $\Delta\delta(^2H)$ of [D_1]**1 b** upon Lewis acid coordination was measured. Therefore, we applied the procedure which we developed for quinolizidine probe [D_1]**5**.[11a] Therein, [D_1]**5** is treated with a tenfold excess of Lewis acid in CH_2Cl_2 at room temperature. In case of [D_1]**1 b** this excess was diminished to five equivalents of Lewis acids, since in the case of insoluble Lewis acids that form soluble complexes, for example, $AlCl_3$ or InI_3, a better signal-to-noise ratio was observed. ^2H NMR spectroscopic titration experiments of [D_1]**1 b** with InI_3 showed a single, downfield shifted peak throughout the titration, and minimal difference of $\Delta\delta(^2H)$ at five or ten equivalents of InI_3. Therefore, we embarked on further studies including all acids under these conditions (Table 1).

The ^2H NMR spectroscopic studies using excess Lewis acid revealed several interesting aspects. The activation $\Delta\delta(^2H)$ is connected to the quantified or the perceived acidity of Lewis acids, for example, $BF_3{\cdot}Et_2O$ activates [D_1]**1 b** less than $AlCl_3$ or BBr_3.[14] Furthermore, some Lewis acids displayed none or hardly any activation, for example, ZnI_2 or $InCl_3$. Finally, some Lewis acid–CBS adducts exhibited several signals in the respective ^2H NMR spectra, hence more than one species must be formed.[15]

The rationale for more than one peak in ^2H NMR spectra could be traced back to coordination of the Lewis acid to the oxygen atom of [D_1]**1 b**,[16] as well as via adducts with simultaneous coordination of two Lewis acid molecules to the nitrogen and the oxygen atom of [D_1]**1 b**. The latter could be responsible for the very high $\Delta\delta(^2H)$ values observed in some cases, for example, for $AlBr_3$ or $TiCl_4$ (see the Supporting Information for quantum chemical calculations on the stability of N–, O–, and N–O-coordinated adducts **9**; Table S2). We additionally suspected decomposition of adducts **9** since no clear precedence was present, as Corey mentioned a stability of **9 e** only below −20 °C,[5] whereas Paddon-Row used the $SnCl_4$

© 2016 Wiley-VCH Verlag GmbH & Co. KGaA, Weinheim

Table 1. ^{2}H NMR spectroscopic quantified activation $\Delta\delta(^2H)$ of [D$_1$]**1b** upon Lewis acid coordination at −40 °C.

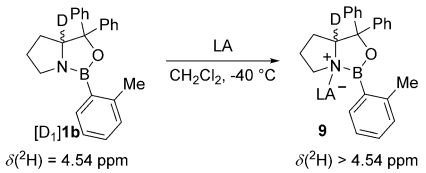

Entry[a]	Lewis acid	CBS adduct	$\Delta\delta(^2H)$ [ppm] (−40 °C)
1	$BF_3{\cdot}Et_2O$	**9a**	0.00
2	BCl_3	**9b**	**1.14**, 0.28[d]
3	BBr_3	**9c**	1.20
4	$AlCl_3$	**9d**	**1.22**, 0.29[d]
5	$AlBr_3$	**9e**	1.27[b]
6	AlI_3	**9f**	1.28[c]
7	$InCl_3$	**9g**	0.00
8	$InBr_3$	**9h**	0.00
9	InI_3	**9i**	0.81
10	$SnCl_4$	**9j**	0.16
11	$TiCl_4$	**9k**	0.49
12	ZnI_2	**9l**	–
13	$HNTf_2$	**3b**	**0.83**, 0.46, 0.22[d]

[a] Adducts **3b** and **9** were prepared according to the general procedure 1 (see the Supporting Information): [D$_1$]**1b** (64 μmol, 1.0 equiv), Lewis acid (64 μmol, 1.0 equiv), CH_2Cl_2 (0.50 mL), preparation below −70 °C, NMR spectroscopic measurement was then performed at −40 °C. [b] CH_2Br_2 was used as solvent instead of CH_2Cl_2. [c] CH_2I_2 was used as solvent instead of CH_2Cl_2. [d] The most intensive peak is given in bold format.

adduct **9j** at 40 °C.[17] We found the $AlCl_3$ adduct **9d** to decompose at room temperature over the course of 24 h.

To circumvent these problems the 1:1 adducts (ratio of Lewis acid/[D$_1$]**1b**) were synthesised below −70 °C and investigated by ^{2}H NMR spectroscopy at three different temperatures. As expected, the number of signals was reduced at low temperatures whereas at room temperature several species were observable (for the complete data set at different temperatures, see the Supporting Information, Table S1).

No $\Delta\delta(^2H)$ value could be obtained for $BF_3{\cdot}Et_2O$, since a precipitate formed at −70 °C, which we assume to be either solid $BF_3{\cdot}Et_2O$ (m.p. about −58 °C) or **9a**. The most consistent data set of $\Delta\delta(^2H)$ values was found at −40 °C (Table 1) and is used for further discussion (25 °C in case of $BF_3{\cdot}Et_2O$). In case of the 1:1 adducts a clearer connection between Lewis acidity and activation of [D$_1$]**1b** was notable, that is, an increase of $\Delta\delta(^2H)$ values for a given central atom with heavier halide substituents, for example, Table 1, entries 1–3. In addition, it became clear that several Lewis acids, for example, BCl_3, BBr_3, or $AlCl_3$, exerted a similar polarising effect on [D$_1$]**1b** as $AlBr_3$.

Considering all employed acids, four groups of activators could be distinguished based on the $\Delta\delta(^2H)$ values (Figure 3). This classification matches to a good degree with the acidities of these Lewis acids as determined by other experimental quantification methods.[14] Accordingly, we assumed that the adducts **9** formed with these Lewis acids should be equally good catalysts in Diels–Alder reactions, if the catalytic activity would correlate strictly to the activation of **1b**.

strong activation $\Delta\delta(^2H)$ > 1.00 ppm **BCl_3, BBr_3** **$AlCl_3$, $AlBr_3$** **AlI_3**	**moderate activation** 0.50 ppm < $\Delta\delta(^2H)$ < 1.00 ppm **InI_3** **$HNTf_2$**
weak activation 0.00 ppm < $\Delta\delta(^2H)$ < 0.50 ppm **$SnCl_4$** **$TiCl_4$** **$BF_3{\cdot}Et_2O$ (at 25 °C)**	**no activation** $\Delta\delta(^2H) \cong$ 0.00 ppm **ZnI_2** **$InCl_3$** **$InBr_3$**

Figure 3. Classification of the investigated Lewis acids depending on their activation of [D$_1$]**1b**.

In situ FT-IR spectroscopic kinetic studies of Diels–Alder reactions catalysed by Lewis acid-CBS complexes 9

The transformation has the advantage that the progress of the reaction can easily be monitored by in situ FT-IR spectroscopy. Another aspect was that the enantioselectivity was not excellent when the $AlBr_3$–CBS catalyst was used which leaves room to track the influence of other Lewis acids.[7]

The Diels–Alder reactions were performed under pseudo-first-order conditions regarding **10** with a tenfold excess of isoprene (**11**) and by using 4.0 mol% of active catalyst adduct **3b** or **9** (Scheme 3). In contrast to Corey's procedure, the Lewis acid–CBS adducts **3b** and **9** were prepared in a separate flask and added to the reactant mixture, since in some cases, for example, BBr_3, a precipitate was observed, if Lewis acid–CBS catalysts were mixed with **10** before **11** was added. A slight excess of oxazaborolidine **1b** with respect to the Lewis acid was used to avoid racemic background reaction.

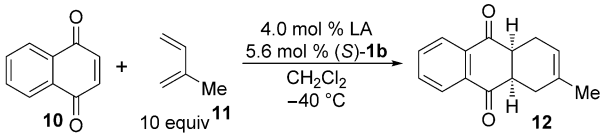

Scheme 3. Diels–Alder reaction to determine rate constants for different Lewis acids (LA).

The reaction progress was monitored by following the carbonyl bands of **10** and **12**, at 1670 and 1696 cm^{-1}, respectively. The changes in concentrations were then used to calculate the rate constants k_{DA}. A comparison of all measured concentration profiles for adducts **9** is given in Figure 4, and an overview of the kinetic data (averages of at least three measurements) is given in Table 2.

The profiles, excluding the one obtained with BF_3 adduct **9a**, showed a bend after 150 to 250 seconds, which we so far attribute to experimental constraints. Before and after the bend straight fits were observed, as expected for a reaction under pseudo-first-order conditions. Therefore, we calculated the constants before, $k_{DAStart}$ (see the Supporting Information), and after the bend k_{DA} (Table 2). In case of full conversion the

© 2016 Wiley-VCH Verlag GmbH & Co. KGaA, Weinheim

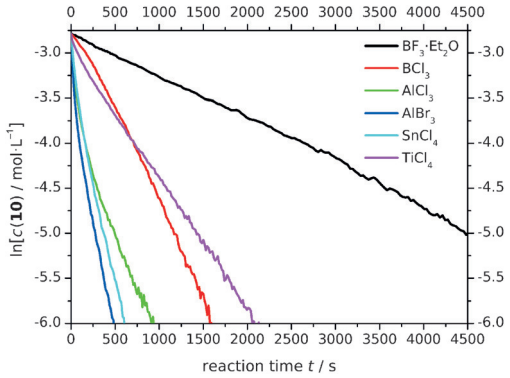

Figure 4. Plots of the natural logarithms of the concentration profiles versus the reaction time obtained with Lewis acid–CBS adducts **9a**, **9b**, **9d**, **9e**, **9j**, and **9k** as catalysts in the Diels–Alder reaction between **10** and **11**.

Table 2. Kinetic data and enantioselectivities of Diels–Alder reactions between **10** and **11** catalysed by CBS adducts **3b** and **9**.

Entry[a]	LA/adduct	$k_{DA}\times10^{-4}$ [s^{-1}][a]	e.r.
1	BF_3·Et_2O/**9a**	4.2 ± 0.8	69:31
2	BCl_3/**9b**	23.7 ± 1.9	55:45
3	BBr_3/**9c**	–[b]	90:10
4	$AlCl_3$/**9d**	34.5 ± 20.5	86:14
5	$AlBr_3$/**9e**	43.0 ± 10.5	83:17
6	AlI_3/**9f**	–[c]	81:19
7	$InCl_3$/**9g**	–[c]	–
8	$InBr_3$/**9h**	–[c]	–
9	InI_3/**9i**	–[c]	89:11
10	$SnCl_4$/**9j**	45.6 ± 8.8	93:7
11	$TiCl_4$/**9k**	14.0 ± 4.2	89:11
12	ZnI_2/**9l**	–[c]	–
13	$HNTf_2$/**3b**	–[c]	–

[a] Reaction conditions according to the general procedure 3 (see the Supporting Information): 1,4-naphthoquinone (**10**, 0.50 mmol, 1.0 equiv), isoprene (**11**, 5.00 mmol, 10.0 equiv), **1b** (28 μmol, 5.6 mol%), Lewis acid (20 μmol, 4.0 mol%), CH_2Cl_2 (7.6 mL), −40 °C, see the Supporting Information for details. The given value is the mean of three reactions. [b] Reactions with BBr_3 were irreproducible, hence no k_{DA} is given. [c] The conversion was below 10% after 8 h reaction time.

reaction was quenched followed by a short work-up to determine the enantiomeric ratios by chiral LC analysis (Table 2). The kinetic measurements showed several surprising features. First of all, some adducts exhibited none or a very small catalytic activity in the monitored timeframe of up to ten hours, namely the adducts of **1b** with AlI_3, all indium halides, ZnI_2, BBr_3 and $HNTf_2$. This was not surprising for $InCl_3$ and $InBr_3$, since they do not activate **1b** according to the $\Delta\delta(^2H)$ values. Adduct **3b** was employed by Corey in similar reactions and usually 20 mol% of **3b** are used or reaction times of at least 12 h are necessary. So despite its moderate activation of **1b**, which is still higher than that of catalytically highly active adducts, for example, **9j**, the formation of contact ion pairs in **3b** seems to prevent a higher activity and measurable rates under the reaction conditions employed in this study.[4a]

While InI_3 adduct **9i** was found to be active at room temperature in preliminary studies, the Diels–Alder reaction with AlI_3 adduct **9f** did not reach full conversion even after 12 h at room temperature. The interpretation of the kinetic data for the activation with the BBr_3–CBS adduct **9c** was hampered based on competing oligomerisation of the isoprene. For the visualisation of a correlation the Lewis acidity strength, determined by the $\Delta\delta(^2H)$ values, and the catalytic activities, namely, the rate constants k_{DA}, were plotted (Figure 5; a plot of $k_{DAStart}$ vs. $\Delta\delta(^2H)$ is given in the Supporting Information, Figure S3).

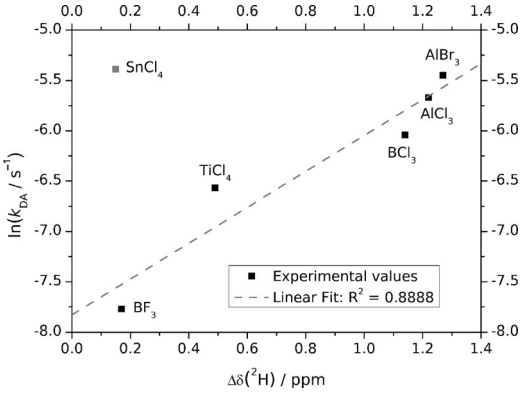

Figure 5. Plot of the natural logarithms of k_{DA} values versus the $\Delta\delta(^2H)$ values. The linear fit was obtained with exclusion of $SnCl_4$ adduct **9j**.

First, with exclusion of $SnCl_4$ adduct **9j** a moderate correlation is observed. The activity of adducts **9** and activation of **1b** is in agreement with the usually perceived and experimentally quantified acidity of the respective Lewis acids,[11a,14] that is, $AlBr_3$ activates **1b** more and adduct **9e** is more active than $TiCl_4$ and its adduct **9k**. Second, an unexpected discrepancy is observed for $SnCl_4$ adduct **9j**, which catalysed the Diels–Alder reaction between **10** and **11** much faster than the $\Delta\delta(^2H)$ suggested. This runaway value prompted the quantum chemical investigations shown in the next subsection.

Overall, the NMR spectroscopic chemical shifts $\Delta\delta(^2H)$ correlated well with the rate constants which are in agreement to Corey's observations as well as to Fujimoto's theoretical studies.[16] Generally, a higher Lewis acidity of a given Lewis acid leads to a stronger activation of **1b**, which was measurable by ^2H NMR spectroscopy employing [D_1]**1b**, and a higher catalytic activity of Lewis acid–CBS adducts **9**. The $AlBr_3$ adduct **9e** shows the highest activation, and with the $SnCl_4$ adduct **9j** the highest activities as catalysts in Diels–Alder reactions.[18]

Despite the low activities or side reactions observed with adducts **9c**, **9f**, and **9i** the enantioselectivities were decent (**9f**) to good (**9c**, **9i**) and even better for the $SnCl_4$–CBS adduct (**9j**) reaching the highest e.r. of 93:7. Concerning the enantioselectivities of active adducts **9** nearly no enantioselectivity was found for **9a** and **9b**. Good enantioselectivities were observed for **9i**, **9j** and **9k**, while the $AlBr_3$ adduct **9e** yielded a lower e.r. value than reported by Corey.[7] This could be attributed to the higher reaction temperature applied in this study, or the fact that $AlBr_3$ was used in substance instead of a commercially available 1.0 M solution.

© 2016 Wiley-VCH Verlag GmbH & Co. KGaA, Weinheim

Quantum chemical calculations: frontier molecular orbitals

The surprising findings for InI_3 (no catalytic activity despite significant $\Delta\delta(^2H)$ value) and $SnCl_4$ (very high catalytic activity despite moderate $\Delta\delta(^2H)$ value) prompted computational investigation of the Lewis acid interactions with the CBS catalyst. We used density functional theory approaches with two different functionals for structural optimisation (M06-2X/def-2TZVP) and bonding analysis (BP86/TZ2P$^+$).

Frontier molecular orbital (FMO) theory is a common approach to estimate the reactivity change of a dienophile upon Lewis acid coordination and can be expressed as LUMO lowering $\Delta E_{LUMO} = E_{LUMO(\mathbf{10}\text{–CBS–LA})} - E_{LUMO(\mathbf{10})}$.[19] A correlation between ΔE_{LUMO} and rate constants has been elucidated by Laszlo for simple aluminium halides several decades ago in a rather unnoticed account.[20] The appeal of FMO theory is its simplicity and its applicability to reactants instead of a tedious transition state analysis.

Based on these studies we started our approach by optimising the structures of the complexes formed from 1,4-naphthoquinone (**10**) and Lewis acid–CBS adducts **9** (in the following referred to as **10**–Lewis acid–CBS complexes **13**) in order to check whether it is possible to use ΔE_{LUMO} to predict the reactivity of 1,4-naphthoquinone (**10**). A preliminary justification for this approach is given in Figure 6, showing the LUMO of **13 j**, which is completely localised on the 1,4-naphthoquinone moiety. Subsequently, the energy differences ΔE_{LUMO} were calculated for all Lewis acids applied in the spectroscopic and kinetic studies (these are summarised in the Supporting Information, Table S2). To verify the predictive power of ΔE_{LUMO} for the catalytic activity of adducts **9** in the Diels–Alder reaction of **10** with **11** ΔE_{LUMO} was plotted against the measured rate constants k_{DA}. The results for adducts **9** that showed significant rate constants are presented in Figure 7. In contrast to the plot of $\Delta\delta(^2H)$ versus $\ln(k_{DA})$ (Figure 5), there is a much better correlation between ΔE_{LUMO} and $\ln(k_{DA})$ for all catalytically active adducts **9** obtained with $AlCl_3$, $AlBr_3$, $TiCl_4$, BF_3, BCl_3, and especially with $SnCl_4$. Furthermore, the Lewis acids with no significant k_{DA} showed low ΔE_{LUMO} as well, demonstrating the predictive power of the FMO approach.

In case of the indium-based Lewis acids, a rather simple explanation for the low reactivity could be found. Although all indium Lewis acids coordinate quite well to CBS catalyst **1 b** (see the Supporting Information, Table S3), and therefore show a significant NMR shift $\Delta\delta(^2H)$, 1,4-naphthoquinone (**10**) does not coordinate to the boron atom in complexes **13 g–i**, but to the indium atom (Tables S5 and S6).[21] Thereby, the activation of **10** is only mediocre and CBS adducts **9 g–i** exhibit only very small catalytic activity as catalyst in Diels–Alder reactions.

As we were able to explain the low activity of the indium Lewis acid–CBS adducts **9 g–i**, we turned our attention to the strange behaviour of $SnCl_4$–CBS adduct **9 j**. The low activation of **1 b** but very good activation of **10** by $SnCl_4$-based adduct **9 j** in the model Diels–Alder reaction is confusing at first sight. In most studies, $SnCl_4$ is usually regarded as a weak to moderate strong Lewis acid and thus the low activation $\Delta\delta(^2H)$ of **1 b** is in line with existing evidence.[11a,14] Hence, the notwithstanding

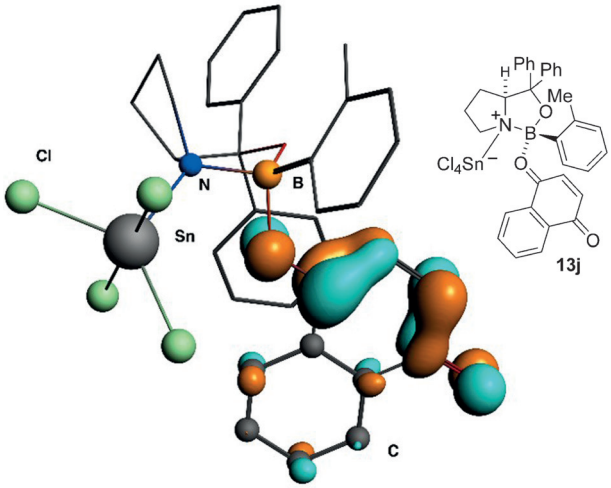

Figure 6. Plot of the calculated LUMO of complex **13 j** at BP86/TZ2P$^+$ (energy cut-offs of MO plots 0.033).

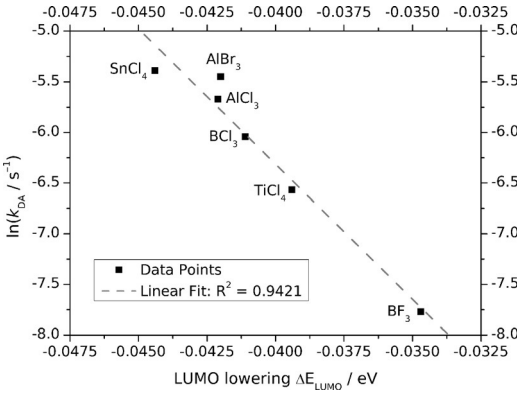

Figure 7. Plot of the LUMO shifts ΔE_{LUMO} (M06-2X/def2-TZVP) of **10** upon formation of adducts **13** versus the $\ln(k_{DA})$ of the Diels–Alder reaction.

strong activation of **10** by adduct **9 j** in catalysis of the model Diels–Alder reaction and the calculated high ΔE_{LUMO} required a more detailed investigation.

To explain the unusual behaviour of $SnCl_4$, the optimised structures and especially the geometry of $SnCl_4$ in **9 j** and **13 j** were analysed more closely (Figure 8). A rather unusual change in coordination geometry of $SnCl_4$ was found when comparing $SnCl_4$–CBS adduct **9 j** and **10**–$SnCl_4$–CBS adduct **13 j**. In **9 j**, the chlorine atoms are arranged axially resulting in a triangular bipyramidal environment for the tin atom. In **13 j** the axial chlorine atom Cl4 is bent in the plane by 37.0° resulting in an equatorial conformation. Furthermore, this is accompanied by a shortening of the tin–nitrogen bond by 0.18 Å.

Only limited reports on structural aspects on the coordination of $SnCl_4$ to different Lewis bases are available.[22] A theoretical study by Frenking et al. dealt with the coordination of $SnCl_4$ to ammonia and pyridine, respectively. They exclusively observed the axial isomer for coordination of $SnCl_4$ to ammonia and for coordination to pyridine both isomers were identified as two closely spaced minima.[23] They postulated steric reasons for this effect but did not further investigate this

© 2016 Wiley-VCH Verlag GmbH & Co. KGaA, Weinheim

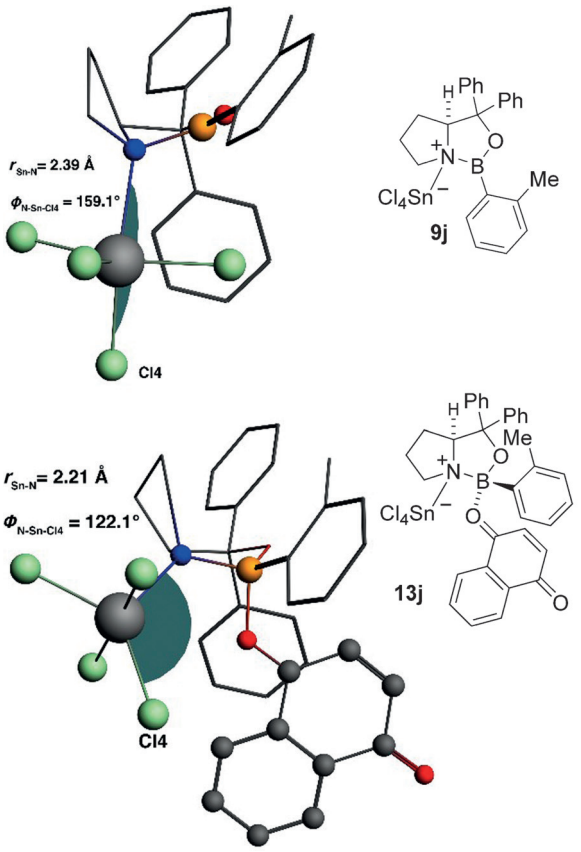

Figure 8. Optimised geometries for $SnCl_4$–CBS complex **9j** and **10**–$SnCl_4$–CBS adduct **13j** at M06-2X/def2-TZVP level, showing the change of the coordination geometry at the tin atom from **9j** to **13j** upon coordination of **10**.

aspect. Experimental insights in coordination geometries are even rarer. To the best of our knowledge, there is only one crystal structure of a classical Lewis acid base adduct present in literature where $SnCl_4$ adopted an axial conformation upon coordination to quinuclidine.[24]

Quantum chemical calculations: bonding analysis

In order to quantify the impact of this conformational change as well as its rationale, the bonding situation in **9** and **13** were studied in more detail. Therefore, the bond between the Lewis acids and the CBS fragment in adducts **9** and **13** were analysed using EDA-NOCV (energy decomposition analysis combined with natural orbitals for chemical valence). EDA analysis allows a partition of the bond energy ΔE_{int} (interaction energy) into its components ΔE_{Pauli} (Pauli repulsion energy), $\Delta E_{orbital}$ (orbital interaction energy) and ΔE_{elstat} (electrostatic interaction energy) and furthermore by linkage with NOCV theory a breakdown of $\Delta E_{orbital}$ in contributions of different fragment orbitals, thus allowing assessment of the proportion of different bond types.[25]

The results of the EDA calculations for **9** and **13** are shown exemplarily for $AlCl_3$, $SnCl_4$ and $TiCl_4$ in Table 3. A closer look on the energy terms gives an indication for the unusual strong activation of **10** by $SnCl_4$–CBS adduct **9j** within the 1,4-naphthoquinone complex **13j**. The interaction energy ΔE_{int} of $SnCl_4$ in the Lewis acid–CBS **9j** adduct is by 10.7 kcal mol^{-1} lower than that of $AlCl_3$–CBS adduct **9d** whereas $TiCl_4$–CBS adduct **9k** is only 4.7 kcal mol^{-1} less stable than **9d**. This is qualitatively in line with the observed $\Delta\delta(^2H)$ values. The lower bond energy ΔE_{int} in **9j** can mainly be ascribed to high Pauli repulsion ΔE_{Pauli} and lower electrostatic interaction energy ΔE_{elstat} and simultaneously nearly the same orbital interaction energy $\Delta E_{orbital}$. As $\Delta E_{orbital}$ should predominantly be responsible for Lewis acid activation of the CBS fragment, it was further analysed by NOCV theory. By this method, the electron flow induced by bond formation can be visualised and quantified. The by far most important NOCV (Figure 9a and b) term $\Delta\rho_{\sigma,1}$ could be assigned to the $\sigma(CBS \rightarrow \sigma^*_{LA-Cl})$ bond. This term is nearly identical for **9d** and **9j** with 36.0 and 35.6 kcal mol^{-1}, respectively. This can be traced back to the number of participating chlorine atoms. In both structures, just three chlorine atoms seem to engage in donor–acceptor interaction. The axially positioned fourth chlorine atom (Cl4) in the $SnCl_4$–CBS adduct **9j** does not contribute to donor–acceptor interaction and does not show any electron-density change (Figure 9b). Accordingly, this complex geometry leads to a similar orbital interaction as in the $AlCl_3$–CBS adduct **9d**. Even if this conformation does not allow efficient interaction with the Lewis base, it seems to be sterically favoured due to a lower necessary preparation energy $\Delta E_{prep}(SnCl_4)$ of 20.7 kcal mol^{-1} for the axial conformation compared to 38.8 kcal mol^{-1} (entry **9j fixed** in Table 3, see discussion below) necessary for the equatorial conformation.

Furthermore, it allows direct stabilising interaction of the tin atom with one of the phenyl rings of the CBS backbone contributing to $\Delta E_{orbital}$ with 3.9 kcal mol^{-1}. This situation changes dramatically when 1,4-naphthoquinone (**10**) coordinates to $SnCl_4$–CBS adduct **9j** resulting in **13j**. The fourth chlorine atom changes from an axial to an equatorial conformation. EDA calculation of **13j** now show an interaction energy ΔE_{int} similar to **13d** due to a disproportional increase in orbital (−56.6 to −88.4 kcal mol^{-1}) and electrostatic interaction. The increase of the orbital term can be attributed by NOCV calculation to the conformational change and a concomitant participation of the now equatorial chlorine atom (Cl4) in donor–acceptor interaction. The most important interaction $\Delta\rho_{\sigma,1}$ with −58.8 kcal mol^{-1} is shown in Figure 9d, which is the $\sigma(HOMO_{10-CBS} \rightarrow \sigma^*_{Sn-Cl})$ bond, and it clearly verifies a participation of all four chlorine atoms. In addition, the enhanced orbital interaction seems to lead to a by 0.18 Å contracted tin–nitrogen bond, which in turn leads to a stronger electrostatic interaction. As a consequence of the change from axial to equatorial conformation seems to be clear, the question for the cause of the change arises. Especially since a comparable increase in orbital interaction could not be verified for the $TiCl_4$ adducts **13d** and **13k**.

In order to analyse the conformational change in more detail, an EDA-NOCV calculation of the $SnCl_4$–CBS adduct **9j fixed** (**9j** in the geometry of the corresponding **10**–CBS–$SnCl_4$ complex **13j**) was carried out to determine the impact of the conformational change without taking interactions with **10** into account. As shown in Table 3, the distortion of **9j** into **9j**

© 2016 Wiley-VCH Verlag GmbH & Co. KGaA, Weinheim

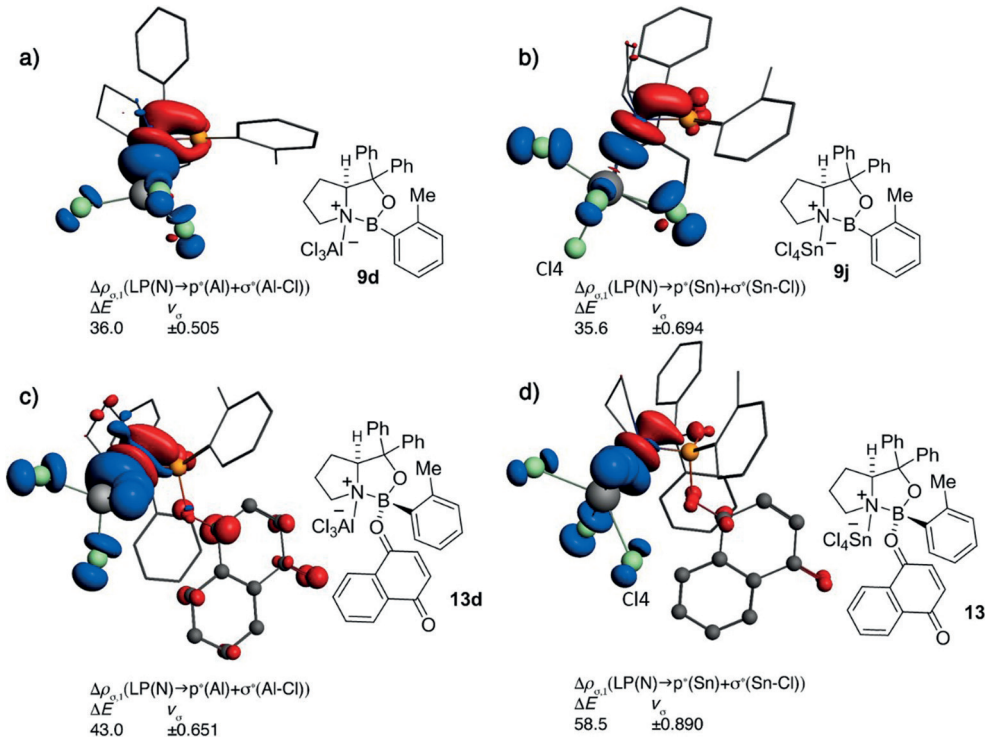

Figure 9. Plots of the NOCVs with the highest eigenvalue ($\Delta\rho_{\sigma,1}$) representing the donor–acceptor interaction ($LP(N_{CBS})\rightarrow LP^*(Al/Sn)+\sigma^*(LA\text{-}Cl)$) in: a) **9d**, b) **9j**, c) **13d**, and d) **13j** at BP86/TZ2P$^+$. b) The missing participation of the fourth chlorine atom of $SnCl_4$ in the CBS–$SnCl_4$ bond in **9j** can be seen. d) The deformation-induced participation of this atom in the **10**–CBS–$SnCl_4$ bond upon coordination of **10** to **9j** is visible. Colour coding: red = decrease of electron density; blue = increase of electron density.

Table 3. Overview of the energy terms given by bonding analysis (EDA-NOCV) of complexes **9e**, **9j**, and **9k**, as well as adducts **13e**, **13j**, and **13k**.

Lewis acid	$AlCl_3$		$SnCl_4$			$TiCl_4$	
energy contributions	complex **9d** [kcal mol^{-1}]	adduct **13d** [kcal mol^{-1}]	complex **9j** [kcal mol^{-1}]	**9j fixed** [kcal mol^{-1}]	adduct **13j** [kcal mol^{-1}]	complex **9k** [kcal mol^{-1}]	adduct **13k** [kcal mol^{-1}]
ΔE_{int}[a]	−60.3	−79.8	−49.6	−62.0 (25.0)[e]	−80.4 (30.0)[f]	−55.6	−65.2
ΔE_{Pauli}	104.2	116.9	111.5	140.2 (25.7)[e]	148.8 (6.1)[f]	106.0	109.3
ΔE_{elstat}	−87.5	−102.7	−77.2	−106.4 (37.8)[e]	−112.8 (6.0)[f]	−83.6	−79.1
$\Delta E_{orbital}$	−58.0	−72.7	−56.6	−74.3 (31.3)[e]	−88.4 (19.0)[f]	−54.1	−67.1
ΔE_{Disp}	−19.0	−21.3	−27.3	−21.5 (−21.2)[e]	−28.0 (30.2)[f]	−23.9	−28.3
ΔE_{prep}	18.4	23.9	27.2	74.7 (174.6)[e]	44.5	39.2	39.0
$\Delta E_{prep(LA)}$[b]	10.3	17.1	20.7	38.8 (87.4)[e]	38.8	28.0	33.4
ΔE_{bond} ($-D_e$)[c]	−41.9	−56.0	−22.5	12.7 (−156.7)[e]	−35.9 (135.4)[f]	−16.4	−26.2
$E_{HOMO(CBS)}$[d]	−0.283	−0.254	−0.290	−0.280 (3.4)[e]	−0.251 (11.8)[f]	−0.282	−0.253

[a] $\Delta E_{int}=\Delta E_{Pauli}+\Delta E_{elstat}+\Delta E_{orb}+\Delta E_{Disp}$. [b] Contribution of the preparation energy from the LA fragment to ΔE_{prep}. [c] $\Delta E_{bond}=\Delta E_{int}+\Delta E_{prep}$. [d] Energy of the HOMO of the respective CBS fragment [eV] at M06-2X/def2-TZVP. [e] Change [%] from **9j** to **9j fixed**. [f] Change [%] from **9j fixed** to **13j**.

fixed has two important impacts on interaction energies. First, the attractive interaction energies ΔE_{elstat} and ΔE_{orb} are amplified. In particular orbital interaction is increased to −74.3 kcal mol^{-1} (+31%) due to participation of all four chlorine atoms in donor–acceptor interaction, which is in line with the results for **13j**. Even if the Pauli repulsion is increased by 28.7 kcal mol^{-1}, ΔE_{int} is 12.4 kcal mol^{-1} (25.0%) higher in energy than in the relaxed structure of **9j**. However, the increase in ΔE_{int} is overcompensated by a disproportional increase of the preparation energy ΔE_{prep} by 175% resulting in a bonding energy ΔE_{bond} of +12.7 kcal mol^{-1}. This means that although the attractive interaction in **9j fixed** is somewhat higher than in **9j**, high ΔE_{prep} and an increase in ΔE_{Pauli} makes this conformation unstable, forcing $SnCl_4$ to adopt a trigonal bipyramidal conformation **9j**.

Only after introduction of naphthoquinone, the equatorial conformation becomes thermodynamically stable mainly due to an increase of orbital interaction by 19%. The increase in ΔE_{orb} can be assigned to the enhancement of Lewis basicity of the CBS fragment **1b** upon coordination of **10** which can be seen in the increase of $\Delta E_{HOMO(\mathbf{10}\text{–}CBS)}$ by 12% after coordination of **13**.

© 2016 Wiley-VCH Verlag GmbH & Co. KGaA, Weinheim

Apparently, the increase in Lewis basicity of the **10**–CBS fragment leads to exceeding a threshold, which only allows efficient interaction of all four chlorine atoms of $SnCl_4$ with the CBS fragment. In complex **13j** (Figure 9d) the distortion of the complex geometry leads to an enhanced Lewis acidity where all four chlorine atoms show participation in electron density delocalisation. This results in an increased Lewis acidity of $SnCl_4$ in **13j** compared to **9j**, which can be observed in a high k_{DA} value making $SnCl_4$ in the equatorial conformation a similar potent Lewis acid as $AlBr_3$.

Although the threshold in Lewis basicity for efficient interaction is the main factor that influences the interplay between both conformations, a second interaction that pushes **13j** towards the equatorial conformation could be found by analysing the NOCV interactions in **13j**. An C–H···Cl interaction $\Delta\rho_{\sigma,6}$ between the hydrogen atom of **10** at position 5 with the chlorine atom Cl3 could be found, which contributes about -1.9 kcal mol^{-1} (Figure 10). This further stabilizes the equatorial conformation and might be a reason for the high enantioselectivity of **9j** in the model Diels–Alder reaction. A similar halogen–hydrogen bond has been found by Fujimoto in his detailed theoretical study on $AlBr_3$–CBS adduct **9e** in the reaction of methacrolein with cyclopentadiene.[16]

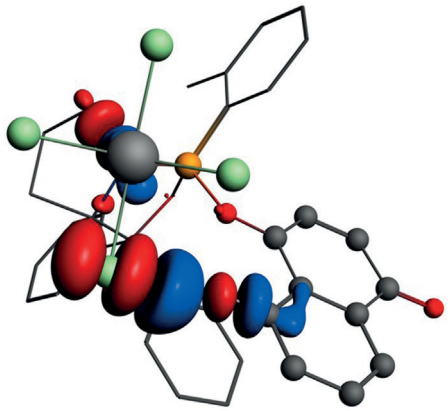

Figure 10. Plot of the NOCV interaction $\Delta\rho_{\sigma,6}$ between the $SnCl_4$ chlorine atoms and the hydrogen atom at position 5 of **10** in adduct **13j** with fragments **10**–CBS and $SnCl_4$ at BP86/TZ2P$^+$.

Conclusions

In conclusion, by combining ^{2}H NMR spectroscopic studies with in situ-IR kinetic measurements, we could demonstrate that several Lewis acids are able to activate CBS catalyst **1b** adequately for Diels–Alder reactions. This suggests the use of less aggressive acids than the commonly employed $AlBr_3$ or $HNTf_2$. The low experimentally quantified activation $\Delta\delta(^2H)$ of **1b** but large catalytic activity of $SnCl_4$–CBS adduct **9j** could be attributed to a conformational change of the chlorine atoms of $SnCl_4$ upon coordination of 1,4-naphthoquinone (**10**). This leads to a massively enhanced Lewis acidity of $SnCl_4$ within the **10**–$SnCl_4$–CBS complex **13j** and thereby to a higher activation of **10** in the Diels–Alder reaction. This behaviour could only be observed for $SnCl_4$. Trivalent Lewis acids such as $AlCl_3$, but also the tetravalent Lewis acid $TiCl_4$ did not show such a behaviour as they adopted only trigonal pyramidal or in case of $TiCl_4$ quadratic pyramidal conformation. The conformational change could be attributed to a more efficient Lewis acid base interaction upon complexation of 1,4-naphthoquinone (**10**) by raising the electron density within the CBS fragment and thus allowing an efficient donor–acceptor interaction of all four chlorine atoms of $SnCl_4$, which overcompensates the high necessary preparation energy. Furthermore, interactions of the hydrogen-atom in position 5 of the naphthoquinone with one of the chlorine atoms could be found which further stabilises the equatorial conformation.

The dependency of the acidity of group 13 based Lewis acids on their structure has been known for some time,[26] and has inspired the design of pre-organised tetrahedral group 13 Lewis acids.[27] A similar behaviour for group 4 and 14 Lewis acids has only been briefly touched on.[23] Through the presented study, both experimental and theoretical results could unravel the impact of the structural change of $SnCl_4$ on its acidity. Similar to the group-13-based Lewis acids, the design of sterically fixed tin-based Lewis acids should therefore lead to the development of novel, highly reactive catalysts.

Experimental Section

Procedure for the preparation of Lewis acid adducts [D$_1$]9 of [D$_1$]1b with stoichiometric amounts of Lewis acid

Inside a glovebox, deuterated CBS-catalyst ([D$_1$]**1b**, 32 mg, 90 μmol, 1.0 equiv) was weighed in a vial, equipped with a magnetic stirring bar. The vial was sealed with a rubber septum, transferred out of the glovebox and connected to a Schlenk line. Then CH_2Cl_2 (0.61 mL) was added, and the solution cooled to below $-70\,^\circ$C. A solution of the respective Lewis acid in CH_2Cl_2 (1.0 M, 90 μL, 90 μmol, 1.0 equiv) and 1 μL of $CDCl_3$ were added under constant stirring. After 15 min an aliquot of the solution (0.50 mL, 64 μmol adduct [D$_1$]**9**) was transferred into a below $-70\,^\circ$C pre-cooled NMR tube, which was sealed with a rubber/PTFE septum. The sample was kept below $-70\,^\circ$C and analysed by NMR spectroscopy at the desired temperature.

Exemplary procedure for the ReactIR kinetic analysis of the Diels–Alder reaction of 10 with 11 by using catalysts of type 9

A 25 mL two-neck Schlenk flask was equipped with a magnetic stirring bar and the ReactIR probe head, and was connected to a Schlenk line. Under argon atmosphere, the flask was cooled to $-40\,^\circ$C and CH_2Cl_2 (3.0 mL), an aliquot of stock solution of **10** (4.0 mL, 0.50 mmol, 1.0 equiv, CH_2Cl_2 ($c = 125$ mmol L^{-1})), as well as isoprene (**11**, 500 μL, 4.99 mmol, 10.0 equiv) were added. Depending on the amount of catalyst solution added later, CH_2Cl_2 (0.1 or 0.4 mL) was added. The in situ FTIR spectroscopic measurement was started, as soon as there were at least 3.0 mL solution in the flask. When the temperature ($-40(\pm 1)\,^\circ$C) as well as the intensity of the IR carbonyl band of dienophile **10** at 1670 cm^{-1} were stable, an aliquot of the respective adduct **9** in CH_2Cl_2 (0.02 mmol, 4.0 mol% active complex, preparation see below) was added under vigorous stirring (final concentrations: c(**10**) = 61.7 mmol L^{-1}, c(**11**) = 617 mmol L^{-1}, c(**9**) = 2.5 mmol L^{-1}, total volume: 8.1 mL).

© 2016 Wiley-VCH Verlag GmbH & Co. KGaA, Weinheim

After 1 min the stirring speed was slightly reduced and the reaction progress was monitored until no further increase of the intensity of the IR carbonyl band of product **12** at 1696 cm^{-1} was observed. To confirm full conversion, a sample (max. 50 μL) was taken, eluted over a small pad of silica gel with *tert*-butyl methyl ether, and subjected to GC-MS analysis. The reaction was stopped by addition of saturated aqueous $NaHCO_3$ solution (4.0 mL) and stirred at room temperature for 15 min. The phases were separated and the aqueous phase was extracted with CH_2Cl_2 (4×10 mL). The combined organic phases were dried over $MgSO_4$, the solvent was removed under reduced pressure, and the raw product was stored at −20 °C under inert atmosphere until HPLC analysis. The enantiomeric ratio of the raw product was determined by HPLC analysis (Agilent Technologies 1200 Series, Chiralpak IA column, 4.6 mm× 250 mmL, 20 °C, *n*-hexane/isopropanol 99:1, flow rate: 1.0 mL min^{-1}, $\lambda = 254$ nm, $t_R = 16.0$ min (major), $t_R = 17.8$ min (minor)).

Preparation of the Lewis acid–CBS adduct solution

Inside a glove box, CBS-catalyst (**1b**; 28–30 mg, 79–85 μmol) was weighed in a vial equipped with a magnetic stirring bar. The vial was sealed with a rubber septum, transferred out of the glovebox and connected to a Schlenk line. CH_2Cl_2 (0.54 mL) was added, the solution was cooled to below −30 °C, and a solution of the respective Lewis acid in CH_2Cl_2 (1.0 m, 60 μL, 60 μmol) was added under stirring. The solution was cooled to about −50 °C and was ready for use after 10 min.

Computational details

Unconstrained structural optimisation was carried out using Gaussian 09 in version C.01.[28] Pre-optimisations were carried out using the B1B95[29] functional with the def2-SVP[30] basis set. For each structure several possible conformers were tested but only the lowest energy conformer was used for further optimisation. Refined structures were obtained by optimisation using the M06–2X[31] functional and the def2-TZVP[30] basis set with an ultra fine integration grid. This choice of computational level was motivated by previous studies of Fujimoto et al. for the CBS-catalyst.[16] Character of a stationary point was identified by subsequent frequency calculation (number of imaginary frequencies (NIMAG): 0 for minimum structures). Formation enthalpies (ΔH) including zero-point vibrational energy (ZPVE) and thermal corrections were obtained from theses frequency calculation with $T = 298.15$ K and $P = 1$ atm. HOMO/LUMO energies are given as $\Delta E_{HOMO}/\Delta E_{LUMO}$ with respect to the HOMO/LUMO energy of free CBS/naphthoquinone molecules. EDA-NOCV analysis was carried out with the ADF program version 2014.10[32] on the BP86[33]/TZ2P$^+$[34] level using the empirical dispersion correction scheme DFT-D3.[35] All fragments were used in their singlet ground states.

Acknowledgements

We thank the Deutsche Forschungsgemeinschaft for financial support and we thank Prof. G. Frenking and L. Vondung for helpful discussions. We thank Prof. E. Meggers and Prof. P. von Zezschwitz for providing their equipment to determine enantioselectivies, as well as T. Mietke (Meggers group) and C. Pfaff (von Zezschwitz group) for their assistance.

Keywords: ab initio calculations · CBS catalyst · Diels–Alder reactions · frontier molecular orbitals · kinetics

[1] a) S. Itsuno, K. Ito, A. Hirao, S. Nakahama, *J. Chem. Soc. Chem. Commun.* **1983**, 469–470; b) S. Itsuno, K. Ito, A. Hirao, S. Nakahama, *J. Org. Chem.* **1984**, *49*, 555–557.

[2] a) E. J. Corey, R. K. Bakshi, S. Shibata, *J. Am. Chem. Soc.* **1987**, *109*, 5551–5553; b) E. J. Corey, R. K. Bakshi, S. Shibata, C.-P. Chen, V. K. Singh, *J. Am. Chem. Soc.* **1987**, *109*, 7925–7926.

[3] E. J. Corey, C. J. Helal, *Angew. Chem. Int. Ed.* **1998**, *37*, 1986–2012; *Angew. Chem.* **1998**, *110*, 2092–2118.

[4] a) E. J. Corey, T. Shibata, T. W. Lee, *J. Am. Chem. Soc.* **2002**, *124*, 3808–3809; b) D. H. Ryu, T. W. Lee, E. J. Corey, *J. Am. Chem. Soc.* **2002**, *124*, 9992–9993; c) D. H. Ryu, E. J. Corey, *J. Am. Chem. Soc.* **2003**, *125*, 6388–6390.

[5] E. J. Corey, *Angew. Chem. Int. Ed.* **2009**, *48*, 2100–2117; *Angew. Chem.* **2009**, *121*, 2134–2151.

[6] K. Futatsugi, H. Yamamoto, *Angew. Chem. Int. Ed.* **2005**, *44*, 1484–1487; *Angew. Chem.* **2005**, *117*, 1508–1511.

[7] D. Liu, E. Canales, E. J. Corey, *J. Am. Chem. Soc.* **2007**, *129*, 1498–1499.

[8] K. Mahender Reddy, E. Bhimireddy, B. Thirupathi, S. Breitler, S. Yu, E. J. Corey, *J. Am. Chem. Soc.* **2016**, *138*, 2443–2453.

[9] a) G. Zhou, Q.-Y. Hu, E. J. Corey, *Org. Lett.* **2003**, *5*, 3979–3982; b) Q.-Y. Hu, G. Zhou, E. J. Corey, *J. Am. Chem. Soc.* **2004**, *126*, 13708–13713; c) Q.-Y. Hu, P. D. Rege, E. J. Corey, *J. Am. Chem. Soc.* **2004**, *126*, 5984–5986; d) S. A. Snyder, E. J. Corey, *J. Am. Chem. Soc.* **2006**, *128*, 740–742; e) S. Hong, E. J. Corey, *J. Am. Chem. Soc.* **2006**, *128*, 1346–1352; f) J. Y. Sim, G.-S. Hwang, H. K. Kim, E. M. Ko, D. H. Ryu, *Chem. Commun.* **2007**, 5064–5064; g) S. Mukherjee, A. P. Scopton, E. J. Corey, *Org. Lett.* **2010**, *12*, 1836–1838; h) B. K. Senapati, L. Gao, S. I. Lee, G. S. Hwang, D. J. Ryu, *Org. Lett.* **2010**, *12*, 5088–5091; i) M. Y. Jin, G.-S. Hwang, H. I. Chae, S. H. Jung, D. H. Ryu, *Bull. Korean Chem. Soc.* **2010**, *31*, 727–730; j) D. R. Hookins, A. R. Burns, R. J. K. Taylor, *Eur. J. Org. Chem.* **2011**, 451–454.

[10] a) E. J. Hicken, E. J. Corey, *Org. Lett.* **2008**, *10*, 1135–1138; b) S. Jones, D. Valette, *Org. Lett.* **2009**, *11*, 5358–5361; c) M. Schubert, P. Metz, *Angew. Chem. Int. Ed.* **2011**, *50*, 2954–2956; *Angew. Chem.* **2011**, *123*, 3011–3013.

[11] a) G. Hilt, F. Pünner, J. Möbus, V. Naseri, M. A. Bohn, *Eur. J. Org. Chem.* **2011**, 5962–5966; b) G. Hilt, A. R. Nödling, *Eur. J. Org. Chem.* **2011**, 7071–7075; c) A. R. Nödling, K. Müther, V. H. G. Rohde, G. Hilt, M. Oestreich, *Organometallics* **2014**, *33*, 302–308; d) A. R. Nödling, G. Jakab, P. R. Schreiner, G. Hilt, *Eur. J. Org. Chem.* **2014**, 6394–6398.

[12] C. Sparr, E.-M. Tanzer, J. Bachmann, R. Gilmour, *Synthesis* **2010**, 1394–1397.

[13] J. N. Payette, H. Yamamoto, *Angew. Chem. Int. Ed.* **2009**, *48*, 8060–8062; *Angew. Chem.* **2009**, *121*, 8204–8206.

[14] a) R. F. Childs, D. L. Mulholland, A. Nixon, *Can. J. Chem.* **1982**, *60*, 801–808; b) M. A. Beckett, D. S. Brassington, S. J. Coles, M. B. Hursthouse, *Inorg. Chem. Commun.* **2000**, *3*, 530–533; c) L. O. Müller, D. Himmel, J. Stauffer, G. Steinfeld, J. Slattery, G. Santiso-Quiñones, V. Brecht, I. Krossing, *Angew. Chem. Int. Ed.* **2008**, *47*, 7659–7663; *Angew. Chem.* **2008**, *120*, 7772–7776; d) H. Böhrer, N. Trapp, D. Himmel, M. Schleep, I. Krossing, *Dalton Trans.* **2015**, *44*, 7489–7499.

[15] The formation of multiple species is known from Corey's reports on Brønsted acid adduct **3a** (see ref. [4c]), but in this case different ion pair species are formed.

[16] K. Sakata, H. Fujimoto, *J. Org. Chem.* **2013**, *78*, 3095–3103.

[17] M. N. Paddon-Row, L. C. H. Kwan, A. C. Willis, M. S. Sherburn, *Angew. Chem. Int. Ed.* **2008**, *47*, 7013–7017; *Angew. Chem.* **2008**, *120*, 7121–7125.

[18] Preliminary proof-of-principle studies of **9j** as catalyst in further Diels–Alder reactions showed performances of **9j** comparable to **9e**, see the Supporting Information for further details.

[19] a) R. B. Woodward, R. Hoffmann, in *The Conservation of Orbital Symmetry*, Verlag Chemie, Weinheim, **1970**; b) J. Sauer, R. Sustmann, *Angew. Chem. Int. Ed. Engl.* **1980**, *19*, 779–807; *Angew. Chem.* **1980**, *92*, 773–801; c) O. F. Guner, R. M. Ottenbrite, D. D. Shillady, P. V. Alston, *J. Org. Chem.* **1987**, *52*, 391–394.

© 2016 Wiley-VCH Verlag GmbH & Co. KGaA, Weinheim

[20] a) P. Laszlo, M. Teston, *J. Am. Chem. Soc.* **1990**, *112*, 8750 – 8754; b) P. Laszlo, M. Teston, *Tetrahedron Lett.* **1991**, *32*, 3837 – 3838.
[21] Coordination of indium-based Lewis acids to the CBS-fragment was confirmed by analysis of the crucial bond lengths and by EDA-NOCV calculation.
[22] E. I. Davydova, T. N. Sevastianova, A. V. Suvorov, A. Y. Timoshkin, *Coord. Chem. Rev.* **2010**, *254*, 2031 – 2077.
[23] E. I. Davydova, A. Y. Timoshkin, T. N. Sevastianova, A. V. Suvorov, G. Frenking, *Comput. Theor. Chem.* **2006**, *767*, 103 – 111.
[24] W. A. Grigsby, T. S. Morien, C. L. Raston, B. W. Skelton, A. H. White, *Aust. J. Chem.* **2004**, *57*, 507 – 508.
[25] a) K. Kitaura, K. Morokuma, *Int. J. Quantum Chem.* **1976**, *10*, 325 – 340; b) T. Ziegler, A. Rauk, *Theor. Chim. Acta* **1977**, *46*, 1 – 10; c) M. Mitoraj, A. Michalak, *J. Mol. Model.* **2008**, *14*, 681 – 687; d) A. Michalak, M. Mitoraj, T. Ziegler, *J. Phys. Chem. A* **2008**, *112*, 1933 – 1939; e) M. Mitoraj, A. Michalak, T. Ziegler, *J. Chem. Theory Comput.* **2009**, *5*, 962 – 975; f) M. Mitoraj, A. Michalak, T. Ziegler, *Organometallics* **2009**, *28*, 3727 – 3733; g) M. Srebro, A. Michalak, *Inorg. Chem.* **2009**, *48*, 5361 – 5369; h) I. Purushothaman, S. De, P. Parameswaran, *RSC Adv.* **2014**, *4*, 60421 – 60428.
[26] a) C. Loschen, K. Voigt, J. Frunzke, A. Diefenbach, M. Diedenhofen, G. Frenking, *Z. Allg. Anorg. Chem.* **2002**, *628*, 1294 – 1304; b) G. Frenking, K. Wichmann, N. Fröhlich, C. Loschen, M. Lein, J. Frunzke, V. M. Rayón, *Coord. Chem. Rev.* **2003**, *238 – 239*, 55 – 82; c) F. Bessac, G. Frenking, *Inorg. Chem.* **2006**, *45*, 6956 – 6964; d) L. A. Mück, A. Y. Timoshkin, M. von Hopffgarten, G. Frenking, *J. Am. Chem. Soc.* **2009**, *131*, 3942 – 3949; e) A. S. Lisovenko, A. Y. Timoshkin, *Inorg. Chem.* **2010**, *49*, 10357 – 10369; f) L. A. Mück, A. Y. Timoshkin, G. Frenking, *Inorg. Chem.* **2012**, *51*, 640 – 646.
[27] H. Zhu, E. Chen, *Inorg. Chem.* **2007**, *46*, 1481 – 1487.
[28] Gaussian 09, Revision C.01, M. J. Frisch, G. W. Trucks, H. B. Schlegel, G. E. Scuseria, M. A. Robb, J. R. Cheeseman, G. Scalmani, V. Barone, B. Mennucci, G. A. Petersson, H. Nakatsuji, M. Caricato, X. Li, H. P. Hratchian, A. F. Izmaylov, J. Bloino, G. Zheng, J. L. Sonnenberg, M. Hada, M. Ehara, K. Toyota, R. Fukuda, J. Hasegawa, M. Ishida, T. Nakajima, Y. Honda, O. Kitao, H. Nakai, T. Vreven, J. A. Montgomery, Jr., J. E. Peralta, F. Ogliaro, M. Bearpark, J. J. Heyd, E. Brothers, K. N. Kudin, V. N. Staroverov, R. Kobayashi, J. Normand, K. Raghavachari, A. Rendell, J. C. Burant, S. S. Iyengar, J. Tomasi, M. Cossi, N. Rega, J. M. Millam, M. Klene, J. E. Knox, J. B. Cross, V. Bakken, C. Adamo, J. Jaramillo, R. Gomperts, R. E. Stratmann, O. Yazyev, A. J. Austin, R. Cammi, C. Pomelli, J. W. Ochterski, R. L. Martin, K. Morokuma, V. G. Zakrzewski, G. A. Voth, P. Salvador, J. J. Dannenberg, S. Dapprich, A. D. Daniels, Ö. Farkas, J. B. Foresman, J. V. Ortiz, J. Cioslowski, D. J. Fox, Gaussian, Inc., Wallingford CT, **2009**.
[29] A. D. Becke, *J. Chem. Phys.* **1996**, *104*, 1040 – 1046.
[30] F. Weigend, R. Ahlrichs, *Phys. Chem. Chem. Phys.* **2005**, *7*, 3297 – 3305; b) B. Metz, H. Stoll, M. Dolg, *J. Chem. Phys.* **2000**, *113*, 2563 – 2569; c) F. Weigend, *Phys. Chem. Chem. Phys.* **2006**, *8*, 1057 – 1065.
[31] a) Y. Zhao, D. G. Truhlar, *Theor. Chem. Acc.* **2008**, *120*, 215 – 241; b) Y. Zhao, D. G. Truhlar, *Acc. Chem. Res.* **2008**, *41*, 157 – 167.
[32] a) G. te Velde, F. M. Bickelhaupt, E. J. Baerends, C. Fonseca Guerra, S. J. A. van Gisbergen, J. G. Snijders, T. Ziegler, *J. Comput. Chem.* **2001**, *22*, 931 – 967; b) C. Fonseca Guerra, J. G. Snijders, G. te Velde, E. J. Baerends, *Theor. Chem. Acc.* **1998**, *99*, 391 – 403; c) ADF2014, SCM, Theoretical Chemistry, Vrije Universiteit, Amsterdam, The Netherlands: http://www.scm.com.
[33] a) J. Perdew, *Phys. Rev. B* **1986**, *33*, 8822 – 8824; b) A. Becke, *Phys. Rev. A* **1988**, *38*, 3098 – 3100.
[34] E. van Lenthe, E. J. Baerends, *J. Comput. Chem.* **2003**, *24*, 1142 – 1156.
[35] a) S. Grimme, J. Antony, S. Ehrlich, H. Krieg, *J. Chem. Phys.* **2010**, *132*, 154104; b) S. Grimme, S. Ehrlich, L. Goerigk, *J. Comput. Chem.* **2011**, *32*, 1456 – 1465.

Received: May 19, 2016
Published online on August 5, 2016

© 2016 Wiley-VCH Verlag GmbH & Co. KGaA, Weinheim

Electrosynthesis

International Edition: DOI: 10.1002/anie.201711293
German Edition: DOI: 10.1002/ange.201711293

Electrochemical Synthesis of Aryl Iodides by Anodic Iododesilylation

*Robert Möckel, Jessica Hille, Erik Winterling, Stephan Weidemüller, Tabea Melanie Faber, and Gerhard Hilt**

Dedicated to Professor Reinhart Möckel

Abstract: *An electrochemical access to iodinated aromatic compounds starting from trimethylsilyl-substituted arenes is presented. By design of experiments, highly efficient and mild conditions were identified for a wide range of substrates. A functional group stability test and the synthesis of an important 3-iodobenzylguanidine radiotracer illustrate the scope of this process.*

Aryl iodides are used as precursors in contemporary carbon–carbon bond-forming reactions,[1] for the synthesis of hypervalent iodine compounds,[2] or as radiopharmaceuticals,[3] and a variety of approaches have been developed for their synthesis. Most often, their synthesis is accomplished by electrophilic aromatic substitution, either by using pregenerated electrophilic iodinating reagents such as *N*-iodosuccinimide (NIS) or by in situ oxidation of iodide or iodine to reactive iodonium ions with various oxidants.[4] The central problem to all possibilities is the lack of atom efficiency as pregenerated reagents or oxidants have to be used in stoichiometric amounts. The electrochemical generation of electrophilic iodinating species offers a unique solution to reduce the amount of waste chemicals. A seminal example of this approach was reported by Yoshida and co-workers who directly iodinated aromatic substrates by electrochemical generation of iodonium ions (Scheme 1).[5] The only drawback of this and similar methods is the decreased control over substitution site selectivity when performing the reaction in a one-pot fashion, and the restriction to electron-rich substrates.

An iodination method reported recently by our group relied on the generation of reactive *tert*-butyl hypoiodite by the reaction of zinc iodide with *tert*-butyl hydrogen peroxide (TBHP), which was reacted in situ with trimethylsilyl arenes (Scheme 1).[6] The introduction of a trimethylsilyl group allowed for selective iodination. The major limitation was, apart from low atom economy, a diminished substrate range,

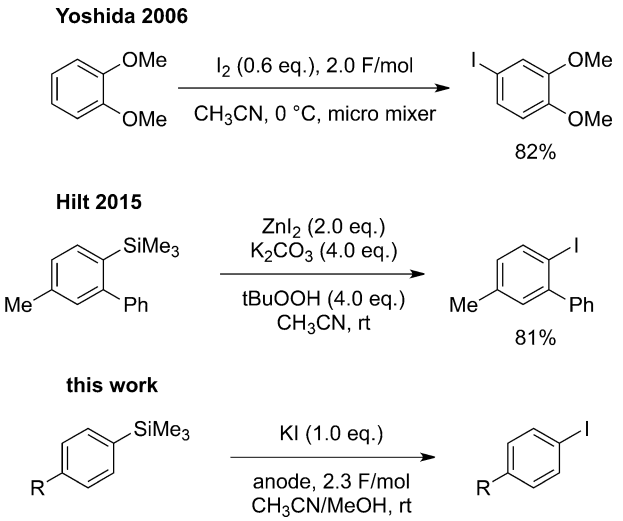

Scheme 1. Iodination reactions.[5,6]

as mainly electron-rich substrates and preferably *ortho*-substituted trimethylsilyl arenes could be employed with satisfying yields. Nevertheless, the method showed excellent selectivity, and the substrates were easily accessible from regioselective cobalt-catalysed Diels–Alder reactions of trimethylsilyl-substituted alkynes with 1,3-dienes.[7]

Herein, we describe the combination of our strategy with sustainable electrochemical methods into a novel protocol. We sought to introduce, in analogy to our initial iodination procedure, a trimethylsilyl group as the directing group for an iododesilylation reaction. The use of a directing group to enhance selectivity combined with high reactivity and short reaction times would outweigh the negative impact on atom economy.

As part of the optimisation, a number of preconditions were drawn to guarantee the design of a simple, mild, green, and inexpensive process. The reaction should be conducted at room temperature, no inert conditions should be necessary, and the iodine source should be potassium iodide as we were hoping to thereby obviate the need for an additional supporting electrolyte. Furthermore, a constant current density of 6.7 $mA\,cm^{-1}$ was applied to allow for a chemoselective electrochemical reaction and to keep the reaction times relatively short.

In a first test reaction with trimethyl(phenyl)silane (**1**) as the substrate, no product was detected upon using an undivided cell (Table 1, entry 1). Therefore, the screening of commonly used solvents (entry 2–5) and all following reac-

[*] M. Sc. R. Möckel, J. Hille, E. Winterling, S. Weidemüller, T. M. Faber, Prof. Dr. G. Hilt
Fachbereich Chemie, Philipps-Universität Marburg
Hans-Meerwein-Straße 4, 35043 Marburg (Germany)
M. Sc. R. Möckel, Prof. Dr. G. Hilt
Institut für Chemie, Universität Oldenburg
Carl-von-Ossietzky-Straße 9–11, 26111 Oldenburg (Germany)
E-mail: gerhard.hilt@uni-oldenburg.de
Supporting information and the ORCID identification number(s) for the author(s) of this article can be found under: https://doi.org/10.1002/anie.201711293.

 © 2018 Wiley-VCH Verlag GmbH & Co. KGaA, Weinheim

Table 1: Electrochemical iododesilylation of trimethyl(phenyl)silane **1**.

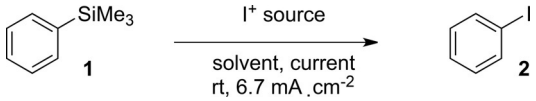

Entry	Solvent	KI [equiv]	Applied charge [F mol^{-1}]	Yield [%]
1[a]	MeCN	1.0	2.0	0
2	MeCN	1.0	2.0	40
3	$(MeOCH_2)_2$	1.0	2.0	10
4	CH_2Cl_2	1.0	2.0	37
5	MeOH	1.0	2.0	10
6	MeCN/MeOH (1:1)	1.0	2.0	64
7	MeCN/MeOH (7:3)	1.0	2.0	80
8	MeCN/MeOH (7:3)	1.1	2.2	84
9	**MeCN/MeOH (7:3)**	**1.1**	**2.4**	**97**
10	MeCN/MeOH (7:3)	1.2	2.4	86
11	MeCN/MeOH (7:3)	1.2	2.6	94
12[b]	MeCN/MeOH (7:3)	1.0	2.0	48
13[c]	MeCN/MeOH (7:3)	1.1	2.4	–[f]
14[d]	MeCN/MeOH (7:3)	1.1	2.4	–[f]
15[e]	MeCN/MeOH (7:3)	1.1	2.4	87

Unless otherwise stated, a divided cell with platinum electrodes with 0.5 mL conc. H_2SO_4 in the cathode compartment was used. The yields were determined by GC analysis using mesitylene as the internal standard (for experimental details, see the Supporting Information). [a] An undivided cell was used. [b] Graphite electrodes were used. [c] Instead of H_2SO_4, acetic acid (1 mL) was used. [d] Instead of H_2SO_4, methanesulfonic acid (0.5 mL) was used. [e] Instead of H_2SO_4, $LiClO_4$ (3 mmol, 0.3 M) was used. [f] No conductivity observed.

tions were performed in H-type divided cells. Disappointingly, the best yield of **2** was quite low (40%) even when acetonitrile was used as the solvent. When CH_2Cl_2, methanol, or dimethoxyethane were used, the yields amounted only to 10–37% (entry 1–5). The low yields were attributed to the formation of large quantities of the protodesilylation side product benzene. Only a solvent mixture of acetonitrile/methanol (1:1) led to an improved yield of 64%, mainly owing to a significant decrease in the protodesilylation side reaction.[8] A slight decrease in the methanol content to a 7:3 mixture further increased the yield to 80%. A final improvement was achieved by slightly increasing the KI loading to 1.1 equiv and adjusting the applied charge to 2.4 F mol^{-1}, which resulted in an almost quantitative yield of 97%. However, a further increase in the amount of the iodine source or the applied charge (entries 10 and 11) led to decreases in yield. Unfortunately, changing the electrodes from platinum plates to graphite decreased the yield to 48% (entry 12). Finally, the acid or supporting electrolyte that was used in the cathode compartment to lower the cell potential was changed from sulfuric acid to acetic acid, methanesulfonic acid, or lithium perchlorate, but all of them led to reduced yields (entry 13–15).

To our disappointment, when we applied our optimized reaction conditions to substrates other than trimethylsilyl benzene, the yields were only moderate (68–71%; see the Supporting Information). The main reason was determined by profound GC/MS analysis of the reaction products: Significant quantities of the starting materials were found to be methoxylated at the benzylic position, if present. Control experiments without an iodonium source in the reaction or with a substrate without a TMS group (toluene) suggested that the methoxylation occurs mainly under participation of iodonium ions and only when TMS-substituted substrates are present.

To improve the yields and decrease the extent of methoxylation, we investigated the influence of the iodide loading and the solvent in more detail. To cover the methoxylation side reaction as well, (*para*-tolyl)trimethylsilane was used as a test substrate for this series of experiments. To be able to address all important interactions between the parameters, we used a design of experiment approach applying a central composite plan.[9,10] Parameters being optimized were a) the methanol concentration (1:1–9:1 acetonitrile/methanol (lower methanol concentrations were excluded because they lead to poor conductivity and therefore need an additional electrolyte)), b) the KI stoichiometry (1.0–1.2 equiv), and c) the applied charge (2.2–2.5 F mol^{-1}) as those three parameters seemed to have the biggest impact on yields according to our previous optimization. The resulting plan contained 18 reactions covering one- and two-factor and quadratic interactions (Table 2).

Table 2: Optimisation by design of experiments.[a]

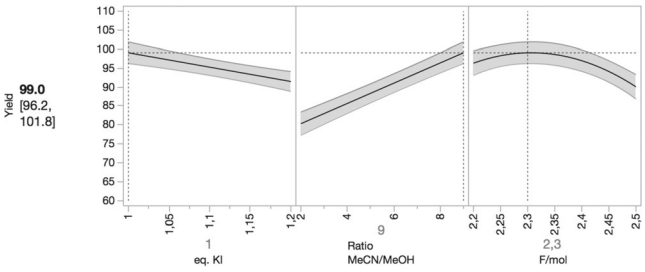

Factor	*p* Value
MeCN/MeOH ratio	0.0000
(applied electricity)^2	0.0001
amount of KI	0.0003
applied electricity × MeCN/MeOH ratio	0.0031

[a] All reactions were carried out on 0.5 mmol scale using a divided cell and platinum electrodes. The yields were determined by GC-FID analysis using mesitylene as the internal standard (see the Supporting Information for details). Numbers in grey indicate the optimal values for the three parameters and the corresponding yield (with its confidence interval in brackets). The *p* values indicate the probability of whether the respective effect can be explained by the null hypothesis (effects below 0.01 are regarded as significant).[9e]

Four important interactions returning a model with an R^2 value of 0.95 (which confirms that there are only slight differences between the observed and predicted values) were found: a) the methanol concentration, b) the quadratic term of the applied electricity, c) a two-factor interaction between methanol concentration and charge consumption, and d) the KI equivalents. According to the obtained model, the optimal values for the three parameters are a methanol concentration of 10 vol% in acetonitrile, 1.0 equiv of KI, and an applied charge of 2.3 F mol^{-1}.

These observations are in line with the previously obtained results as a minimal iodide loading and a minimal

 © 2018 Wiley-VCH Verlag GmbH & Co. KGaA, Weinheim

methanol concentration should supress methoxylation. The greater applied charge than the theoretically needed 2.0 F mol^{-1} can be ascribed to partial oxidation of the solvent. This can be seen in the two-factor interaction, which shows that the necessary applied electricity is higher (and the yields are lower) for higher methanol concentrations as oxidation of methanol becomes more decisive.

The optimised reaction conditions were tested on a variety of *ortho*-, *meta*-, and *para*-functionalized TMS-substituted arenes (Scheme 2) with electron-donating and electron-withdrawing substituents. Good to excellent yields of 70–97% were mostly obtained for both electron-deficient substrates, such as (4-fluorophenyl)trimethylsilane (**4c**, 88%), and electron-rich substrates, such as (4-methoxyphenyl)trimethylsilane (**4b**, 73%). A steric influence as in our initial paper could not be detected as the yields for *para*- and *ortho*-substituted substrates were comparable. Very electron-poor substrates (**3f**) showed diminished reactivity, leading to low yields or extended reaction times. Furthermore, (3-methoxyphenyl)trimethylsilane (**3h**) gave the corresponding product in a poor yield of 31%, which, according to GC-MS analysis, can be explained by direct iodination between the methoxy and the TMS group without affecting the trimethylsilyl group.

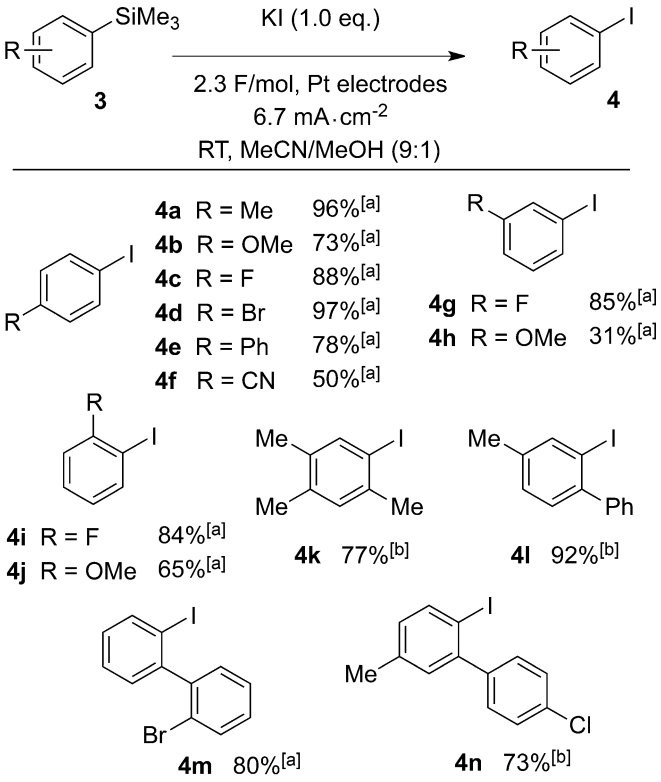

Scheme 2. Results of the electrochemical TMS–iodine exchange reaction. [a] Yield determined by GC-FID analysis using mesitylene as the internal standard. [b] Yield of isolated product.

To check for further functional group tolerance, a method developed by Glorius and co-workers was used.[11] This method is based on the addition of additives containing a certain functional group. To test the reaction compatibility, the yield of the desired product and the amount of additive recovered after the reaction are determined, which gives an indication for the stability of the respective additional functional group under the applied reaction conditions (Table 3).

Table 3: Functional group tolerance test using (*para*-tolyl)trimethylsilane as the substrate.[a]

Additive	Yield (starting material)	Yield (product)	Yield (additive)
1-octene	71%	13%	0%
1-dodecyne	62%	4%	13%
benzonitrile	5%	89%	96%
butyl phenyl ketone	0%	86%	78%
methyl benzoate	4%	82%	81%
aniline	5%	0%	0%
nitrobenzene	0%	84%	100%
carbazole	0%	83%	0%
indole	0%	65%	0%
sulfolane	0%	76%	100%
4-FC_6H_4-CH_2-PPh_3Br	12%	56%	86%[b]
1,2-epoxy-*n*-octane	37%	38%	0%
cyclopropylbenzene	86%	8%	32%

[a] If not stated otherwise, the yields were determined by GC-FID analysis. [b] Determined by ^{19}F NMR analysis using C_6F_6 as an internal standard.

In general, functional groups that lack oxidative stability, such as many heteroaromatic compounds, alcohols, and primary amines, do not withstand the strong oxidative reaction conditions of the electrolysis. Likewise, groups that show reactivity towards iodonium ions, such as alkenes and alkynes, are not compatible. However, a number of other functional groups, such as aromatic halides, ester, amide, keto, nitrile, nitro, or sulfone moieties, as well as phosphonium salts were stable under these conditions.

To demonstrate an application of our method, we chose the iododesilylation of Boc-protected 3-trimethysilylbenzyl guanidine **5** as the Boc-deprotected variant of the iododesilylation product is used as an ^{121}I tracer in SPECT tomography and as a tumour therapeutic in its ^{129}I-marked version.[12] The Boc-protected substrate was employed as we knew from the compatibility test that primary amines are not tolerated (Scheme 3). Nevertheless, this structure still has a high functional group density, which renders it a challenging

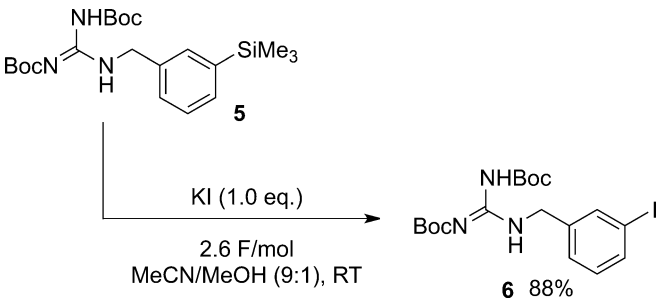

Scheme 3. Electrochemical TMS–iodine exchange for the synthesis of the derivative of a tumour therapeutic.

 © 2018 Wiley-VCH Verlag GmbH & Co. KGaA, Weinheim

substrate for an electrochemical reaction under oxidative conditions. Fortunately, we were able to isolate the product **6** on a 0.25 mmol scale without the need for column purification in 88%. This example not only demonstrates the overall good functional group tolerance but furthermore a possible application in the synthesis of isotopically labelled iodine molecules for applications in the life sciences. As the reaction time depends solely on the amount of used starting material and reactions for isotope labelling are typically conducted on very small scales, this process should be a highly useful alternative to existing iodination methods.[12]

In conclusion, we have developed a new approach for the synthesis of aryl iodides by electrochemical iododesilylation that is atom-economic and only requires sulfuric acid as the supporting electrolyte within the cathode compartment. Various products were obtained in good to very good yields upon rational optimization by design of experiments. The broad functional group tolerance was illustrated with a large variety of substrates and furthermore by a compatibility test. Finally, we applied the method for the synthesis of Boc-protected 3-iodobenzylguanidine, which yielded the product in 88% yield without the need for further expensive purification.

Experimental Section

General procedure for the electrochemical iododesilylation: In an H-type cell, the anode chamber was charged with the aryl trimethylsilane (1.00 mmol, 1.00 equiv) and potassium iodide (1.00 mmol, 1.00 equiv), and the cathode chamber was charged with sulfuric acid (0.5 mL). The respective solvent was added simultaneously to the anode (10 mL) and cathode (9.5 mL + 0.5 mL H_2SO_4 conc.) chambers. The cell was equipped with platinum electrodes, and the solutions were stirred until all solids had dissolved. The reaction was electrolysed under constant current (6.7 mA cm^{-2}) at room temperature until the conversion (GC/MS monitoring; normally complete conversion could be observed with the naked eye as the colour of the anode chamber changed from dark red to yellow) reached completion. The yield was either determined by GC analysis (mesitylene as the standard) or the solution was diluted with diethyl ether, washed with potassium carbonate and sodium thiosulfate, dried over magnesium sulfate, and concentrated under reduced pressure. If necessary, the crude product was purified by flash chromatography on silica gel.

Acknowledgements

We thank the Hochschulrechenzentrum Marburg and Oldenburg for providing computer time and for the excellent service. We thank C. Kohlmeyer for valuable help with the synthesis of starting materials and for helpful discussions. R.M. thanks Reinhart Möckel for an introduction into "design of experiments".

Conflict of interest

The authors declare no conflict of interest.

Keywords: arenes · compatibility test · design of experiments · electrochemistry · iododesilylation

How to cite: *Angew. Chem. Int. Ed.* **2018**, *57*, 442–445
Angew. Chem. **2018**, *130*, 450–454

[1] a) T. Dohi, Y. Kita in *Iodine Chemistry and Applications* (Ed.: T. Kaiho), Wiley, Hoboken, **2014**, pp. 303–310.
[2] a) L. Skulski, *Molecules* **2000**, *5*, 1331; b) E. A. Merritt, B. Olofsson, *Angew. Chem. Int. Ed.* **2009**, *48*, 9052; *Angew. Chem.* **2009**, *121*, 9214; c) Y. Li, D. P. Hari, M. V. Vita, J. Waser, *Angew. Chem. Int. Ed.* **2016**, *55*, 4436; *Angew. Chem.* **2016**, *128*, 4512; d) A. Yoshimura, V. V. Zhdankin, *Chem. Rev.* **2016**, *116*, 3328.
[3] a) M. H. Bourguignon, E. K. J. Pauwels, C. Loc'h, B. Mazière, *Eur. J. Nucl. Med.* **1997**, *24*, 331; b) S. J. Goldsmith, *Semin. Nucl. Med.* **1975**, *5*, 125; c) M. H. Rønnest, F. Nissen, P. J. Pedersen, T. O. Larsen, W. Mier, M. H. Clausen, *Eur. J. Org. Chem.* **2013**, 3970.
[4] a) S. Stavber, M. Jereb, M. Zupan, J. Stefan, *Synthesis* **2008**, 1487; b) S. R. Waldvogel, K. M. Wehming, *Sci. Synth.* **2007**, *31*, 235.
[5] a) K. Midorikawa, S. Suga, J.-i. Yoshida, *Chem. Commun.* **2006**, 3794; b) K. Kataoka, Y. Hagiwara, K. Midorikawa, S. Suga, J.-i. Yoshida, *Org. Process Res. Dev.* **2008**, *12*, 1130.
[6] R. Möckel, G. Hilt, *Org. Lett.* **2015**, *17*, 1644.
[7] G. Hilt, J. Janikowski, W. Hess, *Angew. Chem. Int. Ed.* **2006**, *45*, 5204; *Angew. Chem.* **2006**, *118*, 5328.
[8] Initial isodesmic and mechanistic DFT calculations suggested that the addition of methanol leads to the formation of MeOI instead of HSO_4I as the iodinating species, which might be the reason for the reduced extent of protodesilylation owing to the aprotic character of methyl hypoiodite compared to HSO_4I; see: V. D. Filimonov, O. K. Poleshchuk, E. A. Krasnokutskaya, G. Frenking, *J. Mol. Model.* **2011**, *17*, 2759.
[9] JMP, Version 13.1., SAS Institute Inc., Cary, NC, **1989–2013**.
[10] a) P. M. Murray, F. Bellany, L. Benhamou, D.-K. Bučar, A. B. Taborb, T. D. Sheppard, *Org. Biomol. Chem.* **2016**, *14*, 2373; b) S. A. Weissman, N. G. Anderson, *Org. Process Res. Dev.* **2015**, *19*, 1605; c) E. N. Bess, A. J. Bischoff, M. S. Sigman, *Proc. Natl. Acad. Sci. USA* **2014**, *111*, 14698; d) P. Renzi, M. Bella, *Synlett* **2017**, *28*, 306; e) R. Nuzzo, *Nature* **2014**, *506*, 150; f) a central composite design consists of a full factorial plan in which each factor is measured on two levels and an additional centre point that is augmented with points on each face of the design ("star points") in order to measure curvature (quadratic functions of the factors).
[11] a) K. D. Collins, F. Glorius, *Nat. Chem.* **2013**, *5*, 597; b) K. D. Collins, A. Rühling, F. Glorius, *Nat. Protoc.* **2014**, *9*, 1348; c) T. Gensch, F. Glorius, *Science* **2016**, *352*, 294.
[12] a) G. Vaidyanathan, S. Shankar, M. R. Zalutsky, *Bioconjugate Chem.* **2001**, *12*, 786; b) A. van Berkel, K. Pacak, J. W. M. Lenders, *Clin. Endocrinol.* **2014**, *81*, 329; c) J. J. Mukherjee, G. A. Kaltsas, N. Islam, P. N. Plowman, R. Foley, J. Hikmat, K. E. Britton, P. J. Jenkins, S. L. Chew, J. P. Monson, G. M. Besser, A. B. Grossman, *Clin. Endocrinol.* **2001**, *55*, 47.

Manuscript received: November 3, 2017
Version of record online: December 7, 2017

 © 2018 Wiley-VCH Verlag GmbH & Co. KGaA, Weinheim

Elektrosynthese

Deutsche Ausgabe: DOI: 10.1002/ange.201711293
Internationale Ausgabe: DOI: 10.1002/anie.201711293

Elektrochemische Synthese von Aryliodiden durch anodische Iododesilylierung

*Robert Möckel, Jessica Hille, Erik Winterling, Stephan Weidemüller, Tabea Melanie Faber und Gerhard Hilt**

Professor Reinhart Möckel gewidmet

Abstract: *Ein neuer elektrochemischer Zugang zu Iodaromaten ausgehend von Trimethylsilyl-substituierten Aromaten wird präsentiert. Durch statistische Versuchsplanung konnten sehr effiziente und milde Reaktionsbedingungen gefunden und auf eine Vielzahl von Substraten angewendet werden. Ein Kompatibilitätstest und die Verwendung der Methode zur Synthese eines 3-Iodbenzylguanidin-Derivats (Radiomarker) illustrieren die Anwendungsbreite.*

Aryliodide werden in der modernen Chemie als Edukte für die Bildung von Kohlenstoff-Kohlenstoff-Bindungen,[1] zur Synthese von hypervalenten Iodverbindungen[2] und als Radiopharmazeutika genutzt.[3] Folgerichtig sind eine Reihe von unterschiedlichen Syntheserouten für Aryliodide entwickelt worden. Sehr häufig werden elektrophile Substitutionen genutzt, wobei entweder elektrophile Iodierungsmittel wie etwa NIS eingesetzt oder reaktive Iodonium-Ionen in situ durch Oxidation von Iodid oder elementarem Iod hergestellt werden.[4] Das zentrale Problem dieser Zugangswege ist ihre fehlende Atomeffizienz, denn vorgefertigte Iodierungsmittel oder stöchiometrische Mengen von Oxidationsmitteln müssen eingesetzt werden. Dahingegen eröffnet die elektrochemische Oxidation einen Weg, elektrophile Iodierungsmittel in situ zu generieren und die Abfallmenge drastisch zu verringern. Ein wegweisendes Beispiel wurde von Yoshida und Mitarbeitern beschrieben, die eine direkte Iodierung von aromatischen Edukten durch elektrochemische Erzeugung der Iodonium-Ionen realisierten (Schema 1).[5] Ein Nachteil dieser und ähnlicher Methoden ist die verminderte Regiokontrolle der Iodierung und die Beschränkung auf elektronenreiche Aromaten.

Eine alternative Iodierungsmethode wurde kürzlich von uns beschrieben, bei der das reaktive *t*-Butylhypoiodit durch eine Reaktion von Zinkiodid mit TBHP erzeugt und anschließend mit Trimethylsilyl-substituierten Aromaten in situ umgesetzt wird (Schema 1).[6]

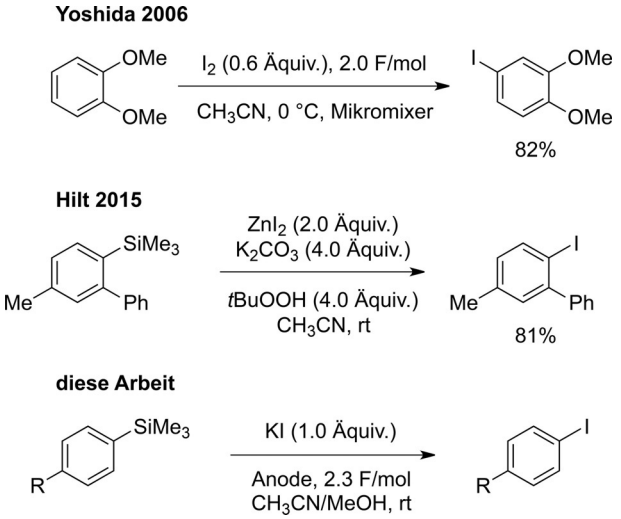

Schema 1. Iodierungsreaktionen.[5,6]

Die Einführung der Trimethylsilylgruppe erlaubt eine selektive Iodierung, wobei die hauptsächliche Limitierung, abgesehen von der niedrigen Atomökonomie, eine eingeschränkte Substratbreite war, da hauptsächlich elektronenreiche Aromaten, vornehmlich mit einem Substituenten in *ortho*-Position, in guten Ausbeuten umgesetzt werden konnten. Nichtsdestotrotz zeichnet sich die Methode durch eine ausgezeichnete Regioselektivität aus, und die Substrate sind relativ leicht durch eine Cobalt-katalysierte Diels-Alder-Reaktion von Trimethylsilyl-substituierten Alkinen mit 1,3-Dienen zugänglich.[7]

Im Folgenden beschreiben wir die Kombination dieser Methode mit nachhaltigen elektrochemischen Methoden, um ein breit anwendbares Protokoll zu entwickeln. Dazu verwendeten wir auch hier die Trimethylsilylgruppe als dirigierende Gruppe, um eine regioselektive Iodierung zu erhalten. Die Verwendung der dirigierenden Gruppe erlaubt eine vorhersagbaren Regiochemie bei hoher Reaktivität und kurzer Reaktionszeit und gleicht damit den Nachteil der verringerten Atomökonomie aus.

Für die Optimierungen wurden einige Randbedingungen definiert, um eine einfache, milde, nachhaltige und kostengünstige Methode zu entwickeln. Die Reaktion sollte bei Raumtemperatur und unter Umgebungsatmosphäre stattfin-

[*] M. Sc. R. Möckel, J. Hille, E. Winterling, S. Weidemüller, T. M. Faber, Prof. Dr. G. Hilt
Fachbereich Chemie, Philipps-Universität Marburg
Hans-Meerwein-Straße 4, 35043 Marburg (Deutschland)
M. Sc. R. Möckel, Prof. Dr. G. Hilt
Institut für Chemie, Universität Oldenburg
Carl-von-Ossietzky-Straße 9–11, 26111 Oldenburg (Deutschland)
E-Mail: gerhard.hilt@uni-oldenburg.de
Hintergrundinformationen und die Identifikationsnummer (ORCID) eines Autors sind unter https://doi.org/10.1002/ange.201711293 zu finden.

 © 2018 Wiley-VCH Verlag GmbH & Co. KGaA, Weinheim

den. Zudem sollte das kostengünstige Kaliumiodid als Iodonium-Quelle dienen, auch in der Hoffnung, auf ein zusätzliches Leitsalz verzichten zu können. Zusätzlich sollten die Elektrolysen bei einer konstanten Stromdichte von 6.7 mA cm^{-1} durchgeführt werden, um eine chemoselektive elektrochemische Reaktion mit einer kurzen Reaktionszeit zu ermöglichen.

Nachdem in einer ersten Testreaktion mit Trimethyl(phenyl)silan (**1**) als Edukt in einer ungeteilten Zelle kein gewünschtes Produkt erhalten werden konnte (Tabelle 1, Nr. 1), wurden alle weiteren Reaktionen zur Optimierung des Lösungsmittels (Nr. 2–5) in geteilten H-Zellen durchgeführt.

Leider war die beste erhaltene Ausbeute des Produkts **2** mit 40 % bei Verwendung von Acetonitril als Lösungsmittel nur moderat. Die Reaktionen in Dichlormethan, Methanol oder Dimethoxyethan als Lösungsmittel ergaben noch geringere Ausbeuten zwischen 10 und 37 % (Nr. 1–5). Die geringen Ausbeuten sind auf eine unerwünschte Protodesilylierungsreaktion zurückzuführen, die Benzol als Nebenprodukt generiert. Einzig eine Mischung aus Acetonitril und Methanol (1:1) ergab eine verbesserte Aubeute von 64 %, vornehmlich durch eine deutlich verringerte Tendenz zur Protodesilylierung.[8] Eine geringfügige Verringerung des Methanolgehalts zu einer 7:3 Mischung ergab eine deutlich bessere Ausbeute von 80 %. Eine nahezu quantitative Ausbeute (97 %) wurde erreicht, indem die Menge an KI auf 1.1 Äquivalente und die verwendete Ladungsmenge auf 2.4 F mol^{-1} erhöht wurde, wohingegen weitere Erhöhungen der Menge an KI oder der verwendeten Ladungsmenge wiederum zu einer Verschlechterung führten (Nr. 10/11). Auch der Ersatz der Platinelektroden gegen Graphitanoden führte zu einer Ausbeuteverringerung auf 48 % (Nr. 12). Zum Schluss wurde der Elektrolyt im Kathodenraum variiert und Schwefelsäure gegen Essigsäure, Methansulfonsäure oder Lithiumperchlorat getauscht was jedoch in allen Fällen zu einer Verringerung der Ausbeute führte (Einträge 13–15).

Tabelle 1: Ergebnisse der elektrochemischen Iododesilylierung von Trimethyl(phenyl)silan **1**.

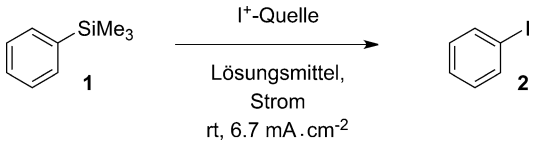

Nr.	Lösungsmittel	KI (Äquiv.)	Ladungsmenge [F mol^{-1}]	Ausbeute [%]
1[a]	MeCN	1.0	2.0	0
2	MeCN	1.0	2.0	40
3	$(MeOCH_2)_2$	1.0	2.0	10
4	CH_2Cl_2	1.0	2.0	37
5	MeOH	1.0	2.0	10
6	MeCN/MeOH 1:1	1.0	2.0	64
7	MeCN/MeOH 7:3	1.0	2.0	80
8	MeCN/MeOH 7:3	1.1	2.2	84
9	**MeCN/MeOH 7:3**	**1.1**	**2.4**	**97**
10	MeCN/MeOH 7:3	1.2	2.4	86
11	MeCN/MeOH 7:3	1.2	2.6	94
12[b]	MeCN/MeOH 7:3	1.0	2.0	48
13[c]	MeCN/MeOH 7:3	1.1	2.4	–[f]
14[d]	MeCN/MeOH 7:3	1.1	2.4	–[f]
15[e]	MeCN/MeOH 7:3	1.1	2.4	87

Soweit nicht anders erwähnt, wurde eine geteilte Zelle mit Platinelektroden und mit 0.5 mL H_2SO_4 konz. in der Kathodenkammer genutzt. Die Ausbeuten wurden durch GC-Analyse mit Mesitylen als interner Standard bestimmt (siehe Hintergrundinformationen). [a] Eine ungeteilte Zelle wurde verwendet. [b] Graphitelektroden wurden verwendet. [c] Anstatt H_2SO_4 wurde 1 mL Essigsäure verwendet. [d] Anstatt H_2SO_4 wurde 0.5 mL Methansulfonsäure verwendet. [e] Anstatt H_2SO_4 wurde 3.0 mmol (0.3 M) $LiClO_4$ verwendet. [f] Keine Leitfähigkeit der Lösung.

Leider stellte sich heraus, dass diese für **1** optimierten Bedingungen sich nicht in dem Maß auf andere Substrate übertragen ließen und eher moderate Resultate erhalten wurden (68–71 %, siehe Hintergrundinformationen). Der Hauptgrund für die verringerten Ausbeuten konnte durch gründliche GC/MS-Analyse der Reaktionsmischung aufgedeckt werden. Es stellte sich heraus, dass unter den Reaktionsbedingungen eine Methoxylierung in der benzylischen Position eintrat, insofern eine solche vorhanden war. In Kontrollexperimenten konnte gezeigt werden, dass die elektrochemische Methoxylierung in Abwesenheit einer Iodonium-Quelle nicht stattfand. Auch wurde eine benzylische Methoxylierung nicht beobachtet, wenn keine Trimethylsilylgruppe im Molekül vorhanden war.

Um die Ausbeute weiter zu optimieren und den Grad der Methoxylierung zu minimieren, wurde der Einfluss der Iodid-Beladung und des Lösungsmittels im Detail untersucht. Um die Methoxylierungsnebenreaktion zu erfassen, wurde diesmal (*p*-Tolyl)trimethylsilan als Substrat gewählt.

Um in der Lage zu sein, alle relevanten Interaktionen der Reaktionsparameter (Faktoren) zu erfassen, nutzten wir statistische Versuchsplanung in Form eines zentral zusammengesetzten Plans.[9,10] Die Parameter, die für die Optimierung untersucht wurden, waren: a) die Methanol-Konzentration (1:1–9:1 Acetonitril/Methanol (geringere Methanol-Konzentrationen wurden ausgeschlossen, da diese zu geringer Leitfähigkeit führen und somit ein weiteres Leitsalz benötigen würden)), b) die KI Beladung (1.0–1.2 Äquiv.) und c) die verwendete Strommenge (2.2–2.5 F mol^{-1}). Ausgehend von der vorangegangenen Optimierung erschienen diese drei Parameter den größten Einfluss auf die Ausbeute zu haben. Der daraus resultierende Versuchsplan umfasste 18 Reaktionen, um ein- und zweifaktorielle als auch quadratische Interaktionen abzudecken (Tabelle 2.).

Es konnten vier signifikante Interaktionen gefunden werden, die ein Modell mit einem R^2 von 0.95 ergaben (wodurch gezeigt ist, dass nur geringe Schwankungen zwischen beobachteten und vorhergesagten Werten auftreten sollten). Diese sind: a) die Methanol-Konzentration, b) der quadratische Term der verwendeten Strommenge, c) eine zweifaktorielle Wechselwirkung zwischen der Methanol-Konzentration und der verwendeten Strommenge und d) die KI-Beladung.

Dem erhaltenen Modell zufolge sind die optimalen Werte für die Methanol-Konzentration 10 % in Acetonitril, 1.0 Äquivalente KI und eine verwendete Strommenge von 2.3 F mol^{-1}.

Diese Beobachtungen sind in Einklang mit den bisherigen Erkenntnissen, die zu einer minimalen Iodid-Beladung und einer möglichst geringen Methanol-Konzentration führten, um eine Methoxylierung zu unterdrücken. Die höhere ver-

 © 2018 Wiley-VCH Verlag GmbH & Co. KGaA, Weinheim

Tabelle 2: Ergebnisse der Optimierung mittels statistischer Versuchsplanung.[a]

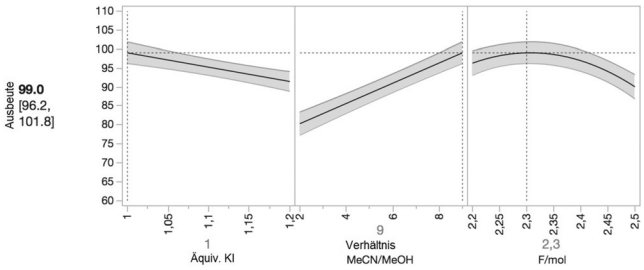

Faktor	p-Wert
MeCN/MeOH-Verhältnis	0.0000
(verwendete Strommenge)^2	0.0001
KI-Beladung	0.0003
verwendete Strommenge × MeCN/MeOH-Verhältnis	0.0031

[a] Alle Reaktionen wurden in einem 0.5-mmol-Maßstab in einer geteilten Zelle mit Platinelektroden durchgeführt. Die Ausbeuten wurden mittels GC-Analyse mit Mesitylen als interner Standard ermittelt (weitere Details, siehe Hintergrundinformationen). Die Zahlen in grau geben die optimalen Werte für die drei Parameter und die zugehörigen optimalen Ausbeuten an (Vertrauensbereich in Klammern). Die p-Werte geben die Wahrscheinlichkeit an, ob der betreffende Effekt durch eine Null-Hypothesenannahme erklärt werden kann (Effekte mit p-Werten unter 0.01 werden als signifikant betrachtet).[9e]

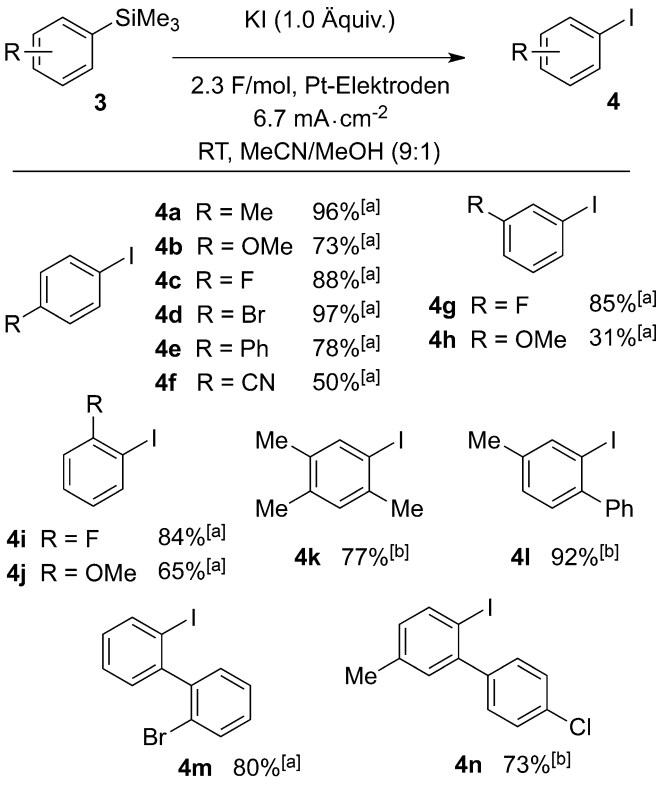

Schema 2. Ergebnisse der elektrochemischen TMS-Iod-Austauschreaktion. [a] Die Ausbeute wurde mittels GC-Analyse mit Mesitylen als internem Standard ermittelt. [b] Isolierte Ausbeute.

wendete Strommenge ($>2.0\,F\,mol^{-1}$) ist wohl auf eine teilweise elektrolytische Zersetzung des Lösungsmittels zurückzuführen. Dies kann an der zweifaktoriellen Wechselwirkung der verwendeten Strommenge mit der Methanol-Konzentration abgelesen werden, die bei höheren Methanol-Konzentrationen eine höhere erforderliche Strommenge zeigt, was durch einen Zugewinn der Relevanz der Methanoloxidation als Nebenreaktion erklärt werden kann.

Die optimierten Reaktionsbedingungen wurden auf eine Reihe von *ortho*-, *meta*- und *para*-funktionalisierten TMS-substituierten Arenen mit sowohl elektronenreichen als auch elektronenarmen Substituenten angewendet (Schema 2). In vielen Fällen wurden gute bis exzellente Ausbeuten erhalten (70–97 %), sowohl für elektronenreiche (**4b**, 73 %) als auch elektronenarme (**4c**, 88 %) Produkte. Ein ausgeprägter sterischer Einfluss auf die Ausbeuten, wie in der vorangegangenen Publikation, konnte nicht erkannt werden, da sowohl *para*- als auch *ortho*-substituierte Substrate ähnliche Ergebnisse lieferten. Lediglich sehr elektronenarme Substrate (z. B. **3f**) zeigten eine verringerte Reaktivität, die zu längeren Reaktionszeiten und niedrigeren Ausbeuten führten. Außerdem zeigte sich für das Substrat 3-Methoxyphenyltrimethylsilan (**3h**) eine verringerte Ausbeute von lediglich 31 %, welche, basierend auf der GC/MS Analyse, durch eine direkte Iodierung des Substrats zwischen der Methoxygruppe und der TMS-Gruppe erklärt werden kann.

Um die Verträglichkeit zu weiteren funktionellen Gruppen zu überprüfen, wurde ein Kompatibilitätstest nach Glorius durchgeführt.[11] Dieser Test basiert darauf, dass zu einer Umsetzung weitere Substrate (Additive) zugegeben werden, die eine weitere funktionelle Gruppe tragen. Um die Kompatibilität zu testen, werden dann der Umsatz des Edukts in das gewünschte Produkt und die Menge des nicht umgesetzten Additivs untersucht. Dies gibt einen Hinweis auf die Stabilität der funktionellen Gruppe des Additivs unter den verwendeten Reaktionsbedingungen (Tabelle 3).

Diejenigen funktionellen Gruppen, die leicht zu oxidieren sind, wie Heterocyclen, Alkohole oder primäre Amine, werden den oxidativen Reaktionsbedingungen der Elektrolyse nicht standhalten. Zusätzlich sind funktionelle Gruppen, die eine intrinsische Reaktivität gegenüber Iodonium-Ionen

Tabelle 3: Funktionsgruppentoleranztest mit (*p*-Tolyl)trimethylsilan als Testsubstrat.[a]

Additiv	Ausbeute (Edukt)	Ausbeute (Produkt)	Ausbeute (Additiv)
1-Octen	71 %	13 %	0 %
1-Dodecin	62 %	4 %	13 %
Benzonitril	5 %	89 %	96 %
Butylphenylketon	0 %	86 %	78 %
Benzoesäuremethylester	4 %	82 %	81 %
Anilin	5 %	0 %	0 %
Nitrobenzol	0 %	84 %	100 %
Carbazol	0 %	83 %	0 %
Indol	0 %	65 %	0 %
Sulfolan	0 %	76 %	100 %
4-FC_6H_4-CH_2-PPh_3Br	12 %	56 %	86 %[b]
1,2-Epoxyoctan	37 %	38 %	0 %
Cyclopropylbenzol	86 %	8 %	32 %

[a] Soweit nicht anders erwähnt, wurde die Ausbeute durch GC-Analyse ermittelt. [b] Die Ausbeute wurde durch ^{19}F-NMR-Spektroskopie mit C_6F_6 als internem Standard ermittelt.

© 2018 Wiley-VCH Verlag GmbH & Co. KGaA, Weinheim

aufweisen, auch nicht kompatibel unter den Reaktionsbedingungen. Trotz dieser Einschränkungen zeigt sich, dass Arylhalogenide, Ester, Amide, Ketone, Nitrile, Nitrogruppen, Sulfone und Phosphoniumsalze stabil unter den Reaktionsbedingungen sind.

Um eine potentielle Anwendungsmöglichkeit zu demonstrieren, untersuchten wir zum Abschluss die Iododesilylierung von Boc-geschütztem 3-Trimethysilylbenzylguanidin **5**, welches in der Boc-entschützten Variante als ^{121}I-markierte Verbindung in der SPECT-Tomographie Verwendung findet; das ^{129}I-Derivat wird als Tumortherapeutikum genutzt.[12]

Wir verwendeten das Boc-geschützte Substrat **5**, da wir aus dem Kompatibilitätstest erkannten, dass primäre Amine nicht kompatibel mit den Reaktionsbedingungen sind (Schema 3). Trotzdem stellt **5** ein Edukt mit hoher Dichte an

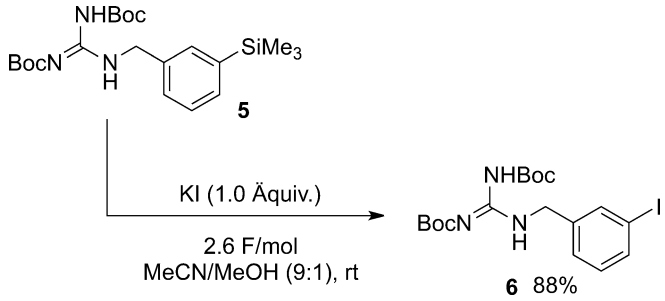

Schema 3. Elektrochemischer TMS-Iod-Austausch zur Synthese eines Tumortherapeutikums.

funktionellen Gruppen dar und ist eine herausfordernde Verbindung für eine oxidative elektrochemische Iododesilylierung. Glücklicherweise konnte das Produkt **6** in einem 0.25-mmol-Maßstab ohne säulenchromatographische Aufreinigung in 88 % Ausbeute erhalten werden. Dies demonstriert die gute Toleranz der elektrochemischen Methode gegenüber funktionellen Gruppen und zeigt prinzipiell die Möglichkeit zum Einsatz der Methode bei der Herstellung isotopenmarkierter Iodderivate auf, die in den Lebenswissenschaften von großer Bedeutung sind.

Da die Elektrolysedauer direkt mit der Stoffmenge korreliert und die Mengen an Startmaterial für eine Isotopenmarkierung oft recht klein sind, sollten die Elektrolysezeiten im Rahmen von einigen Minuten liegen, sodass eine Alternative zu den herkömmlichen Markierungsmethoden realisiert werden könnte.[12]

Wir konnten zeigen, dass die Synthese von Aryliodiden durch elektrochemische Iododesilylierung eine atomökonomische Alternative darstellt, die lediglich Schwefelsäure im Kathodenraum verwendet, um die Leitfähigkeit zu erhöhen. Es konnten sehr gute Ergebnisse mittels statistischer Versuchsplanung erhalten werden, und die optimierten Reaktionsbedingungen ließen sich auf eine Reihe von Substraten übertragen. Eine hohe Toleranz gegenüber funktionellen Gruppen konnte im Kompatibilitätstest gefunden werden, und letzlich gelang die Synthese eines Boc-*m*-iodguanidins durch elektrochemische Iododesilylierung in einer guten Ausbeute (88 %) ohne eine teure und zeitraubende Reinigung.

Experimentelles

Allgemeine Prozedur für die elektrochemische Iododesilylierung: In einer H-Zelle wird in die Anodenkammer das Aryltrimethylsilan (1.00 mmol, 1.00 Äquiv.) und Kaliumiodid (1.00 mmol, 1.00 Äquiv.) gegeben. In die Kathodenkammer gibt man konzentrierte Schwefelsäure (0.5 mL). Das Lösungsmittelgemisch (Acetonitil:Methanol = 9:1) wird gleichzeitig in Anodenraum (10 mL) und Kathodenraum (9.5 mL) gegeben. Die Platinelektroden werden eingebracht und die Lösung so lange gerührt, bis alle Feststoffe gelöst sind. Danach wird die Lösung bei konstantem Strom (6.7 mA cm^{-2}) bei Raumtemperatur bis zum vollständigem Umsatz (GC/MS-Kontrolle) elektrolysiert. Der Umsatz ist meist vollständig, wenn die Farbe der Lösung im Anodenraum von dunkelrot nach gelb umschlägt. Die Ausbeute wird entweder über GC-Analyse bestimmt (Mesitylen als interner Standard), oder die Lösung des Anodenraums wird mit Diethylether verdünnt, mit wässriger Kaliumcarbonat- und wässriger Natriumthiosulfat-Lösung gewaschen, über Natriumsulfat getrocknet, unter vermindertem Druck wird das Lösungsmittel entfernt und falls nötig über Kieselgel säulenchromatographisch gereinigt.

Danksagung

Wir danken dem Hochschulrechenzentrum Marburg und Oldenburg für die bewilligte Computerrechenzeit und für den exzellenten Service und C. Kohlmeyer für wertvolle Hilfe bei der Synthese der Ausgangsverbindungen und für hilfreiche Diskussionen. R.M. dankt Reinhart Möckel für die Einführung in das Konzept der statistischen Versuchsplanung.

Interessenkonflikt

Die Autoren erklären, dass keine Interessenkonflikte vorliegen.

Stichwörter: Aromaten · Elektrochemie · Iododesilylierung · Kompatibilitätstest · Statistische Versuchsplanung

Zitierweise: *Angew. Chem. Int. Ed.* **2018**, *57*, 442 – 445
Angew. Chem. **2018**, *130*, 450 – 454

[1] a) T. Dohi, Y. Kita in *Iodine Chemistry and Applications* (Hrsg.: T. Kaiho), Wiley, Hoboken, **2014**, S. 303 – 310.
[2] a) L. Skulski, *Molecules* **2000**, *5*, 1331; b) E. A. Merritt, B. Olofsson, *Angew. Chem. Int. Ed.* **2009**, *48*, 9052; *Angew. Chem.* **2009**, *121*, 9214; c) Y. Li, D. P. Hari, M. V. Vita, J. Waser, *Angew. Chem. Int. Ed.* **2016**, *55*, 4436; *Angew. Chem.* **2016**, *128*, 4512; d) A. Yoshimura, V. V. Zhdankin, *Chem. Rev.* **2016**, *116*, 3328.
[3] a) M. H. Bourguignon, E. K. J. Pauwels, C. Loc'h, B. Mazière, *Eur. J. Nucl. Med.* **1997**, *24*, 331; b) S. J. Goldsmith, *Semin. Nucl. Med.* **1975**, *5*, 125; c) M. H. Rønnest, F. Nissen, P. J. Pedersen, T. O. Larsen, W. Mier, M. H. Clausen, *Eur. J. Org. Chem.* **2013**, 3970.
[4] a) S. Stavber, M. Jereb, M. Zupan, J. Stefan, *Synthesis* **2008**, 1487; b) S. R. Waldvogel, K. M. Wehming, *Sci. Synth.* **2007**, *31*, 235.
[5] a) K. Midorikawa, S. Suga, J.-i. Yoshida, *Chem. Commun.* **2006**, 3794; b) K. Kataoka, Y. Hagiwara, K. Midorikawa, S. Suga, J.-i. Yoshida, *Org. Process Res. Dev.* **2008**, *12*, 1130.
[6] R. Möckel, G. Hilt, *Org. Lett.* **2015**, *17*, 1644.
[7] G. Hilt, J. Janikowski, W. Hess, *Angew. Chem. Int. Ed.* **2006**, *45*, 5204; *Angew. Chem.* **2006**, *118*, 5328.
[8] Isodesmische und mechanistische DFT-Rechnungen legen nahe, dass die Zugabe von Methanol die Bildung von MeO-I austatt

 © 2018 Wiley-VCH Verlag GmbH & Co. KGaA, Weinheim

von HSO_4-I als Iodierungsreagenz bewirkt. Dies könnte der Grund für die verringerte Protodesilylierung sein, aufgrund des weniger protischen Charakters von Methylhypoiodit im Vergleich zu HSO_4I. V. D. Filimonov, O. K. Poleshchuk, E. A. Krasnokutskaya, G. Frenking, *J. Mol. Model.* **2011**, *17*, 2759.

[9] JMP, Version *13.1.* SAS Institute Inc., Cary, NC, 1989–2013.

[10] a) P. M. Murray, F. Bellany, L. Benhamou, D.-K. Bučar, A. B. Taborb, T. D. Sheppard, *Org. Biomol. Chem.* **2016**, *14*, 2373; b) S. A. Weissman, N. G. Anderson, *Org. Process Res. Dev.* **2015**, *19*, 1605; c) E. N. Bess, A. J. Bischoff, M. S. Sigman, *Proc. Natl. Acad. Sci. USA* **2014**, *111*, 14698; d) P. Renzi, M. Bella, *Synlett* **2017**, *28*, 306; e) R. Nuzzo, *Nature* **2014**, *506*, 150; f) Ein zentral zusammengestzter Plan besteht aus einem vollfaktoriellen Plan, in welchem jeder Faktor auf zwei Stufen gemessen wird, und einem zusätzlichen Mittelpunktsversuch, der auf die Flächen des vollfaktoriellen Plans projeziert wird, um nicht-lineare Effekte bestimmen zu können.

[11] a) K. D. Collins, F. Glorius, *Nat. Chem.* **2013**, *5*, 597; b) K. D. Collins, A. Rühling, F. Glorius, *Nat. Protoc.* **2014**, *9*, 1348; c) T. Gensch, F. Glorius, *Science* **2016**, *352*, 294.

[12] a) G. Vaidyanathan, S. Shankar, M. R. Zalutsky, *Bioconjugate Chem.* **2001**, *12*, 786; b) A. van Berkel, K. Pacak, J. W. M. Lenders, *Clin. Endocrinol.* **2014**, *81*, 329; c) J. J. Mukherjee, G. A. Kaltsas, N. Islam, P. N. Plowman, R. Foley, J. Hikmat, K. E. Britton, P. J. Jenkins, S. L. Chew, J. P. Monson, G. M. Besser, A. B. Grossman, *Clin. Endocrinol.* **2001**, *55*, 47.

Manuskript erhalten: 3. November 2017
Endgültige Fassung online: 7. Dezember 2017

 © 2018 Wiley-VCH Verlag GmbH & Co. KGaA, Weinheim

ChemPubSoc Europe

DOI: 10.1002/chem.201804152

CHEMISTRY
A European Journal
Communication

Electrocatalysis

Iodine(III)-Mediated Electrochemical Trifluoroethoxylactonisation: Rational Reaction Optimisation and Prediction of Mediator Activity

Robert Möckel,*[a, b] Emre Babaoglu,[a, b] and Gerhard Hilt*[a]

Abstract: A new electrochemical iodine(III)-mediated cyclisation reaction for the synthesis of 4-(2,2,2-trifluoroethoxy)isochroman-1-ones is presented. Based on this reaction design of experiments and multivariate linear regression analysis were used to demonstrate their first application in an electrochemical reaction. The broad applicability of these reaction conditions could be shown by a range of substrates and an extensive compatibility test.

Organic electrochemistry has recently drawn much attention due to an increased demand for more environmentally friendly reactions, that is, the substitution of oxidants and reductants by electricity.[1] Electrochemical batch reactions are also easy to implement into flow conditions which is an appealing point with regard to industrial applications.[2] Although an electrochemical approach often simplifies reactions as oxidants or reductants are avoided and often no inert conditions are required, it brings new challenges especially when it comes to reaction optimisation. In this regard, new reaction parameters, such as electrode material, cell design (e.g., divided, undivided, pseudo-divided), supporting electrolytes and, most importantly, frequently employed mediators are noteworthy. Furthermore, the fact that special cells and power supplies have to be used limits the number of experiments that can be carried out in parallel which aggravates the optimisation process.[3]

As optimisation is a fundamental problem, not only for chemical method development, a range of statistical tools are available in order to accelerate, hedge and simplify optimisation processes. One tool which is well-known but nonetheless seldom used in academic research, is design of experiments (DOE). It deals with the challenge of distributing measuring points as efficiently as possible within their experimental space in order to reduce the number of necessary experiments with at the same time higher statistical significance.[4] Another method which has found increasing use in recent years is multivariate linear regression analysis (MLR). This tool deals with the prediction of one or even more variables from multiple descriptor variables. In chemistry it is often combined with theoretical methods like DFT calculations in order to predict outcome variables like yield or enantiomeric excess from computationally accessible predictors.[5]

Even though these methods have been used (extensively in case of MLR) for the optimisation of general chemical reactions their application in electrochemistry is rare.[5] Two examples for multivariate modelling of electrochemical reactions have been reported by Sigman regarding reaction yield prediction of a TEMPO-mediated oxidation[6] and for the prediction of the stability of anolytes.[7] The only example for the usage of DOE in an electrochemical reaction has, to our knowledge, been reported recently by us in which we used DOE for the optimisation of an electrochemical iododesilylation reaction.[8]

On the basis of the promising results we obtained with DOE in this reaction, we were interested in whether we could expand the use of DOE and furthermore combine it with multivariate modelling to be able to optimise the used mediator in a virtual screening.

In order to prove the concept, we chose the field of hypercoordinate iodine(III) chemistry. The choice for an iodine(III)-mediated reaction was governed by several reasons; most importantly, the fascinating reactivity of those compounds that show reactivity patterns comparable to that of transition metals.[9] Although iodine(III)-mediated reactions depend on a stoichiometric use of oxidants, only a rare number of examples of their application as in-cell mediators in electrochemical reactions has been reported. In addition, these examples cover exclusively simple oxidative fluorination reactions at highly activated substrates (thioacetals, 1,3-dicarbonyls).[10] More challenging reactions at unactivated substrates with more complicated reaction mechanisms or efforts towards iodine(III)-mediated enantioselective electrochemical reactions have not been reported.[10d]

A substrate class that has been used before in iodine(III)-mediated lactonisation reactions are vinyl benzoic esters (Scheme 1). Fujita reported a lactonisation using tosylate and acetate as nucleophiles together with stoichiometric amounts of the respective iodine(III) reagent.[11] Jacobsen could improve a similar reaction with fluorine as nucleophile by using *meta*-chloroperbenzoic acid as oxidant and thereby facilitating a

[a] R. Möckel, E. Babaoglu, Prof. Dr. G. Hilt
Institut für Chemie, Universität Oldenburg, Carl-von-Ossietzky-Straße 9–11
26129 Oldenburg (Germany)
E-mail: robert.moeckel@uni-oldenburg.de
gerhard.hilt@uni-oldenburg.de

[b] R. Möckel, E. Babaoglu
Fachbereich Chemie, Philipps-Universität Marburg
Hans-Meerwein-Straße 4, 35043 Marburg (Germany)

Supporting information and the ORCID identification number(s) for the author(s) of this article can be found under:
https://doi.org/10.1002/chem.201804152.

© 2018 Wiley-VCH Verlag GmbH & Co. KGaA, Weinheim

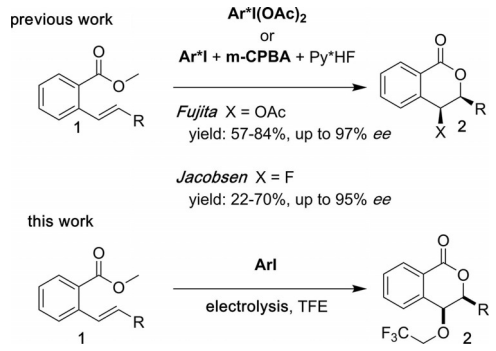

Scheme 1. Previous work on iodine(III)-mediated lactonisation by Fujita[11] and Jacobsen.[12]

sub-stoichiometrically use of the iodine mediator.[12] We wanted to expand this type of reaction by using electrochemical conditions in order to circumvent the use of stoichiometric amounts of oxidant or iodine(III) reagent and furthermore by using a different introduced nucleophile. We chose trifluoroethoxylate as it is a challenging anion due to its low nucleophilicity and furthermore due to its potential application in pharmacologically active compounds.[13]

We started the optimisation process using a D-optimal screening design consisting of 19 reactions (covering only linear terms and, in case of concentrations, their corresponding acids/electrolytes cross terms) in order to probe as many variables as possible with the lowest possible number of experiments. Investigated factors were: the mediator loading (iodobenzene was chosen as mediator to avoid possible substituent effects on the reaction), an additional acid, as preceding test reactions showed an impact on the yield (acetic acid, trifluoroacetic acid and methanesulfonic acid) and the supporting electrolyte (tetrabutylammonium tetrafluoroborate, lithium perchlorate and lithium hexafluorophosphate), their respective concentrations, the electrodes (graphite and platinum), temperature (6 to 35 °C), the current density (2.5 to 7.5 mA cm^{-2}) and the applied charge (1.8 to 2.4 F mol^{-1}). The styrene derivative **1a** was chosen as screening substrate in order to be able to follow the reaction progress and determine yields using ^{19}F NMR spectroscopy.

By this means, we could exclude the current density and the applied charge as impact factors. In case of the categorical factors, we constricted the design to the top scorers meaning lithium perchlorate as electrolyte and trifluoroacetic acid as supporting acid. The remaining design was expanded by only six reactions in order to cover quadratic terms as well as the cross interactions of the acid and the electrolyte concentration. The resulting model consists of nine factors with a very good R^2 of >0.99, p-values <0.01 and a very good lack of fit of 0.31. The most important factor was found to be the applied electrolyte together with its respective concentration. The single quadratic term which is relevant is the acid concentration. The thereby derived optimal conditions are shown in Figure 1. Not surprisingly, the mediator loading showed an equally small positive effect but was set to 25 mol% in all following investigations to obtain catalytic conditions. Using those optimised conditions,

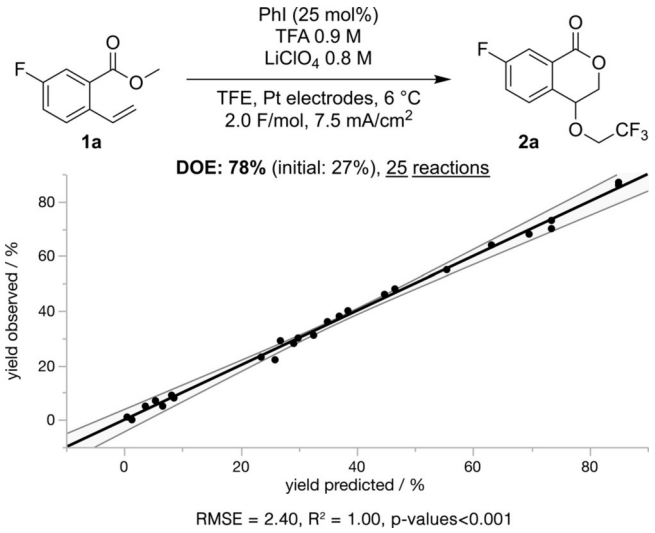

Figure 1. DOE optimised reaction conditions and plot of measured versus predicted yields. Reactions were performed on a 0.5 mmol scale. Yields were determined by ^{19}F NMR analysis using C_6F_6 as internal standard (for detailed information see the Supporting Information).

we were able to increase the yield dramatically from 27 to 78% carrying out only 25 reactions.

With these optimised reaction conditions in hand, the next variable to optimise was the mediator. By screening a set of commercially available aryl iodides and subsequent multilinear regression with theoretically obtained values, a model for the prediction of the yield was to be generated. The second step should be a virtual screening of potentially chiral mediators to reduce the effort invested in the synthesis of those synthetically challenging mediators dramatically. An often-occurring problem when screening new systems is an asymmetrical distribution of the predictor and connected with this of the target values. To minimize this problem, we generated a descriptor set for a large set of 46 mediators. Only commercially available mediators were considered to ensure an as efficient and rapid screening as possible. From this set we selected 18 mediators as fitting and 6 mediators as validation set using a D-optimal design ensuring an even distribution of the predictors and thereby hopefully a uniform yield distribution. The selected mediators span a broad range of electron-rich as well as electron-poor arenes with *ortho*-, *meta*- and *para*-substitution (Figure 2) confirming the DOE approach. Each mediator was used in triplicate to ensure good reproducibility applying the optimised reaction conditions (the reaction temperature was set to 25 °C in ease of preparational simple conditions).

For the generation of the descriptor set, we calculated three distinctive structures: the iodobenzene derivative, its dication, and the respective hypercoordinate iodine(III) structure with two trifluoroacetoxy ligands.[14] The calculated predictors were: the free oxidation enthalpy ΔG_{ox}, the free binding enthalpy of the trifluoroacetoxy ligands $\Delta G_{bond,TFA}$ and for each structure, respectively, the NBO charge on the iodine, HOMO and LUMO energies. Furthermore, an IR deformation vibration in **III** and in order to cover steric effects, various *Sterimol* parameters and finally the distance $L_{O\text{-}O}$ between the two oxygen atoms in struc-

© 2018 Wiley-VCH Verlag GmbH & Co. KGaA, Weinheim

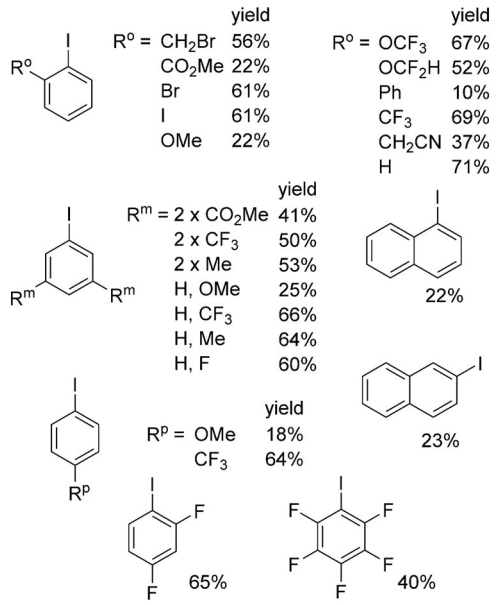

Figure 2. Screened iodoarene mediators for MLR. All reactions were carried out three times (for determination of the standard deviation) on a 0.5 mmol scale. Yields were determined by GC-FID analysis using mesitylene as internal standard at room temperature.

ture **III** (for more information see Scheme 2 and the Supporting Information).

With the theoretical as well as experimental data in hand, multivariate linear regression analysis was applied. To cope with the high number of descriptors we applied various techniques. To initially reduce the number of relevant descriptors, we used principal component analysis and the partial least squares method implemented in JMP 13.[16] Ensuing, the stepwise algorithm implemented in JMP 13 using fivefold internal cross validation—taking quadratic and two-way cross interactions into account—was used (for further information see the Supporting Information). The final model consists of seven descriptors. It shows a high predictive power with a RMSE of 5.59 in the validation set. The model is dominated by two terms,

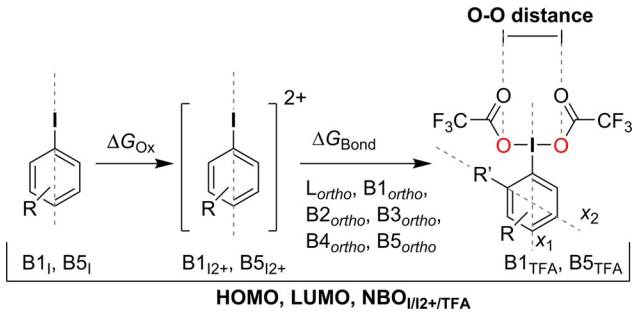

Scheme 2. Calculated molecular descriptors for multivariate linear regression modelling. Respective *Sterimol* parameters B1 and B5 were determined along x_1-axis, $B1_{ortho}$, $B2_{ortho}$, $B3_{ortho}$, $B4_{ortho}$, $B5_{ortho}$ and L_{ortho} along the x_2-axis. Distance $L_{O\text{-}O}$ was measured along the O–O bond axis. IR_{TFA} ring deformation vibration in x_1 direction was measured in **III**. All structures and electronic parameters (ΔG_{ox}: free oxidation enthalpy, ΔG_{bond}: binding free enthalpy, NBO, HOMO and LUMO values) were determined on the M06-2X/def2-TZVPP-D3 level (for computational details, see the Supporting Information).

the $\mathbf{HOMO_I}$ and the $\mathbf{HOMO_{I2+}}$ energy. Less important are the $\mathbf{B5_{I2+}}$, $\mathbf{L_{O\text{-}O}}$, $\mathbf{NBO_I}$, and $\mathbf{LUMO_I}$. Using cyclic voltammetry, some of those terms could be attributed to two different factors that determine the performance of the mediator (see the Supporting Information). $\mathbf{HOMO_I}$ and $\mathbf{HOMO_{I2+}}$ as the most important terms could be connected to their oxidation potential which most likely reflects their stability towards oxidative degradation processes. $\mathbf{LUMO_I}$, $\mathbf{L_{O\text{-}O}}$ and $\mathbf{NBO_I}$ correlate with the peak current ratios *j*, depicting the reactivity of the mediator towards the substrate.

As we found the optimal achiral mediator to be iodobenzene (it possesses nearly ideal descriptor values, thus further virtual screening is not promising) we drew our attention to chiral mediators. This field is much more challenging as all tested chiral mediators, commonly used in literature, decomposed under the reaction conditions (yields are plotted in Figure 3 as test set, see the Supporting Information for a complete list with their respective structures). According to the model, this can be mainly attributed to their low oxidation potential. That is why we calculated in a virtual screening a large set of chiral mediators in order to find a new potential chiral mediator that is stable under the reaction conditions. One of the top scorers **3 g** which could be obtained by directed optimisation of a literature known mediator, is shown in Figure 3. It shows a promising yield of 56% (compared to 71% for iodobenzene) and perfectly illustrates the time saving benefits in synthesis due to a virtual screening. Current investigations on the enantiomeric excess of this and other high yielding chiral mediators are under way and will be reported soon.

In a last step, the performance of iodobenzene as mediator under the optimised reaction conditions should be evaluated. Once again, we wanted to reduce the experimental expenditure by refraining from testing a large range of substrates. Only a small number of substrates were subjected to the reaction in order to check for electronic and steric effects. Electronic effects were examined by modifying the aromatic core. For electron-neutral or electron-deficient substrates no distinct dependency could be observed (Figure 4).

The electron-rich substrate **2 f** decomposed and only product traces could be found. Steric effects were studied at three positions: at the aromatic core and at the two *ortho*-positions using the respective methyl derivatives **2 h** and **2 i** but no significant effect could be observed. The vinylic position was the third position to be modified in order to check for effects on the yield and potential diastereomers. Unfortunately, we observed a negative correlation. For sterically demanding groups, such as cyclohexyl **2 l**, satisfying diastereomer ratios of up to 90:10 could be observed but accompanied with low yields. For sterically less demanding substrates like *n*-propyl **2 j**, good yields were obtained but the diastereomer ratio was lower.

To further reduce the synthetic effort in the determination of the functional group tolerance, a compatibility test was carried out which is based on the addition of additives containing one specific functional group to a screening reaction in order to measure the product and the additive yield and thereby determine the stability or influence on the reaction of the respective functional group.[17] A selection of results is shown in

© 2018 Wiley-VCH Verlag GmbH & Co. KGaA, Weinheim

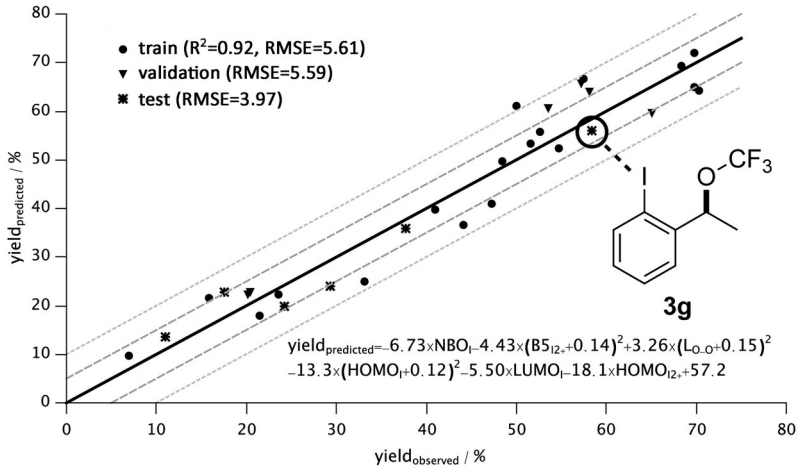

Figure 3. Normalised multivariate linear regression model for the yield of aryl iodide mediators and structure of potentially chiral mediator **3g** (for structures of remaining test set see the Supporting Information).

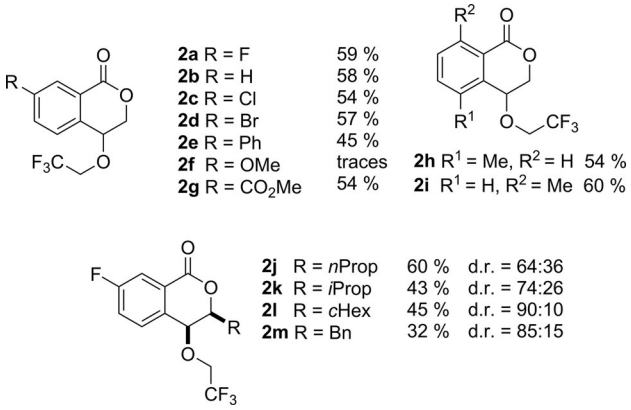

Figure 4. Results of the electrochemical lactonisation reaction using 25 mol% iodobenzene as mediator. All reactions were carried out on a 1.0 mmol scale using the reported optimised reaction conditions. Diastereomer ratios were determined by GC/MS prior to chromatographic purification. For further information see Experimental Section.

Table 1. In general, functional groups that are labile towards oxidative conditions or groups that show intrinsic reactivity towards iodine(III) species show low additive and/or product yields.[18] This is the case for alkenes, alkynes or some heterocycles like furanes or indoles. Nevertheless, a broad range of functional groups is stable. Noteworthy are electron-deficient heterocycles such as chinoline or pyridine, Boc-protected amides but oxidative labile groups like aliphatic amines or aldehydes are stable as well (for complete list, see the Supporting Information).

All reactions were carried out on a 0.5 mmol scale using the reported optimised reaction conditions. Additive yields were determined by GC-FID analysis using mesitylene as the internal standard. For more examples see the Supporting Information.

In conclusion, we have developed a new electrochemical iodine(III)-mediated lactonisation leading to trifluoroethoxy-substituted isochromanones. To our knowledge, this is the first example of an electrocatalytically mediated iodine(III) reaction in which two new bonds are formed and the hypercoordinate iodine species not solely serves as an oxidant. Functional group tolerance could be demonstrated using a compatibility test and furthermore, steric and electronic effects were investigated using a range of substrates. Based on this new reaction we could demonstrate several methods that simplify and simultaneously render reaction optimisation more valid and robust. Using design of experiments theory considering seven parameters of which three are categorical, we could reduce

Table 1. Functional group tolerance test using 25 mol% iodobenzene as mediator with screening substrate **1a**.[a]

Additive	Yield starting material [%]	Yield product [%]	Yield additive [%]
–	0	71	–
1-dodecylamine	0	75	100
benzaldehyde	0	58	77
butanol	0	68	100
1-*N*-Boc-2-piperidone	0	53	69
2,6-lutidine	0	53	64
2-chlorochinoline	0	67	75
2-butylfuran	2	43	0
1-dodecyne	0	40	7
1-octene	0	33	0
2-methylanisole	86	0	0
N-methyl indole	19	10	34
sulfolane	0	68	90
benzothiazole	0	45	94
1-chlorooctane	0	71	92
chlorobenzene	0	67	87
carbazole	9	51	42
dibutyl ether	0	49	100
heptyl cyanide	0	55	100
2-butylfuran	2	43	0
nitrobenzene	0	64	100
4-(TMS)toluene	10	19	0
valerophenone	0	59	82
methyl benzoate	0	69	88

[a] All reactions were carried out on a 0.5 mmol scale using the reported optimised reaction conditions. Additive yields were determined by GC-FID analysis using mesitylene as the internal standard. For more examples see the Supporting Information.

© 2018 Wiley-VCH Verlag GmbH & Co. KGaA, Weinheim

the number of experiments needed for a statistically significant result dramatically to 25 reactions. Using multivariate linear regression, we could build up a model by which we can predict yields for theoretically calculated mediators. This allowed us to carry out a virtual screen yielding inter alia one potentially chiral mediator with a promising yield of 56% doubling the yield of literature known mediators. As far as we know, this is the first reported example for the combination of these methods and we hope that it will be a kick-off for other groups to use design of experiment in combination with multivariate modelling in order to speed up the reaction and mediator optimisation process with simultaneously higher significance of the results.

Experimental Section

In an H-type cell, both chambers were loaded with 10 mL of an 0.9 M trifluoroacetic acid solution in trifluoroethanol and lithium perchlorate (851 mg, 0.8 M). Iodobenzene (0.125 mmol, 25 mol%) and the respective vinyl benzoate (1.00 equiv, 0.5 mmol) were added to the anode compartment. The cell was equipped with platinum electrodes and the solutions were stirred until all solids were dissolved. The reaction was electrolysed under constant current density (7.5 mA cm^{-2}) at RT until complete conversion (GC/MS monitoring) could be detected (normally 2 F mol^{-1}). The anode compartment solution was taken up with a syringe and filtered through a pad of neutral aluminium oxide which was rinsed thoroughly with ethyl acetate. The solvent was evaporated under reduced pressure. The crude product was purified by column chromatography using neutral aluminium oxide as stationary phase.

Acknowledgements

We thank the Hochschulrechenzentrum Marburg and Oldenburg for providing computer time and for the excellent service. We thank Alexander Nödling and Reinhart Möckel for helpful discussions and Marc Schmidtmann for help with crystal structure analysis.

Conflict of interest

The authors declare no conflict of interest.

Keywords: electrochemistry · hypercoordinate iodine · iodine(III) · iodoarenes · multivariate linear regression

[1] a) M. Yan, Y. Kawamata, P. S. Baran, *Chem. Rev.* **2017**, *117*, 13230; b) J.-I. Yoshida, A. Shimizu, R. Hayashi, *Chem. Rev.* **2018**, *118*, 4702; c) K. D. Moeller, *Chem. Rev.* **2018**, *118*, 4817; d) A. Wiebe, T. Gieshoff, S. Möhle, E. Rodrigo, M. Zirbes, S. R. Waldvogel, *Angew. Chem. Int. Ed.* **2018**, *57*, 5594; *Angew. Chem.* **2018**, *130*, 5694; e) S. Möhle, M. Zirbes, E. Rodrigo, T. Gieshoff, A. Wiebe, S. R. Waldvogel, *Angew. Chem. Int. Ed.* **2018**, *57*, 6018; *Angew. Chem.* **2018**, *130*, 6124; f) E. J. Horn, B. R. Rosen, P. S. Baran, *ACS Cent. Sci.* **2016**, *2*, 302.

[2] a) D. Pletcher, R. A. Green, R. C. D. Brown, *Chem. Rev.* **2018**, *118*, 4573; b) M. Atobe, H. Tateno, Y. Matsumura, *Chem. Rev.* **2018**, *118*, 4541; c) K. Mitsudo, Y. Kurimoto, K. Yoshioka, S. Suga, *Chem. Rev.* **2018**, *118*, 5985.

[3] C. Gütz, B. Klöckner, S. R. Waldvogel, *Org. Process Res. Dev.* **2016**, *20*, 26.

[4] a) S. A. Weissman, N. G. Anderson, *Org. Process Res. Dev.* **2015**, *19*, 1605; b) P. Renzi, M. Bella, *Synlett* **2017**, *28*, 306; c) P. M. Murray, F. Bellany, L. Benhamou, D.-K. Bučar, A. B. Tabor, T. D. Sheppard, *Org. Biomol. Chem.* **2016**, *14*, 2373.

[5] a) C. B. Santiago, J. Y. Guo, M. S. Sigman, *Chem. Sci.* **2018**, *9*, 2398; b) A. Milo, A. J. Neel, F. D. Toste, M. S. Sigman, *Science* **2015**, *347*, 737; c) C. B. Santiago, A. Milo, M. S. Sigman, *J. Am. Chem. Soc.* **2016**, *138*, 13424; d) J.-Y. Guo, Y. Minko, C. B. Santiago, M. S. Sigman, *ACS Catal.* **2017**, *7*, 4144; e) F. D. Toste, M. S. Sigman, S. J. Miller, *Acc. Chem. Res.* **2017**, *50*, 609; f) M. S. Sigman, K. C. Harper, E. N. Bess, A. Milo, *Acc. Chem. Res.* **2016**, *49*, 1292; g) E. N. Bess, A. J. Bischoff, M. S. Sigman, *Proc. Natl. Acad. Sci. USA* **2014**, *111*, 14698; h) D. T. Ahneman, J. G. Estrada, S. Lin, S. D. Dreher, A. G. Doyle, *Science* **2018**, *360*, 186.

[6] a) D. P. Hickey, R. D. Milton, D. Chen, M. S. Sigman, S. D. Minteer, *ACS Catal.* **2015**, *5*, 5519; b) D. P. Hickey, M. S. McCammant, F. Giroud, M. S. Sigman, S. D. Minteer, *J. Am. Chem. Soc.* **2014**, *136*, 15917; c) J. E. Nutting, M. R. Rafiee, S. S. Stahl, *Chem. Rev.* **2018**, *118*, 4834.

[7] a) C. S. Sevov, D. P. Hickey, M. E. Cook, S. G. Robinson, S. Barnett, S. D. Minteer, M. S. Sigman, M. S. Sanford, *J. Am. Chem. Soc.* **2017**, *139*, 2924; b) K. H. Hendriks, S. G. Robinson, M. N. Braten, C. S. Sevov, B. A. Helms, M. S. Sigman, S. D. Minteer, M. S. Sanford, *ACS Cent. Sci.* **2018**, *4*, 189.

[8] R. Möckel, J. Hille, E. Winterling, S. Weidemüller, T. M. Faber, G. Hilt, *Angew. Chem. Int. Ed.* **2018**, *57*, 442; *Angew. Chem.* **2018**, *130*, 450.

[9] a) S. Ghosh, S. Pradhan, I. Chatterjee, *Beilstein J. Org. Chem.* **2018**, *14*, 1244; b) A. Parra, S. Reboredo, *Chem. Eur. J.* **2013**, *19*, 17244; c) A. Sreenithya, K. Surya, R. B. Sunoj, *Wiley Interdiscip. Rev.: Comput. Mol. Sci.* **2017**, *7*, 1; d) A. Yoshimura, V. V. Zhdankin, *Chem. Rev.* **2016**, *116*, 3328; e) A. Stirling, *Chem. Eur. J.* **2018**, *24*, 1709; f) S. V. Kohlhepp, T. Gulder, *Chem. Soc. Rev.* **2016**, *45*, 6270; g) S. Haubenreisser, T. H. Wöste, C. Martínez, K. Ishihara, K. Muñiz, *Angew. Chem. Int. Ed.* **2016**, *55*, 413; *Angew. Chem.* **2016**, *128*, 422.

[10] a) T. Broese, R. Francke, *Org. Lett.* **2016**, *18*, 5896; b) S. Hara, T. Hatakeyama, S.-Q. Chen, K. Ishi-i, M. Yoshida, M. Sawaguchi, T. Fukuhara, N. Yoneda, *J. Fluorine Chem.* **1998**, *87*, 189; c) D. Kajiyama, T. Saitoh, S. Nishiyama, *Electrochemistry* **2013**, *81*, 319; d) M. Elsherbini, T. Wirth, *Chem. Eur. J.* **2018**, *24*, 13399 – 13407.

[11] a) M. Fujita, Y. Yoshida, K. Miyata, A. Wakisaka, T. Sugimura, *Angew. Chem. Int. Ed.* **2010**, *49*, 7068; *Angew. Chem.* **2010**, *122*, 7222.

[12] E. M. Woerly, S. M. Banik, E. N. Jacobsen, *J. Am. Chem. Soc.* **2016**, *138*, 13858.

[13] J. Wang, M. Sánchez-Roselló, J. L. Aceña, C. del Pozo, A. E. Sorochinsky, S. Fustero, V. A. Soloshonok, H. Liu, *Chem. Rev.* **2014**, *114*, 2432.

[14] Isodesmic calculations as well as control reactions using stoichiometric amounts of (bis(trifluoroacetoxy)iodo)benzene (PIFA) suggest the respective PIFA analogues to be the active species and not the expected TFE coordinate structures.

[15] *Sterimol* parameters describe the steric demand of a substituent in a multidimensional approach (e.g., B1: minimum width, B5 maximum width from the primary bond); A. Verloop, in *Drug Design, Vol. III, 133* (Ed.: E. J. Ariens), Academic Press, New York, **1976**.

[16] JMP, Version 13.1., SAS Institute Inc., Cary, NC, **1989 – 2013**.

[17] a) K. D. Collins, A. Rühling, F. Glorius, *Nat. Protoc.* **2014**, *9*, 1348; b) K. D. Collins, F. Glorius, *Nat. Chem.* **2013**, *5*, 597; c) K. D. Collins, F. Glorius, *Acc. Chem. Res.* **2015**, *48*, 619.

[18] In a rough MLR analysis, we were able to correlate additive yields with their HOMO energies and an NBO charge, which shows that mainly oxidative degradation processes are important for substrate stability (for more information see the Supporting Information).

Manuscript received: August 14, 2018

Accepted manuscript online: August 21, 2018

Version of record online: October 1, 2018

© 2018 Wiley-VCH Verlag GmbH & Co. KGaA, Weinheim